

**Regulation of metamorphosis and the evolution of life
cycles: insights from the common moon jelly *Aurelia aurita***

Dissertation

Zur Erlangung des Doktorgrades
der Mathematisch-Naturwissenschaftlichen Fakultät
der Christian-Albrechts-Universität zu Kiel

vorgelegt von

Wei Wang

Kiel, im Mai 2013

Erster Gutachter: Prof. Dr. Dr. h.c. Thomas Bosch

Zweiter Gutachter: PD Dr. Konstantin Khalturin

Tag der mündlichen Prüfung: 31.07.2013

Zum Druck genehmigt: 31.07.2013

gez. Prof. Dr. Wolfgang J. Duschl, Dekan

Meinen Eltern und Meiner Frau

献给我的父母和妻子

<u>I. Summary.....</u>	<u>V</u>
<u>II. Zusammenfassung.....</u>	<u>VI</u>
<u>III. Abbreviations.....</u>	<u>VII</u>
<u>1 Introduction.....</u>	<u>1</u>
1.1 Cnidarians as model systems.....	1
1.2 Metamorphosis in animal kingdom.....	2
1.3 The metamorphosis of <i>Aurelia aurita</i> : from polyp to medusa.....	4
1.3.1 Metamorphosis is induced by temperature changes and soluble internal inducer.....	5
1.3.2 Transcriptome sequencing from different stages of <i>Aurelia</i>	7
1.3.3 Cell proliferation and DNA methylation during strobilation.....	8
1.3.4 Unbiased identification of strobilation inducing molecules.....	9
1.3.5 Expression analysis of the potential strobilation inducers <i>CL390</i> , <i>CL112</i> and <i>CL631</i>	11
1.4 Aims of the thesis.....	13
<u>2 Results.....</u>	<u>14</u>
2.1 Induction of strobilation in <i>Aurelia aurita</i>	14
2.1.1 Metamorphosis is induced by the temperature changes.....	14
2.1.2 Uncovering the molecular cascades of strobilation.....	14
2.1.3 Retinoic acid signaling plays a critical role in strobilation.....	15
2.1.4 Candidate strobilation genes.....	18
2.1.5 Temperature dependent "timer" for the onset of metamorphosis.....	19
2.1.6 <i>CL390</i> as strobilation inducer.....	23
2.1.7 Promoter analysis of <i>CL390</i>	25
2.1.8 Strobilation inducers in <i>Aurelia</i>	26
2.1.8.1 Recombinant <i>CL390</i> , <i>CL112</i> and <i>CL631</i> proteins.....	26
2.1.8.2 Synthetic peptides.....	27
2.1.8.3 Chemical inducers.....	28
2.2 Strobilation inhibitors in <i>Aurelia</i>	31
2.2.1 Synthetic peptides.....	31
2.2.2 Chemical inhibitor.....	32
2.3 Segmentation and ephyra morphogenesis in <i>Aurelia aurita</i>	33

2.3.1	Segmentation process and ephyra development	33
2.3.2	Conserved signalling pathways which influence the segmentation and ephyra development ..	35
2.3.2.1	Retinoic acid signaling pathway	35
2.3.2.2	<i>Hedgehog</i> signaling pathway	37
2.3.2.3	<i>Wnt</i> , <i>BMP</i> and <i>ETS</i>	38
2.3.3	Taxonomically restricted genes (<i>TRGs</i>) in segmentation	42
3	<u>Discussion</u>	43
3.1	Regulation of life cycle in <i>Aurelia aurita</i>	43
3.1.1	Temperature induction of strobilation	43
3.1.2	<i>CL390</i> as a temperature dependent molecular timer	44
3.1.3	<i>CL390</i> as a precursor of the strobilation hormone	44
3.1.4	The molecular toolkit controlling induction of strobilation.....	45
3.2	Synthetic inhibitors of strobilation.....	47
3.3	Segmentation and ephyra morphogenesis	48
3.3.1	Retinoic acid signalling pathway controls the formation of segments and ephyrae.....	48
3.3.2	Inhibition of <i>hedgehog</i> signalling pathway represses segmentation.....	49
3.3.3	<i>Wnt</i> signaling and segmentation	50
3.3.4	<i>BMP</i> and <i>ETS</i> in segmentation and ephyra development	50
3.3.5	Novel genes in segmentation and ephyra development.....	52
3.3.6	Model for the regulation of segmentation and ephyra development	52
3.4	What is the ancestral cnidarian life cycle?	53
4	<u>Material</u>	56
4.1	Organisms and cell lines.....	56
4.2	Chemicals	56
4.3	Media	57
4.4	Buffer and Solutions.....	58
4.4.1	General	58
4.4.2	<i>In situ</i> hybridization.....	58
4.4.3	Protein purification	59
4.4.4	gDNA extraction.....	59
4.4.5	Western blot.....	59
4.4.6	DNA sequencing.....	59
4.5	Kits.....	59

4.6 Enzymes	60
4.6.1 General	60
4.6.2 Restriction enzymes.....	60
4.7 Antibodies	60
4.8 Vectors	60
4.9 Size standards	61
4.10 Oligonucleotides (Primer)	61
4.11 Devices	65
4.11.1 PCR- Thermocyclers	65
4.11.2 Power supplies.....	65
4.11.3 Gel electrophoresis chambers	65
4.11.4 Incubators / Shakers.....	66
4.11.5 Electroporation devices	66
4.11.6 Centrifuges	66
4.11.7 Microscopy	66
4.11.8 UV-devices	66
4.11.9 Photometer.....	67
4.11.10 Sequencers.....	67
4.11.11 Other devices	67
4.12 Expendable materials	67
4.13 Other materials	68
4.14 URLs	68
4.15 Software	68
<u>5 Methods</u>	<u>70</u>
5.1 Cultivation of Organisms	70
5.1.1 Cultivation of <i>Aurelia aurita</i>	70
5.1.2 Cultivation of <i>Artemia salina</i>	70
5.1.3 Temperature induction if strobilation in <i>Aurelia aurita</i>	70
5.2 Transplantation and feeding experiments	71
5.2.1 Preparation the tissue pieces for transplantation and feeding.....	71
5.2.2 Transplantation setup.....	71
5.2.3 Feeding procedure	71
5.3 Standard laboratory methods	72
5.3.1 Isolation of mRNA	72
5.3.2 Isolation of gDNA	72

5.3.3	Quantification of nucleic acids	72
5.3.4	First strand cDNA synthesis	72
5.3.5	Double strand cDNA (dscDNA) synthesis	72
5.3.6	Splinkerette synthesis and ligation	72
5.3.7	Polymerase chain reaction (PCR).....	73
5.3.7.1	Standard PCRs.....	73
5.3.7.2	Colony Check PCR.....	74
5.3.7.3	High Fidelity PCR	74
5.3.7.4	Quantitative real-time PCR (qRT-PCR).....	75
5.3.7.5	Splinkerette PCR	75
5.3.8	Electrophoretic separation of DNA samples	76
5.3.9	Extraction of DNA fragments from agarose gel.....	76
5.3.10	Restriction digestion of DNA	77
5.3.11	Ligation of DNA fragments.....	77
5.3.11.1	Ligation of PCR products into pGEM [®] -T vector	77
5.3.11.2	Ligation of DNA fragments into pET-28a(+) vector.....	77
5.3.12	Desalting of ligation products.....	78
5.3.13	Transformation of <i>E. coli</i>	78
5.3.14	Preparation of plasmids	78
5.3.15	Sanger DNA sequencing	78
5.4	Whole mount <i>in situ</i> hybridization.....	79
5.4.1	Preparation of the labeled RNA probes	79
5.4.2	Whole-mount <i>in situ</i> hybridization protocol for <i>Aurelia aurita</i>	80
5.5	Chemical interference experiments.....	80
5.6	5-Brom-deoxy-Uridin (BrdU) labeling and detection.....	81
5.7	RNA interference (RNAi)	81
5.8	Recombinant proteins expression and purification.....	82
5.8.1	Constructs for recombinant proteins.....	82
5.8.2	Expression of recombinant proteins	82
5.8.3	Purification of recombinant proteins	83
5.9	Western blot	83
5.9.1	Preparation of samples.....	83
5.9.2	SDS-PAGE	83
5.9.3	Coomassie brilliant blue staining.....	84
5.9.4	Transfer membranes	84
5.9.5	Western blot.....	85
5.10	Transcriptome sequencing and assembly.....	85

5.11	Microarray Experiments	86
5.12	Phylogenetic Analysis	86
5.13	Microscopic Analysis	86
5.14	IT Software and Hardware.....	87
6	<u>References</u>	88
7	<u>Acknowledgements</u>	94
8	<u>Appendix</u>	96
8.1	Whole-mount <i>in situ</i> hybridization protocol for <i>Aurelia aurita</i>	99
9	<u>Erklärung</u>	103

I. Summary

Life histories of ancient marine invertebrates offer insight into the evolution of life cycles. The archetypal metagenetic life cycle of cnidarians alternates between sessile asexual polyps and pelagic medusa. Transition from one life form to another is triggered by environmental signals, but the molecular cascades involved in these drastic morphological and physiological changes remain unknown.

Here I show in the moon jelly *Aurelia aurita* that the molecular machinery controlling transition of the sessile polyp into a free-swimming jellyfish consists of two counterparts. One is conserved and relies on the retinoic acid signalling which is responsible for the initiation of metamorphosis. The second, novel part, is based on secreted proteins which are strongly up-regulated prior to metamorphosis in response to seasonal temperature changes. One of these secreted proteins is a temperature sensitive "timer" and a precursor of the metamorphosis hormone.

Polyp to jellyfish transition is accompanied by the dramatic changes in morphology. In my thesis, I have identified genes which are responsible for this transformation. Stage specific genes were selected and their expression patterns were examined. I also functionally analyzed several conserved signalling pathways by chemical interference. The data indicate that two taxonomically restricted genes and retinoic acid, *hedgehog*, *Wnt* and *TGF β* signalling pathways in cooperation with *ETS* transcription factor play the central role in *Aurelia* segmentation and the following ephyra morphogenesis.

These findings uncover the molecular framework controlling the life cycle regulation of a basal metazoan and imply that the Urmetazoan ancestors of currently living cnidarians possessed a medusoid stage, which has been secondarily lost in corals and sea anemones.

II. Zusammenfassung

Die Lebensentwicklung mariner Invertebraten ermöglicht einen Einblick in die Evolution des Lebenszyklus. Der archetypische metagenetische Generationswechsel findet bei Cnidarian zwischen dem sessilen asexuellen Polypen und der pelagischen Meduse statt. Die Umwandlung von einer Lebensform zur anderen wird durch Umweltsignale induziert, doch sind die molekularen Signalwege, die an diesem drastischen morphologischen und physiologischen Wechsel beteiligt sind, unbekannt.

In dieser Arbeit zeige ich, dass in der Ohrenqualle *Aurelia aurita* der molekulare Mechanismus, der den Wechsel vom sessilen Polypen zur freischwimmenden Meduse kontrolliert, aus zwei Gegenspielern besteht. Der eine ist konserviert und beruht auf dem Retinolsäure-Signalweg, welcher für die Inhibierung der Metamorphose verantwortlich ist. Der andere basiert auf sekretierten Proteinen, die als Antwort auf saisonale Temperaturwechsel vor Beginn der Metamorphose stark hochreguliert werden. Eins dieser sekretierten Proteine ist ein temperatursensitiver „Wecker“ und ein Vorläufer des Metamorphosehormons.

Der Übergang vom Polyp zur Qualle wird durch einen dramatischen Wechsel der Morphologie begleitet. In meiner Arbeit habe ich Gene identifiziert, die für diese Transformation verantwortlich sind. Es wurden stadiumspezifische Gene ausgewählt und ihre Expressionsmuster untersucht. Außerdem habe ich verschiedene konservierte Signalwege mittels chemischer Interferenz funktionell untersucht. Die Daten deuten daraufhin, dass zwei taxonomisch beschränkte Gene und der Retinolsäure-, der hedgehog-, der Wnt- und der TGF β -Signalweg in Zusammenarbeit mit dem ETS-Transkriptionsfaktor die zentrale Rolle in der *Aurelia*-Segmentation und der anschließenden Ephyra-Morphogenese spielen.

Diese Ergebnisse decken die molekulare Grundstruktur auf, welche den Lebenszyklus basaler Metazoa kontrolliert. Des Weiteren implizieren sie, dass die Urmetazoan-Vorfahren der heute lebenden Cnidaria ein Medusenstadium besaßen, welches in Korallen und Seeanemonen sekundär verloren ging.

III. Abbreviations

% (v/v)	Volume concentration (volume/volume)
% (w/v)	Mass concentration (weight/volume)
A	Adenine or Ampère
aa	amino acids
Amp	Ampicillin
AP	Alkaline Phosphatase
ASW	Artificial Seawater
b	base
BCIP	5-Brome-4-Chlor-3-Indolylphosphate
BLAST	Basic Local Alignment Search Tool
BMP	Bone Morphogenetic Protein
bp	base pairs
BrdU	5-Brom-Deoxy-Uridin
BSA	Bovine Serum Albumin
C	Cysteine or Control
°C	degree Celsius
CAR	Constitutive androstane receptor
cDNA	complementary DNA
CHAPS	3-[(3-Cholamidopropyl) -Dimethylammonio] -1-Propansulfonate
cm	Centimeter
COX	Cyclooxygenase
CTAB	Cetrimonium bromide
d	day
DBD	DNA Binding Domain
ddATP	Dideoxyadenosine triphosphat
ddCTP	Dideoxycytosine triphosphat
ddGTP	Dideoxyguanosine triphosphat
ddNTP	Dideoxynucleotide triphosphat
ddTTP	Dideoxythymidine triphosphat
DEAB	4-Diethylaminobenzaldehyde
DHH	Desert hedgehog
DIG	Digoxigenin
DMSO	Dimethylsulfoxid
DNMT	<i>de novo</i> methyl transferase
DNA	Deoxyribonucleic acid
DNase	Deoxyribonuclease
dNTP	Deoxynucleotide triphosphat
ds	double stranded
E	Ephyra
<i>E. coli</i>	<i>Escherichia coli</i>
EcR	Ecdysone Receptor
EDTA	Ethylenediaminetetraacetic Acid
EF1	Elongation Factor 1
EGF	Epidermal growth factor
ES	Early Strobila
ETS	Erythroblast Transformation Specific transcription factor
F	Forward or Phenylalanine
FGF	Fibroblast growth factor

Fig.	Figure
G	Guanine
g	Gram or g-force
GFP	Green fluorescent protein
GSK-3 β	Glycogen synthase kinase 3 beta
h	hour (s)
H ₂ O	Millipore water
HCl	Hydrochloric Acid
HMM	Hidden Markov Model
IHH	Indian hedgehog
<i>in silico</i>	via computer simulation
<i>in situ</i>	natural location
ITS	Internal Transcribed Spacer
K	Lysine
kb	kilo base pairs
kV	kilovolt
L	Liter or Leucine
LB	Lauria Bertani (bacterial growth broth)
LBD	Ligand Binding Domain
LS	Late Strobila
M	Molar
m	milli
mA	milliampère
MAB	Maleic Acid Buffer
MAB-B	Maleic Acid Buffer with BSA
MAB-T	Maleic Acid Buffer with Tween-20
MEGA	Molecular Evolutionary Genetic Analysis
mg	milligram
min	minute(s)
ml	milliliter
mm	millimetre
mM	millimolar
mRNA	Messenger-RNA
μ	micro
μ g	Microgram
μ l	Microliter
μ M	Micromolar
n	Number of replicates
NaOH	Sodium Hydroxide
NBT	Nitro Blue Tetrazolium
NCBI	National Center for Biotechnology Information
ng	nanogram
NHR	Nuclear Hormone Receptor
OD	Optical Density
ORF	Open reading frame
P	Proline
PBS	Phosphate Buffered Saline
PBT	PBS with Tween-20
PCR	Polymerase Chain Reaction
Ptc	Patched
PTTH	Protheracicotropic Hormone
qRT-PCR	Quantitative Real-Time PCR
R	Reverse or Arginine

RA	Retinoic Acid
RDH	Retinol dehydrogenase
rDNA	Ribosomal DNA
RNA	Ribonucleic Acid
RNAi	RNA Interference
RNase	Ribonuclease
rpm	rounds per minute
rRNA	ribosomal RNA
RT	Room Temperature or Reverse Transcription
RT-PCR	Reverse Transcriptions-PCR
RxR	Retinoic X Receptor
S	Serine
SD	Standard deviation
SDS	Sodiumdodecylsulfate
SDS-PAGE	Sodiumdodecylsulfate polyacrylamide gel electrophoresis
sec	seconds
SEM	Standard Error of the Mean
SHH	Sonic hedgehog
SMART	Simple Modular Architecture Research Tool
sp.	species
ss	single stranded
SXR	Steroid and xenobiotic receptor
T	Thymine
ΔT	temperature shift
T3	Triiodothyronine
T4	Thyroxine
TAE	Tris-Acetate-EDTA-buffer
<i>Taq</i>	<i>Thermophilus aquaticus</i>
TBE	Tris-Boric acid-EDTA-buffer
TEMED	N,N,N',N' - Tetraethylendiamin
TF	Transcription Factor
TGF β	Transforming Growth Factor beta
TH	Thyroid Hormone
THR	Thyroid hormone receptor
T _m	Melting temperature
TR	Thyroid Receptor
TRG	Taxonomically Restricted Gene
Tris	Tris-(Hydroxymethyl) -Aminomethane
TRPA1	Transient receptor potential cation channel subfamily A member 1
TRPM	Transient receptor potential cation channel subfamily M
TSH	Thyroid-stimulating hormone
tRNA	transfer RNA
U	Units or Uracil
USP	Ultraspiracle
UTR	Untranslated region
UV	Ultraviolet Light
V	Volt
VES	Very Early Strobila
W	Tryptophan
Y	Tyrosine

1 Introduction

1.1 Cnidarians as model systems

Cnidarians have existed for about 500 million years on earth (Cartwright *et al.*, 2007) and are the most basal animals with a complex life cycle (see Fig.1A). They possess two germ layers, the endoderm and ectoderm (Ruppert *et al.*, 2004) and are the first metazoans with a nervous system (Lindgens *et al.*, 2004). Their synapomorphic feature is the highly differentiated cnidocytes that have originated from modified neurons (Ruppert *et al.*, 2004). Complex life cycles with alternation of two morphologically and physiologically disparate generations (polyps and jellyfishes) are typical for cnidarians (see Fig.1B; Technau & Steele, 2011). The medusa stage is present in Hydrozoa, Scyphozoa and Cubozoa and is absent in corals and sea anemones.

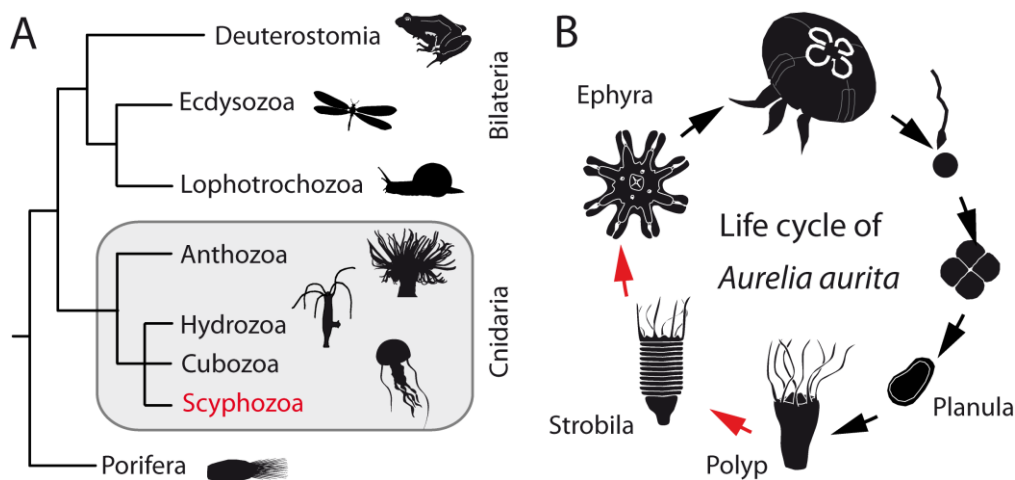


Fig. 1 (A) Phylogenetic tree of animals. Scyphozoa belong to the phylum Cnidaria which is a sister group of all bilateral animals. **(B) Life cycle of *Aurelia aurita*.** Two alternating generations - polyps and jellyfishes follow each other. Each polyp transforms into multiple ephyrae through strobilation process.

In Cnidaria, there are six major model systems belonging to Hydrozoa (*Hydra*, *Hydractinia echinata* and *Clytia hemisphaerica*) and Anthozoa (*Nematostella vectensis*, *Acropora millepora* and *Acropora digitifera*). The genomes of *Hydra magnipapillata*, *Nematostella vectensis* and *Acropora digitifera* have been sequenced (Chapman *et al.*, 2010; Putnam *et al.*, 2007; Shinzato *et al.*, 2011). Transgenic animals were generated in *Hydra vulgaris* AEP, *Nematostella vectensis* and *Hydractinia echinata* (Wittlieb *et al.*, 2006; Siebert *et al.*, 2008; Renfer *et al.*, 2010; Künzel *et al.*, 2010). Transcriptome sequences are available from

Acropora millepora, *Hydractinia echinata*, *Clytia hemisphaerica* and several *Hydra* species (Meyer *et al.*, 2009; Soza-Ried *et al.*, 2010; Houliston *et al.*, 2010; Hemmrich *et al.*, 2012).

Taken together, cnidarians are well studied at the molecular level. However, surprisingly little is known about Scyphozoan and Cubozoan jellyfishes which represent the highest degree of morphological sophistication among cnidarians. These animals possess advanced sensory organs (Garm *et al.*, 2011), exhibit complex behavioral traits (Lewis & Long, 2005; Petie *et al.*, 2011) and have complete life cycles with larvae, polyps and medusa (Ruppert *et al.*, 2004). In my PhD thesis, I used common moon jelly *Aurelia aurita* (Scyphozoan) as a model system to study the life cycle regulation in the basal Metazoa.

1.2 Metamorphosis in animal kingdom

Animal genomes often encode several alternative physical manifestations which are successively realized during ontogeny. The drastic transformation of a body plan, termed metamorphosis, is typical for amphibians, fishes, tunicates, echinoderms, crustaceans, molluscs, parasitic flatworms, cnidarians, and sponges. Intensively studied examples of complex life cycles within the bilaterians (see Fig.2) include the metamorphosis of insect larvae and amphibian tadpoles into adults (McBrayer *et al.*, 2007; Brown & Cai, 2007; Paris & Laudet, 2008).

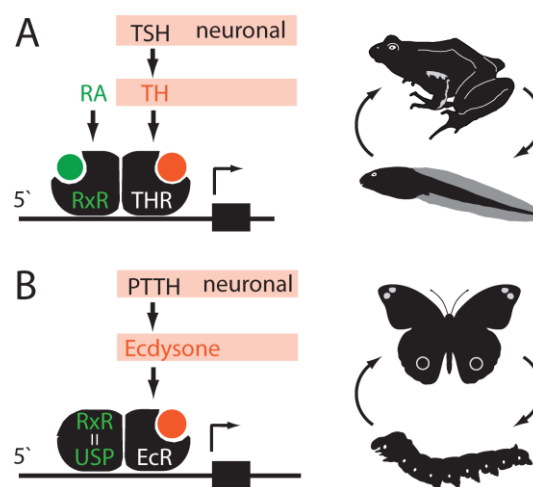


Fig. 2 Retinoic acid signalling plays a role in the regulation of metamorphosis in amphibians and insects. TSH - thyroid-stimulating hormone, TH - thyroid hormone, PTTH - prothoracicotropic hormone, RA - retinoic acid, THR - thyroid hormone receptor, EcR - ecdysone receptor, RxR - retinoic X receptor, USP – ultraspiracles.

In all model systems where the molecular basis of metamorphosis is characterized in detail, there are always two cascades which function cooperatively. These are the retinoic acid (RA) cascade with the retinoid X receptor (RxR) or its homolog ultraspiracles (USP) in insects functioning as a transcription factor and a taxon-specific hormonal system with the corresponding nuclear hormone receptor (see Fig.2). In all the cases metamorphosis activation has two successive steps - neuronal and endocrine.

In amphibians, thyroid-stimulating hormone (TSH) from the pituitary gland regulates the production of thyroid hormone (TH) which induces tadpole transformation into juvenile frog (Gudernatsch, 1912; Furlow & Neff, 2006). TSH in *Xenopus* is a glycoprotein which consists of two polypeptide chains (XP_002933965, XP_002942835) and TH is a condensation product of two iodinated tyrosines. TH is produced from a high molecular weight protein precursor (thyroglobulin) which consists of more than 2000 amino acids with only about 60 of them being tyrosines. Thyroid hormone receptor (THR) and RxR form a heterodimer which activates the cascade of downstream genes leading to metamorphosis (see Fig.2A). THR homologs have not been identified outside Deuterostomia and the TH signaling cascade is restricted to Hemichordata, Cephalochordata, Urochordata and Chordata - the animal groups where thyroid gland or thyroid-like structures are present (Paris *et al.*, 2008; Satou & Satoh, 2003).

In insects, the major components of taxon-specific metamorphosis machinery are the prothoracicotrophic hormone (PTTH) and ecdysone (see Fig.2B). PTTH is a neuropeptide which binds tyrosine kinase Torso, thereby activating ecdysone production in the prothoracic gland (Rewitz *et al.*, 2009). The sequence of PTTH differs in *Manduca*, *Drosophila* and *Bombyx mori* (McBrayer *et al.*, 2007). As shown in Fig.2B, target genes responsible for the metamorphosis are activated by the heterodimer of USP (homologous to RxR) and ecdysone nuclear receptor (EcR).

In cnidarians, the transition from polyp stage to medusa stage is tightly regulated by environmental stimuli and depends on seasonal rhythms (Hofmann *et al.*, 1978; Leitz & Wagner, 1993; Kroihner *et al.*, 2000; Miyake *et al.*, 2002). The only known cnidarian life cycle regulator is a neuropeptide, GLW-amide, which induces larvae-to-polyps transition in the hydrozoan *Hydractinia echinata* (Schmich *et al.*, 1998). Thus, despite a long history of studies, genetic regulation of a metagenetic life cycle remains enigmatic.

1.3 The metamorphosis of *Aurelia aurita*: from polyp to medusa

In order to elucidate the molecular machinery of metamorphosis in the basal Metazoa, the transition from polyp to medusa in the common moon jelly *Aurelia aurita* (see Fig.1B) was investigated. Belonging to the class Scyphozoa, *Aurelia aurita* was first described in 1758 by Carl Linnaeus. In the ocean, *Aurelia* appears in three different morphotypes: planula larva, polyp and medusa (see Fig.1B). First, the zygote develops into a free-swimming planula larva which only exists for a few weeks. Then the planula becomes sessile and develops into a polyp which can proliferate asexually by the process similar to budding. During the second metamorphosis event, which is called strobilation, the polyp turns into several ephyrae (young jellyfishes) that develop to mature medusae within several weeks (Arai, 1997). The mature medusae belong to separate sexes, with either female or male gonads (Arai, 1997). Unlike polyps, medusae have a limited life span and have a lower potential for regeneration (Agata & Inoue, 2012). However, jellyfishes have much more complex nervous system, sensory organs and striated muscles (Wehner & Low, 1995; Petie *et al.*, 2013; Steinmetz *et al.*, 2012).

Polyp to medusa transition can be divided into three successive phases: induction of metamorphosis by environmental stimuli (temperature changes), polyp segmentation and jellyfish morphogenesis. In nature, metamorphosis in *Aurelia* is a seasonal process which usually starts in winter or early spring (Möller, 1980; Miyake *et al.*, 2002). Water temperature in the ocean decreases in winter and that serves as a reliable environmental cue for starting metamorphosis which is perceived by the polyps. In laboratory conditions, similar to that in nature, metamorphosis can be induced by simply lowering the water temperature by several degrees (Kroiher *et al.*, 2000; Berking *et al.*, 2005). The characteristics of temperature modulation needed and its duration are strain specific and depend on the geographical origin of the animal strain (Schroth *et al.*, 2002). After strobilation has been initiated, the body of a polyp is divided into multiple fix-sized segments by a process which resembles somitogenesis in vertebrates. The final step, development of ephyra from a strobila segment, is a drastic transformation of the body plan (see Fig.52 in Appendix). In each segment the channels of the gastro-vascular system, striated musculature, sensory organs and complex neural network are developed (see Fig.52 and Fig.53 in Appendix).

There are at least seven genetically and geographically distinct strains of *Aurelia aurita* (Schroth *et al.*, 2002). In my work, I have used three animal lineages: Roscoff strain, Baltic



Fig. 3 Geographic distribution of three strains of *Aurelia aurita* used in this work. Polyps of Roscoff strain (shown by red circle) inhabit in the Pacific Ocean near Japan and California. Baltic sea strain (shown by red square) originate from the Kiel bay in Germany and White sea strain (shows by red triangle) originate from Shupa bay in Russia.

sea strain and White sea strain, which originate from geographically distant locations (see Fig.3). The phylogenetic trees in Fig.4 show that 16S rDNA sequences as well as ITS-1/5.8S rDNA sequences of Baltic sea strain and White sea strain have a high similarity. In contrast, the sequences of Roscoff strain are highly similar to the ubiquitous lineage. In this study, most of the experiments were carried out using Roscoff strain of *Aurelia aurita*.

A. Genealogy of *Aurelia* lineages based on 16S rDNA **B. Genealogy of *Aurelia* lineages based on ITS-1/5.8S rDNA**

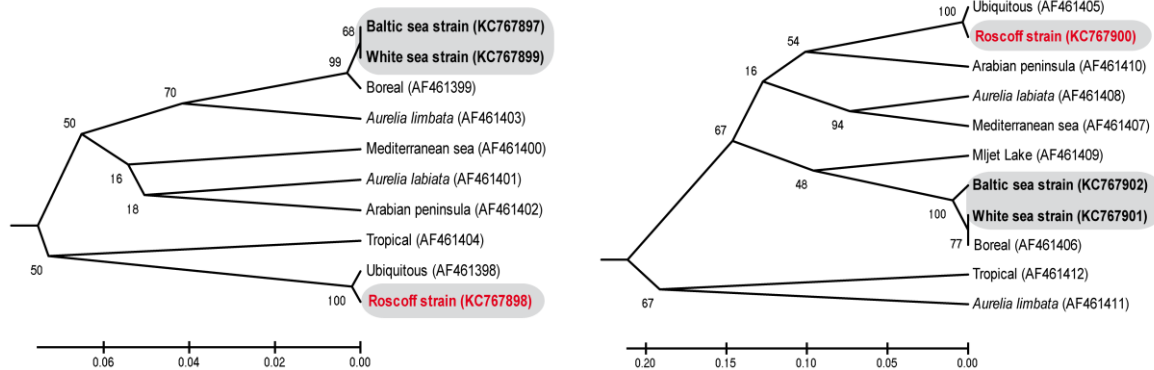


Fig. 4 Genealogy of *Aurelia* lineages. (A) Maximum likelihood tree based on 16S rDNA. (B) Maximum likelihood tree based on ITS-1/5.8S rDNA.

1.3.1 Metamorphosis is induced by temperature changes and soluble internal inducer

Morphologically, strobilation of *Aurelia aurita* is a wave-like segmentation process, which starts at the apical part of the polyp and progresses downwards (see Fig.5A-F). As a result, a stack of disk-shaped segments is generated (see Fig.5B-D). Each of those segments subsequently develops into a young jellyfish called ephyra (see Fig.5E, F). Young jellyfishes

detach from strobila (see Fig.5E, F), start independent planktonic life and within several weeks complete their development into adult jellyfish (see Fig.1B).

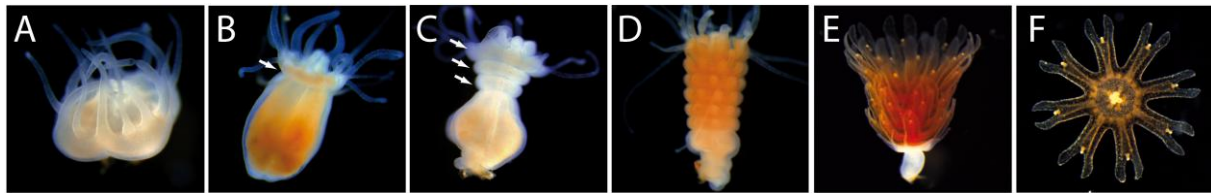


Fig. 5 Metamorphosis process in *Aurelia aurita*. Polyp (A) is divided into multiple segments (B-D) which develop into young jellyfish (E, F). White arrows, strobila segments.

The wave-like nature of strobilation implies the presence of a signalling factor or factors regulating the segmentation process (Kroiher, 2000; Fuchs, 2010). In our laboratory, we recently performed transplantation experiments shown in Fig.6A (Li, 2010). Strobila rings, when transplanted onto non-induced polyps, induce strobilation within 72 hours (see Fig.6B-D). Interestingly, the segmentation process in recipient polyps starts and progresses from the most apical part of the body and not from the site of transplantation. When strobila segments are fed to non-induced polyps (see Fig.6E), the first signs of strobilation are observed within 48 hours after feeding (see Fig.6F-H). According to the feeding experiments, different amounts of the metamorphosis inducer are present in the head, segments and the foot part of the strobila. As shown in Fig.7A, strobila segments have the strongest inductive capacity, head tissue is less potent and the least amount of inducer is present in the foot. Heat treatment of tissue prior to feeding (5 minutes at $+40^{\circ}\text{C}$) completely abolishes its inductive capacity. Co- cultivation of strobila and non-induced polyps cause strobilation only if the animals come

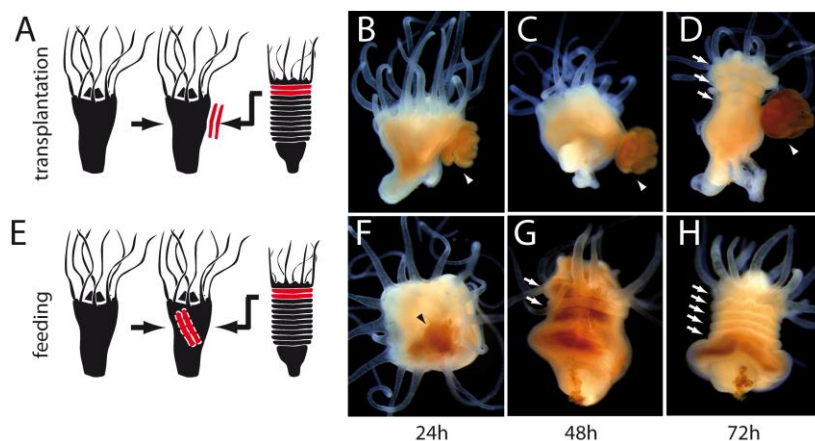


Fig. 6 Transplantation and feeding experiments (modified from Li, 2010). (A-D) Metamorphosis is induced by transplanting strobila segments onto non-induced polyps. (B-D) Segmentation starts 72 hours after transplantation. White arrowheads, transplanted strobila segments; white arrows, newly developed segments. (E-H) Feeding with strobila segments induces metamorphosis. (F) Polyp fed with strobila segments after 24 hours. Black arrowhead, strobila inside of the polyp. (G, H) Polyp strobilation starts 48 hours after feeding. White arrows, strobila segments.

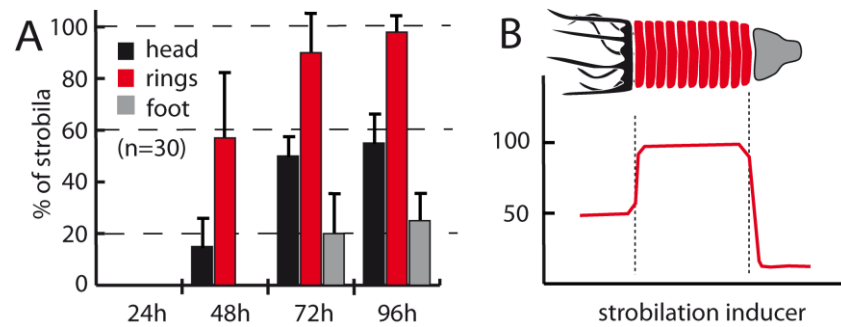


Fig. 7 Distribution of the strobilation inducer along the strobila (modified from Li, 2010). (A) Segmented part of the strobila (rings) contains the highest amount of the strobilation inducer. (B) Putative distribution of the strobilation inducer along the body of the strobila.

into prolonged direct contact with each other. In contrast to the observations of Spangenberg (1971), induction never takes place if direct contact between polyp and strobila tissue is prevented by a fine mesh barrier (Lenk, 2011). Induction of strobilation by transplantation or feeding is successful only between polyps and strobila of the Roscoff strains, while feeding polyps of Baltic sea or White sea strains with Roscoff strobila does not cause strobilation (see Fig.8). Tissues of non-induced polyps or ephyra do not exhibit any capacity to induce strobilation. In sum, internal soluble inducer is present in the strobila rings of *Aurelia*.

	Roscoff	White sea	Baltic sea
Roscoff	+ (20/20)	- (0/20)	- (0/20)

+ strobilation is induced
- strobilation is not induced

Fig. 8 Cross-feeding with Roscoff strobila segments. Segments from Roscoff strain do not induce strobilation in White sea and Baltic sea strains.

1.3.2 Transcriptome sequencing from different stages of *Aurelia*

To identify the nature of the soluble strobilation inducer as well as the molecular machinery responsible for metamorphosis in *Aurelia*, Khalturin, Fuchs and I sequenced and compared the transcriptomes of polyp, strobila and ephyra stages of *Aurelia aurita* Roscoff strain (see PhD thesis of Björn Fuchs, 2010).

As shown in Fig.9, raw reads from GS-FLX sequencer (340 Mbp in 1.478.472 reads) were assembled using Celera v5.0.4 into 29608 contigs. BLASTX search against non-redundant NCBI protein database shows that 43.8% of contigs have similarity to known proteins and

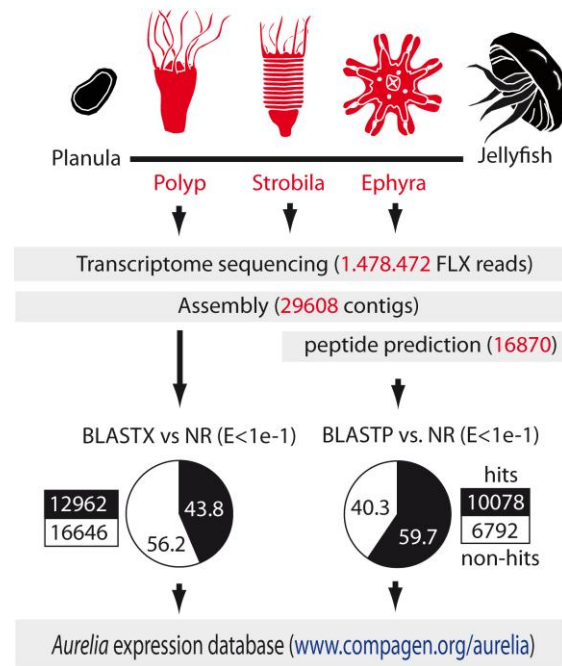


Fig. 9 Identification of the stage-specific genes and regulators of metamorphosis. Stage-specific genes were identified by sequencing of the polyp, strobila and ephyra transcriptomes (see online expression database at www.compagen.org/aurelia). Black sectors of the pie charts represent the percentage of genes having BLASTX and BLASTP hits in the non-redundant NCBI database. The absolute numbers of hits and non-hits are shown near the corresponding pie charts.

56.2% (16646) are non-hits. As a next step of the data analysis, peptides were predicted by EstScan 3.0.3 using Hidden Markov Model (HMM) matrix based on manually curated set of *Aurelia* cDNAs and *Nematostella* transcript models. In total, 16870 peptides were predicted from 29608 contigs. Out of these peptides, 59.7% (10078) show similarity to the entries in the non-redundant protein database of NCBI and 40.3% (6792) represent non-hits (e-value cut-off $\leq 1e-1$). In *Aurelia* transcriptome 190 contigs encode proteins with more than 300 amino acids which have no BLASTP hits with e-value threshold of 10^{-5} . These contigs most likely represent Scyphozoa-specific genes (Khalturin *et al.*, 2009). Contig sequences, their expression values in three life stages, peptide predictions and the results of BLAST searches are available online (see *Aurelia Project* database at www.compagen.org/aurelia).

1.3.3 Cell proliferation and DNA methylation during strobilation

The process of strobilation is accompanied by massive cellular proliferation in the ectoderm and endoderm (see Fig.10). A high number of cells in S-phase can be detected by BrdU particularly in the segmented part of the strobila (Boehm, 2009). High mitotic activity requires the maintenance of methylation patterns of DNA and epigenetic reprogramming might be necessary for *Aurelia* metamorphosis. Supporting this assumption, a gene encoding

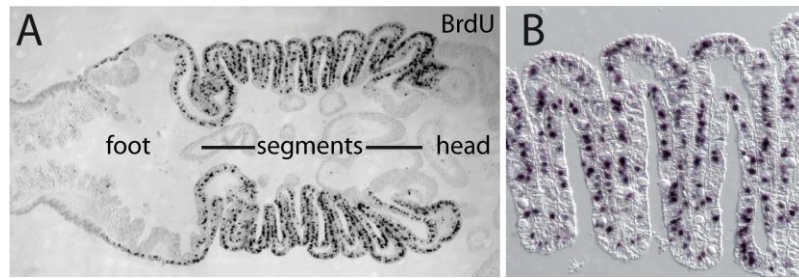


Fig. 10 High level of cellular proliferation is detected in the segmented part of the strobila by BrdU (modified from Boehm, 2009). (B) Cells in S-phase are present in both ectoderm and endoderm.

DNA methyltransferase 1 (*DNMT1*) is up-regulated during strobilation and is down-regulated in polyp and ephyra stages (see Fig.17A, 21). Incubation of *Aurelia* polyps in 5-Aza-cytidin, an inhibitor of DNA methylation, represses temperature induced strobilation (Fuchs, 2010). As shown in Fig.11, after 21 days at +10°C, only 30.0% of polyps undergo metamorphosis in the presence of 5-Aza-cytidin, compared to 67.1% in the DMSO control.

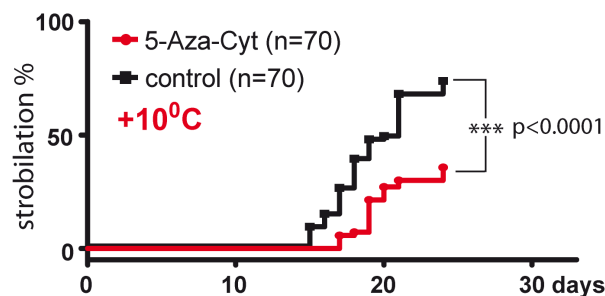


Fig. 11 Inhibition of DNA methylation by 5-Aza-cytidine (5 μ M) represses strobilation (modified from Fuchs, 2010). 5-Aza-cyt, animals treated with 5-Aza-cytidine (5 μ M); control, DMSO. n = total number of animals in three independent experiments. ***, log-rank (Mantel-Cox) test, p<0.0001.

1.3.4 Unbiased identification of strobilation inducing molecules

To identify which secreted molecule induces metamorphosis in feeding experiments and to determine the expression profile of the strobilation inducer in the course of the temperature induction, my colleagues and I analyzed strobilation in *Aurelia* by microarray approach (see PhD thesis of Björn Fuchs, 2010 and Master thesis of Philipp Dirksen, 2010). Based on the results of the transplantation and feeding experiments (see Fig.6) as well as 5-Aza-cytidin incubation (see Fig.11), any potential strobilation inducers must be expressed at the extremely low level 24 hours after the beginning of the temperature induction; expression level should steadily increase (being lower at 14 days than at 16 days) and should reach its highest level in the late strobila (see Fig.12). At the same time, the expression levels at 14 days and 16 days in DMSO control animals should be higher than in 5-Aza-cytidin incubated polyps (see Fig.11).

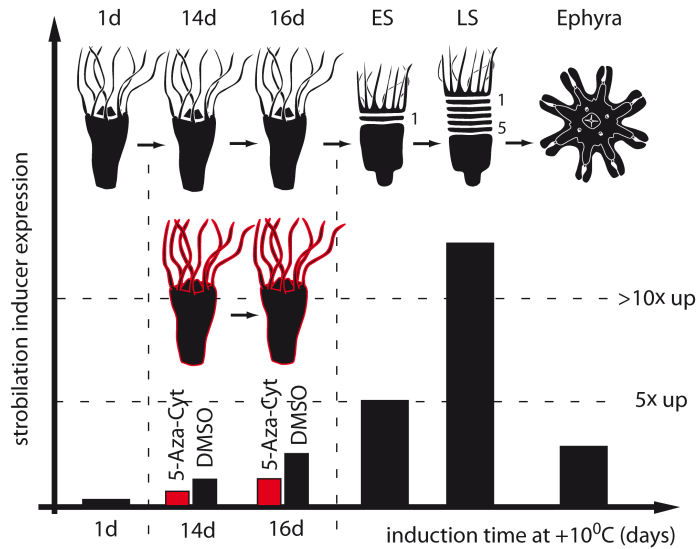


Fig. 12 Microarray experiment design (modified from Fuchs, 2010). The hypothetical expression profile of the strobilation inducer is shown as a bar diagram along X axis. 5-Aza-cyt, animals treated with 5-Aza-cytidine (5 μ M); DMSO, solvent control; ES, early strobila with 1 segment; LS, late strobila with 5 segments.

Based on these criteria we designed the experimental setup for microarray experiments shown in Fig.12. *Aurelia* polyps were placed at +10 $^{\circ}$ C and mRNA was extracted after 24 hours, 14 days, 16 days of incubation as well as from early strobila (having 1 segment), late strobila (having 5 segments) and freshly detached ephyra (maximum 24 hours after detachment). In addition, mRNA was extracted after 14 and 16 days from polyps that were continuously incubated in 5-Aza-Cytidin. Mean expression values of the replicates were normalized using the elongation factor 1 α (*EF1 α*) and the final microarray results are represented in the online database at www.compagen.org/aurelia/aur_atlas_ma.html.

Next, we identified clusters whose expressions profile during induction corresponded to the hypothetical model described in Fig.12 (see www.compagen.org/aurelia/help.html). In total, 27 contigs exhibit expression dynamics predicted for the strobilation inducer. As shown on the heat map in Fig.13 (log₂ transformed *EF1 α* normalized expression values), there are two groups of clusters (I and II) which show strong up-regulation at 14 and 16 days compared to 24 hours and are highly expressed in strobila. In group I, gene expression is drastically down-regulated in ephyra, while in group II down-regulation is not so prominent. Groups of contigs with identical expression dynamics often represent splice variants or 5'/'3' UTRs of the same gene (for example clusters 26669, 26813, 26229, 15345, 1285, 390 and 4884, 631, 913). Three genes (*CL390*, *CL112* and *CL631*) attracted special attention due to their dramatic up-regulation during strobilation.

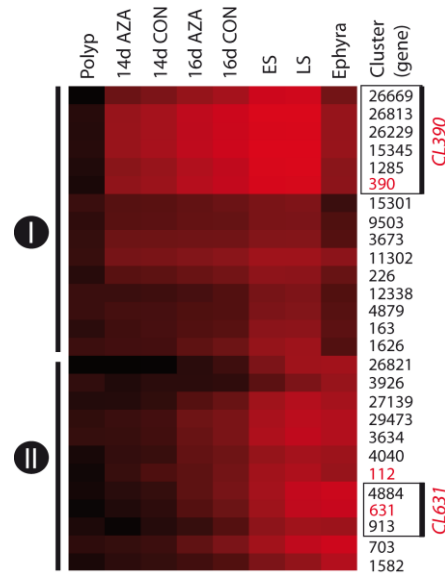


Fig. 13 Twenty seven clusters with the expression profile expected for the strobilation inducer. Numbers, cluster identifiers. Clusters representing the splice variants or 5'/3' UTRs of the same gene are boxed. ES - early strobila, LS - late strobila. I, clusters where expression is strongly down-regulated in ephyra; II, clusters without strong down-regulation in ephyra. log₂ transformed, *EF1a* normalized values.

1.3.5 Expression analysis of the potential strobilation inducers *CL390*, *CL112* and *CL631*

Transcript localization of *CL390*, *CL112* and *CL631* was examined by *in situ* hybridization in non-induced polyps, induced polyps with the first constriction (VES), early strobila (ES), late strobila (LS), during ephyra morphogenesis and in ephyra (see Fig.14). To obtain better comparison of the expression levels, animals from different life stages were always hybridized and stained together. This data have been included in the PhD thesis of Björn Fuchs (2010) and Master thesis of Philipp Dirksen (2010).

In accordance with the microarray results, *CL390* is not expressed in non-induced polyps (see Fig.14A), but is dramatically up-regulated in ectodermal epithelium during strobilation (see Fig.14B). In early strobila *CL390* is evenly expressed everywhere along the body column except tentacles, hypostome and the basal region of the body adjacent to the foot (see Fig.14C). During ephyra morphogenesis, *CL390* expression is strongly down-regulated which is clearly visible as a gradient in Fig.14D. In a freely swimming ephyra, expression of *CL390* is not detectable by *in situ* (see Fig.14E). *CL112* is expressed in a sub-population of endodermal cells (see Fig.14F-J). Similar to *CL390* it is not expressed in tentacles, hypostome and the basal part of the body (see Fig.14G-H). Expression in segments is stronger than in non-segmented part (see Fig.14G-H). In ephyra stage only four groups of endodermal cells in

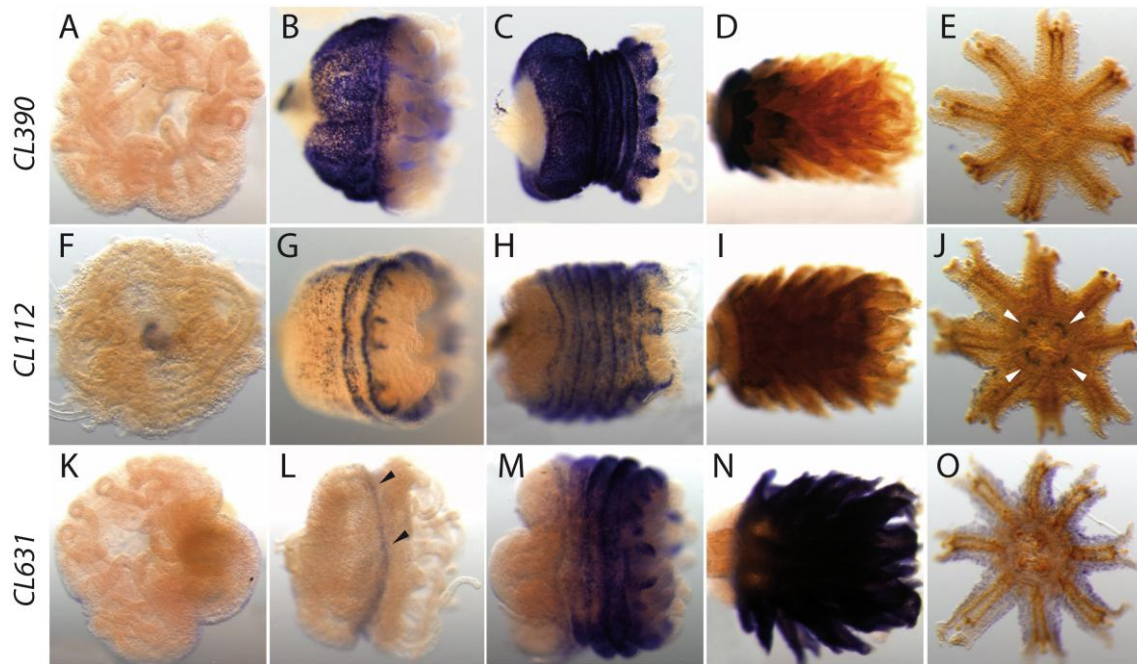


Fig. 14 Transcript localization of *CL390*, *CL112* and *CL631* was examined by *in situ* hybridization. (A-E) *CL390* is strongly up-regulated during strobilation and down-regulated in ephyra. (F-J) *CL112* is expressed in a sub-population of endodermal cells during strobilation and in four circle-like groups of cells in ephyra. (K-O) *CL631* is exclusively expressed in the segments of strobila and in the ectoderm of ephyra.

the manubrium remain *CL112* positive (white arrowheads in Fig.14J). *CL631*, in contrast to *CL390* and *CL112*, is expressed only in the segmented part of the strobila (see Fig.14L-M). The transcript is present in all ectodermal epithelial cells (see Fig.14M). The expression is strong in developing ephyra (see Fig.14N) and is clearly detectable in the ectoderm of freshly detached ephyra (see Fig.14O). All these data indicate that *CL390*, *CL112* and *CL631* might play a role in strobilation.

1.4 Aims of the thesis

Using a combination of cell biology and transcriptomic approaches as well as *in situ* hybridization, chemical interference and transplantation experiments, the following questions were addressed in this thesis:

- Which genes and signaling pathways are involved in polyp to medusa transition in *Aurelia aurita*?
- Are the mechanisms controlling the metamorphosis in *Aurelia* conserved in evolution?
- What is the nature of the strobilation inducer?
- How do the conserved signaling pathways regulate the segmentation and ephyra morphogenesis?
- What is the behavior of stage specific genes during segmentation and ephyra morphogenesis?

2 Results

2.1 Induction of strobilation in *Aurelia aurita*

2.1.1 Metamorphosis is induced by the temperature changes

In *Aurelia aurita* strain Roscoff transition from polyp to jellyfish (termed strobilation) is induced by temperature shift from +18°C to +10°C. After 3 weeks of incubation at +10°C about 25% of polyps (see Fig.15) show the first morphological sign of metamorphosis - tissue constriction below the head (see Fig.5B). Temperature shift is the only necessary manipulation to induce metamorphosis. As shown in Fig.15, timing of strobilation at a given temperature shift is highly precise with only minor fluctuations. From transplantation and feeding experiment (see Fig.6) we know that strobila segments produce diffusible temperature-labile signalling factor(s) capable to induce metamorphosis. This inductive substance is strain-specific (see Fig.8) and is present exclusively in the segmented part of the strobila (see Fig.7B).

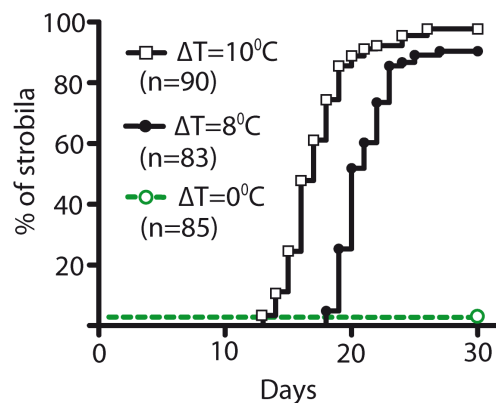


Fig. 15 Polyp-to-jellyfish transition is induced by cooling and the kinetics is dependent on the magnitude of the temperature shift. Polyps maintained at constant temperature (+18°C) do not strobilate. ΔT , temperature change; open square, cooling from +20°C to +10°C; closed circles, cooling from +18°C to +10°C; n=total number of animals in three independent experiments.

2.1.2 Uncovering the molecular cascades of strobilation

Transcriptome sequencing allowed the identification of genes with the differential expression in polyp, strobila and ephyra stages. It also gave the first insight into the signalling cascades regulating metamorphosis in *Aurelia*. Contigs where $\geq 80\%$ of reads originate from either polyp, strobila or ephyra stage were classified as stage-specific (shown in red bold font in

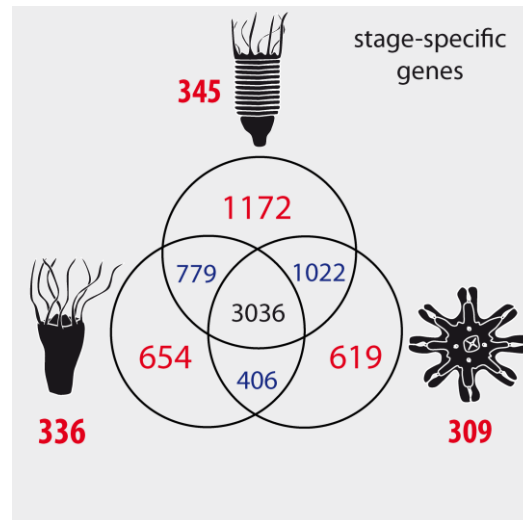


Fig. 16 Venn diagram represents the number of clusters (genes) having more than 2.5 fold up-regulation in polyp, strobila or ephyra stage (shown in red). Genes with >2.5 up-regulation in two stages (for example, polyps and strobila) are shown in blue. Number of genes with the stage-specific expression (>80% of all reads originate from either polyp, strobila or ephyra stage) are shown in red bold font. Results are shown for the clusters with the total number of reads ≥ 10 .

Fig.16). Using the threshold based on the total number of reads per contig (n_r), the stage-specific genes were identified. Values in Fig.16 are shown for $n_r \geq 10$. In all stages the proportion of stage-specific contigs (genes) ranges between 3.6% in ephyra and 4.1% in strobila, giving the mean number of stage-specific genes of about 3.9%. Venn diagram in Fig.16 represents the number of genes which are more than 2.5 fold up-regulated in polyp, strobila or ephyra. The largest number of genes (1172) is up-regulated in the strobila stage. That most probably reflects the intensive morphogenetic processes and the increase in the overall body complexity during transition from polyp to ephyra. Transcriptomes of strobila and ephyra seem to be more similar (1022 common up-regulated genes) than those of ephyra and polyp which share only 406 up-regulated genes. In about 36% of the genes (3036), expression changes throughout the life cycle do not exceed 2.5 fold.

2.1.3 Retinoic acid signaling plays a critical role in strobilation

In the *Aurelia* transcriptome, my colleagues and I identified the homologue of *RxR* nuclear hormone receptor (see also phylogenetic tree and alignment in Fig.54 in Appendix) which is highly similar to *RxR* receptors from *Tripedalia* and *Clytia*. We also identified 12 contigs encoding retinol dehydrogenases (*RDH*) (see Master theses of Simon Graspentner, 2012). Interestingly, *RxR* receptor gene as well as *RDH2* is up-regulated during strobilation, while *RDH1* is gradually down-regulated (see Fig.17A and Fig.21). RDHs convert retinol (vitamin A) into retinaldehyde which is an intermediate in the synthesis of 9-*cis* retinoic acid (RA)

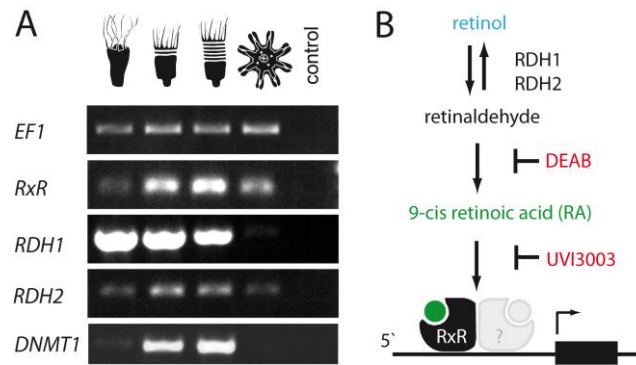


Fig. 17 (A) Retinoic X receptor (*RxR*), retinol dehydrogenase 1 and 2 (*RDH1*, *RDH2*) and *de novo* methyl transferase 1 (*DNMT1*) are differentially expressed during strobilation. *EF1 α* expression was used for equilibration. Compared stages - non-induced polyp, early strobila (1 segment), late strobila (5 segments) and ephyra. **(B) Schematic representation of the retinoic acid signalling.** Retinol is converted into retinaldehyde by retinol dehydrogenases (*RDH1*, *RDH2*). Retinoic acid binds *RxR* nuclear hormone receptor. DEAB inhibits conversion between retinaldehyde and retinoic acid. UVI3003 is a *RxR* receptor antagonist.

which activates *RxR* receptor (see Fig.17B). Up-regulation of *RxR* and *RDH2* led us to hypothesize that this retinoic acid signaling might be involved in the initiation of metamorphosis in *Aurelia* in response to temperature shift. In order to test this we performed chemical interference experiments by incubating polyps in retinol, 9-*cis* RA and retinoic acid cascade inhibitors DEAB and UVI3003. DEAB blocks aldehyde dehydrogenases which are necessary for the production of RA from retinolaldehyde (Chute, *et al.*, 2006) and UVI3003 is a highly specific antagonist of *RxR* which mimics the structure of RA and prevents *RxR* activation (Nahoum, *et al.*, 2007) (see Fig.17B). First we tested whether retinol or RA could induce strobilation in *Aurelia* without temperature shift. In support of the hypothesis, incubation of *Aurelia* polyps at +18⁰C in ASW containing 1 μ M retinol or 1 μ M RA induced strobilation after 7-12 days of incubation. As shown in Fig.18A, after 15 days about 50% of polyps convert into early strobila. Thus, retinol and RA are able to directly induce strobilation bypassing the temperature sensing step. Retinol and RA induce strobilation approximately 2 times quicker than temperature shift from +18⁰C to +10⁰C (7-12 vs. 19-21 days, see Fig.15), but about 2 times slower than transplantation or feeding of strobila rings (3 or 2 days, see Fig.6). Strobilation induction by retinol or RA is repressed in the presence of the *RxR* inhibitor (1 μ M UVI3003, see Fig.18A). In co-incubation experiments (see Fig.18A, retinol + UVI3003 or RA + UVI3003), polyps kept at +18⁰C start to strobilate after 17 days and demonstrate the same strobilation kinetics as polyps undergoing strobilation induced by incubation at +10⁰C (see Fig.15). Thus, *RxR* inhibitor (1 μ M) delays strobilation at +10⁰C for about 6 days (see Fig.18B). First strobila in the presence of UVI3003 appear after 25 days, compared to 19 days in the control and 50% strobilation is reached after 28 days compared to

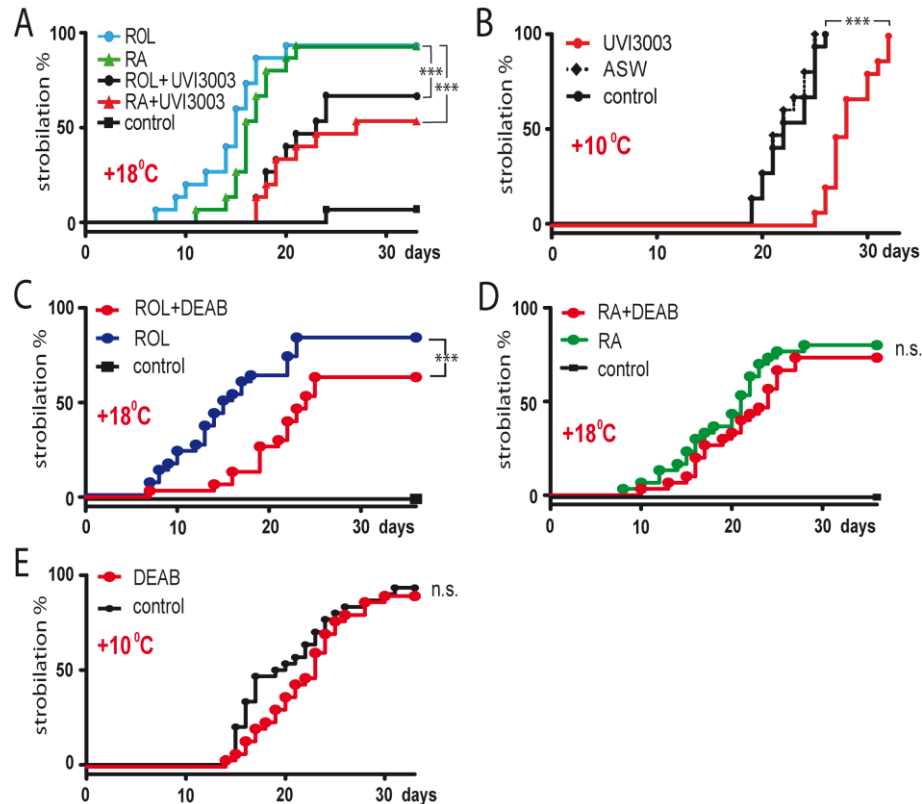


Fig. 18 Retinoic acid signalling is necessary for the metamorphosis in *Aurelia*. (A) Incubation of *Aurelia* polyps in 1 μ M solution of retinol (ROL) or retinoic acid (RA) induces strobilation without temperature shift (at +18 $^{\circ}$ C). Co-incubation of polyps in ROL or RA and 1 μ M UVI3003 slows down strobilation induction. Total number of animals in each treatment n=30. ***, log-rank (Mantel-Cox) test, p<0.0001. (B) Temperature induced strobilation is significantly slowed down in the presence of 1 μ M of RxR antagonist UVI3003. Total number of animals in each treatment n=30. ***, log-rank (Mantel-Cox) test, p<0.0001. (C) 10 μ M DEAB retards induction of strobilation by 1 μ M retinol at +18 $^{\circ}$ C. ROL, 1 μ M retinol; ROL+DEAB, 1 μ M retinol + 10 μ M DEAB; control, solvent (EtOH) in ASW. Mantel-Cox test, p<0.0001. For each treatment three independent experiments with a total number of polyps n=30 have been performed. (D) 10 μ M DEAB does not influence the activation of strobilation by *9-cis* retinoic acid (RA) at +18 $^{\circ}$ C. *9-cis* RA, 1 μ M *9-cis* retinoic acid; *9-cis* RA + DEAB; 1 μ M *9-cis* retinoic acid + 10 μ M DEAB; control, solvent (EtOH) in ASW. Mantel-Cox test, the difference is not significant (n.s.). For each treatment three independent experiments with a total number of polyps n=30 have been performed. (E) 10 μ M DEAB does not repress the activation of strobilation by temperature shift. DEAB, 10 μ M DEAB; control, solvent (EtOH) in ASW. Mantel-Cox test, the difference is not significant (n.s.). For each treatment three independent experiments with a total number of polyps n=30 have been performed.

22 days in control (see Fig.18B). DEAB, which prevents conversions of retinaldehyde into RA (see Fig.17B), slows down strobilation in animals incubated in retinol (see Fig.18C), but does no influence strobilation in polyps incubated in RA (see Fig.18D). Interestingly, DEAB does not inhibit normal temperature-induced strobilation at +10 $^{\circ}$ C (see Fig.18E).

Taken together, these data show that retinoic acid signalling is important for the induction of strobilation and the addition of retinol or RA can completely substitute the temperature shift

which is necessary for strobilation under natural conditions. However, retinol and RA, even in their highest non-toxic concentrations (5 μ M) are not able to induce strobilation within 48 hours like it happens when polyps are fed with strobila segments. This fact indicates that RA is an important, but not the only signaling molecule necessary to induce strobilation. The RA may be referred to as "slow" inducer, which presumably works cooperatively with a "quick" inducer whose presence is strongly indicated by the result of the feeding experiments.

2.1.4 Candidate strobilation genes

From microarray experiment (see Fig.13), three candidate genes (*CL390*, *CL112* and *CL631*) had been selected and their expression pattern in different stages during strobilation have been examined (see Fig.14). All these genes encode proteins without similarity to any known proteins from other animals (BLASTP e-value < 1e-5). Thus, most probably they represent Scyphozoa-specific or even *Aurelia*-specific genes. The common feature of *CL390*, *CL112*



Fig. 19 Putative protein structures of CL390, CL112 and CL631. Signal peptide sequence is shown in red, internal repeats as gray boxes and EGF-like domain of CL112 in light blue.

and *CL360* is the presence of a putative signal peptide sequence at the N-terminus (see Fig.19). *CL390* protein consists of two qualitatively different regions - N-terminal part contains a large proportion of hydrophobic amino acids, while C-terminal part is highly charged and is made of unusual arginine rich repeats with the general motive RRRxxRRR or RRRxxxRRR and several WS and SF repeats (see Fig.20A). *CL112* has a domain containing 6 cysteine residues with low similarity to EGF ($E=1e-2$) (see Fig.20B). *CL631*, similar to *CL390* contains a large proportion of hydrophobic amino acids in its' N-terminal part and three repeats separated by the putative endopeptidase processing sites KR and KK (see Fig.20C).

CL390, *CL112* and *CL631* encode novel secreted proteins which might serve as precursors for epithelial peptides. Taking into consideration their expression dynamics they all might be considered as potential strobilation inducers of *Aurelia*. However, as shown by 454 sequencing, microarray data and *in situ* hybridization, *CL631* is strongly expressed in strobila

A. CL390

```

1  MKVLSILILI GLSVFSCAAT KDAEEKITKD AIRTAGATIE PVESDSDEPE QDQDESEEEP
61  NEAESTSDDQ DEESSATTEA SSDPIFWRRR STRRRCYEAR RRYIARRRYI ARRCYRRRS
121 FRRRLSFRRR WSRRLWLRRR FSYRRRWSRR RSLRRRFSFR RRG

```

B. CL112 EGF-like domain

```

1  MDANRAILAL VLICSLIQSA SLEKSQPIQT ETGGGDCIDN DDCANNIGCR IEKKSKEKGG
61  CNCFVGFTKP NCDAESKVKK LEPGVKGVKAV RRNHIHRHES ASKRYETGSG SYESASKSDE
121 TGSERNLEYD PASDIFGLTP KNLADSGQEF LIYNPDKKVF LRVSKDIKAT GKRMPYIEAR
181 GDRAGLRNIF TFMKVPQDQ KYYIKNKDTN KFLYVSNSKS GFIKYWNNV LGADSVATDD
241 SKTKYIFEFV DEDGDGFYEI KNQKSFYVS SHMLGIPMYR LVKATDQKEL ERWNSQFFQF
301 VLKDKAKAVK FATKGEPRKR LQTVIDAGQS SKSCNKGKSK TDKEDDVQIQ YKETNTETRT
361 YTQTHGFTFN GKLPDPFGGM SFTYSNTQAT QEANTKTKEL TRTVGIKVPV NRCACITISY
421 KAVEYDQDYE VTATSKEGKD LKATGQVKG T SRGEFEVHKK MFNYKDNFKC PYEK

```

C. CL631

```

1  MRAFITALLL FSVLCALPCV MCEEDESETK NEKDEDEVSR YKDEDEVSRV REEDASDAEL
61  EDVSSAAKRS EEEEDAKPFL NFNLRRLRRRL LPHTKDVSSA AKRSEEEEDA KPFLNFLNRR
121 RRRLLPHTKD VSSAAKRSEE EEDAKPFLNF LNRRLRRLLS HTKDVSGAAK RSQ

```

Fig. 20 Putative protein sequences of CL390, CL112 and CL631. (A) Amino acid sequence of CL390. Arginine repeats are highlighted in gray. Cysteine residues are shown in red. The putative signal peptide sequence is underlined. (B) Amino acid sequence of CL112. EGF-like domain is highlighted in blue. (C) Amino acid sequence of CL631. Predicted signal peptide sequences are underlined. Black arrowhead, putative signal peptide cleavage site. Cysteines are highlighted in red. Putative peptidase processing sites in CL631 are highlighted in yellow.

segments as well as in developing and freely swimming ephyra. Exclusive expression in strobila rings corresponds well to the hypothetical distribution of strobilation inducer which has been deduced from feeding and transplantation experiments. However, feeding polyps with ephyra does not induce strobilation. Hence, large amounts of *CL631* transcript in ephyra (if the expression can be taken as a proxy for the abundance of the corresponding protein) speaks against its` role as strobilation inducer. *CL112* exhibits very similar expression dynamics to that of *CL631*. The only difference is that *CL112* is highly up-regulated before the onset of segmentation and positive cells are located in non-segmented part of strobila. *CL112* also has a considerable level of expression in developing and freely swimming ephyra and, thereby, does not completely fulfil the criteria for being a strobilation inducer. It is not possible to exclude the chance that the strobilation inducer of *Aurelia* is a mixture of several molecules with overlapping expression domains. However, if to assume that the strobilation inducer of *Aurelia* is encoded by a single gene, *CL390* seems to be the most probable candidate. This gene is not expressed in polyps, is strongly up-regulated in strobila and the expression is drastically down-regulated in the ephyra stage.

2.1.5 Temperature dependent "timer" for the onset of metamorphosis

According to microarray data, transcript levels of *CL390*, *CL112* and *CL631* are steadily increasing during the temperature induction. Most probably, by incubating polyps at +10⁰C,

we mimic a winter period when the water temperature slowly decreases and then rises again in spring. It is clear that the metamorphosis controlling system has to distinguish winter from any short term temperature fluctuations (day / night cycle and periods of cold weather in summer and fall). Thus, there must be a minimal duration of the "cold" period which should cause metamorphosis and any shorter period should be referred to as weather fluctuation and accordingly ignored. Hence, genes involved in strobilation control must respond to changes in temperature and their expression dynamics must be dependent on the magnitude and duration of the temperature shift.

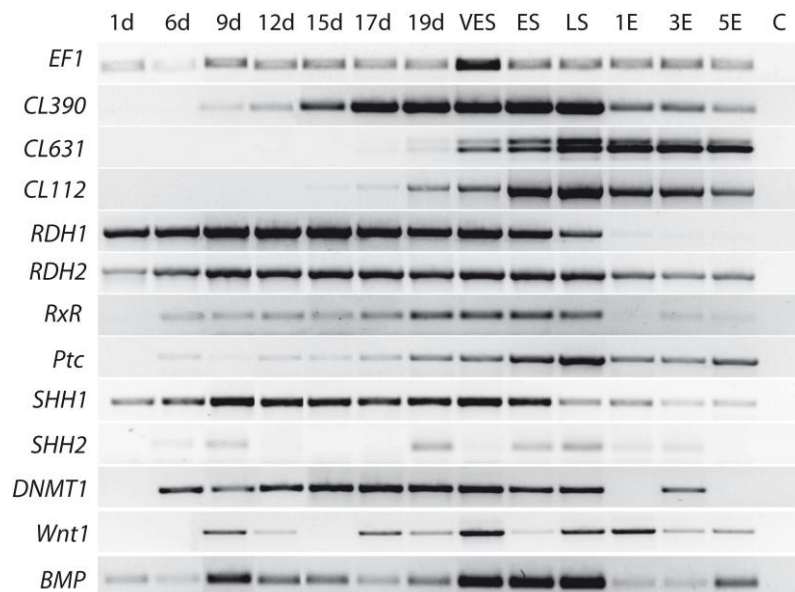


Fig. 21 RT-PCR shows expression of selected genes during the induction of strobilation at +10⁰C. 1d - non-induced polyp, 6d - 19d - polyps incubated at +10⁰C for 6-19 days, VES - very early strobila, ES - early strobila, LS - late strobila, 1E - 5E - detached ephyra for 1-5 days. *EF1* - elongation factor 1-alpha, *RDH1/2*, retinol dehydrogenase 1 and 2; *RxR*, retinoic X receptor; *Ptc*, patched; *SHH1/2*, sonic hedgehog 1 and 2; *DNMT1*, *de novo* methyl transferase 1, *BMP*, bone morphogenetic protein.

Based on this assumption, the expression of *CL390*, *CL112* and *CL631* during the process of temperature induction was examined (see Fig.21) and the minimal duration of the cold period which is sufficient to induce metamorphosis was identified (see Fig.22). As shown in Fig.21, *CL390*, *CL112* and *CL631* respond to the temperature change and the increase in their transcript levels occurs much earlier than the onset of segmentation. The most intriguing dynamic is typical for *CL390*. While *CL112* and *CL631* are highly up-regulated only after 17 days or 19 days, *CL390* is up-regulated already after 9 days of incubation at +10⁰C.

In parallel to the induction experiment, the minimal duration of the cold period needed to induce strobilation was determined. As shown in Fig.22 (inset) and Fig.23, in the course of

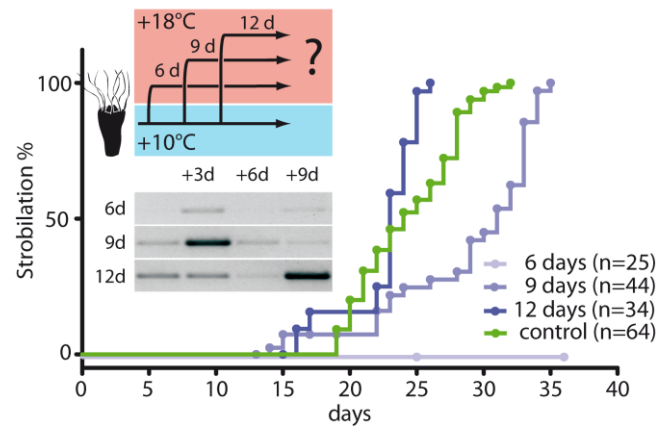


Fig. 22 Minimal duration required for the temperature induction. Polyps were incubated at $+10^{\circ}\text{C}$ for 6, 9, 12 days and then transferred back to $+18^{\circ}\text{C}$. Strobilation curves and *CL390* expression levels after 3, 6 and 9 days (+3d, +6d, +9d in the insert) are shown. Control - polyps continuously incubated at $+10^{\circ}\text{C}$.

the temperature induction, groups of polyps were returned back to $+18^{\circ}\text{C}$ after 6, 9, and 12 days of incubation. mRNA was extracted from these polyps after 3, 6 and 9 days (see insert in the Fig.22 and Fig.23) and the rate of metamorphosis in each group was recorded. Interestingly, none of the polyps which stayed at $+10^{\circ}\text{C}$ for just 6 days undergo strobilation, while the period of 9 days at $+10^{\circ}\text{C}$ is enough to induce strobilation in Roscoff strain of *Aurelia*. In that case, however, the slope of strobilation curve is significantly shallower than in the control group (continuous incubation at $+10^{\circ}\text{C}$). In this group, strobilation is considerably delayed with 50% rate been reached only after 32 days compared to 24 days in the $+10^{\circ}\text{C}$ control. Animals kept at $+10^{\circ}\text{C}$ for 12 days show the same strobilation kinetics as the control group which remained all the time at $+10^{\circ}\text{C}$. Earlier appearance of strobila in the 12 day group is explained by the fact that segmentation in induced polyps is a temperature dependent process and proceeds quicker at $+18^{\circ}\text{C}$ than at $+10^{\circ}\text{C}$. Expression dynamics of *CL390* in the

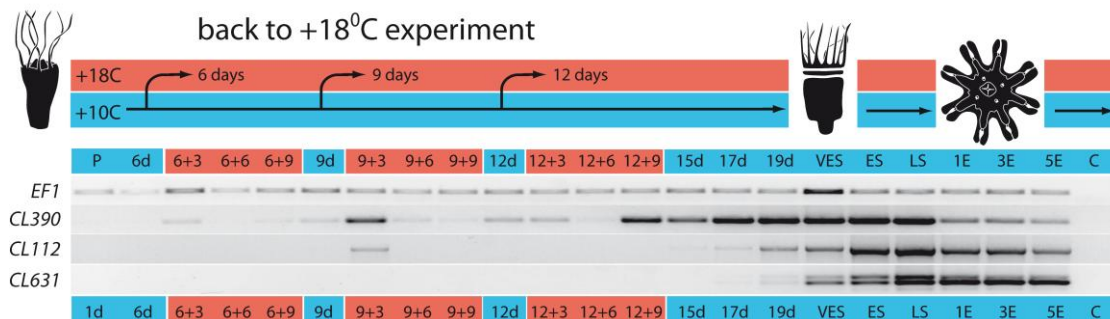


Fig. 23 Expression of *CL390*, *CL112* and *CL631* during strobilation induction. Dishes with polyps were transferred to $+10^{\circ}\text{C}$ and then groups of polyps were returned back to $+18^{\circ}\text{C}$ after 6, 9 and 12 days of cold treatment. *CL390* is up-regulated by cooling and exhibits oscillations after polyps were returned to $+18^{\circ}\text{C}$. Amount of cDNA across the samples was equilibrated with *elongation factor 1-alpha* (*EF1*).

polyps returned back to $+18^{\circ}\text{C}$ after 3, 6 and 9 days of cooling shows intriguing oscillations (see inset in Fig.22 and Fig.23). In the first group (6 days as $+10^{\circ}\text{C}$) transcript level initially increases (+3d), then decreases (+6d) and slightly increases again (+9d) with the second expression peak being weaker than the first one. In the second group (9 days at $+10^{\circ}\text{C}$) expression of *CL390* strongly increases after 3 days and then decreases after 6 days and 9 days. In the third group (12 days as $+10^{\circ}\text{C}$) the expression is initially high, decreases after 6 days and strongly increases after 9 days. Taken together, expression of *CL390* after returning to $+18^{\circ}\text{C}$ seems to behave like a temperature dependent oscillator where the magnitude and phase of fluctuations are dependent on the duration of the cold period.

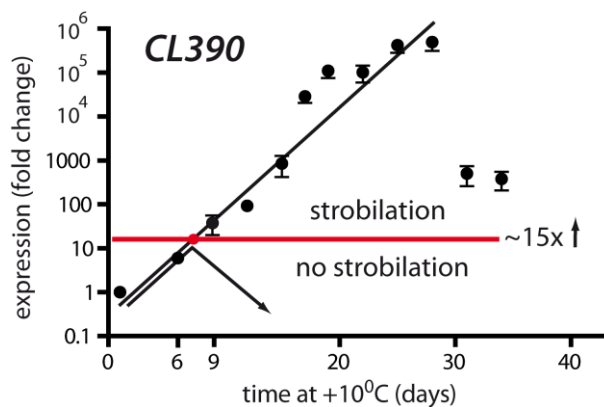


Fig. 24 *CL390* expression is exponentially increased at $+10^{\circ}\text{C}$. Between 6 and 9 days the decision to strobilate is made (horizontal red line). qRT-PCR results, mean values of three independent experiments \pm SD.

Detailed analysis of *CL390* expression by real-time PCR (see Fig.24) indicates that at $+10^{\circ}\text{C}$ the amount of transcript increases exponentially with mean up-regulation of 5.5x after 6 days, 31x after 9 days, 81x after 12 days and 110.000x after 19 days. From the analysis of strobilation kinetics (see Fig.22) we know that 6 days of incubation at $+10^{\circ}\text{C}$ are not enough to induce strobilation, but 9 days are sufficient. Therefore, as soon as the up-regulation exceeds the threshold of about 15 folds, the strobilation program is activated, becomes self-sustainable and independent from the further temperature input (see Fig.24).

Analysis of the expression dynamics indicates that the amount of *CL390* transcript is positively and directly correlated with the amount of time spent by *Aurelia* polyps at low temperature. Thus, the outcome of a temperature induction experiment can be reliably predicted by just monitoring the expression level of *CL390* without knowing the actual duration of the cold exposure. *CL390*, thereby, represents an example of a novel temperature dependent timer, which records the duration of the cold period. On the cellular level, cooling

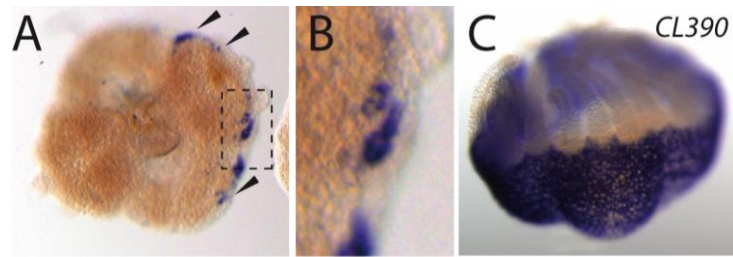


Fig. 25 Expression of *CL390* during induction by low temperature. (A) At +10⁰C, groups of *CL390* positive epithelial cells appear, increase in their size and number. (B) Close up of the area boxed in (A). (C) Several hours before the appearance of the first constriction all ectodermal cells of the polyp are *CL390* positive. Black arrowheads - groups of *CL390* positive cells.

activates the expression of *CL390* in the groups of ectodermal epithelial cells which initially form small patches (see Fig.25) and then increase in their number and grow in size. Finally, several hours before the segmentation process start, all ectodermal epithelial cells of a polyp (except once in the tentacles and in the foot) become *CL390* positive (see Fig.25C).

2.1.6 *CL390* as strobilation inducer

Involvement of *CL390* in strobilation is further supported by its expression dynamics and transcript distribution in transplantation and feeding experiments (see Fig.26). As described previously (see Fig.6), these manipulations induce strobilation in 72 and 48 hours respectively. As shown by *in situ* hybridization in Fig.26A, transplantation of strobila segments induces local up-regulation of *CL390* in the region adjacent to the transplant (see dotted line in Fig.26A). A patch of *CL390* expressing cells surrounds the area where the transplant was located (transplanted strobila tissue has been detached from the recipient animal prior to fixation). In the feeding experiments, *CL390* is systemically and strongly up-regulated in all ectodermal epithelial cells throughout the polyp body within 24 hours (see Fig.26B).

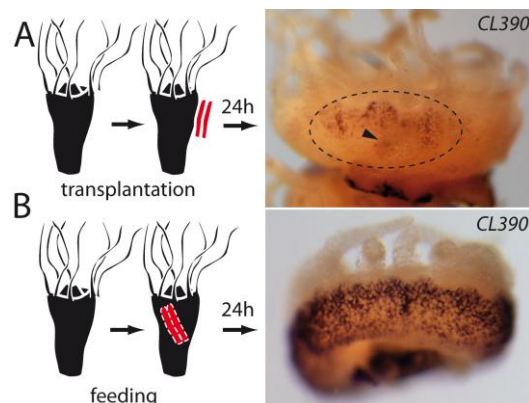


Fig. 26 Expression dynamics of *CL390* in transplantation and feeding experiments. (A) *CL390* is locally up-regulated in recipient polyp at the site of strobila tissue transplantation. dotted line, the area of the tissue contact between polyp and transplant; arrowhead - hole from the fishing line used during transplantation. (B) *CL390* is systemically up-regulated 24h after feeding.

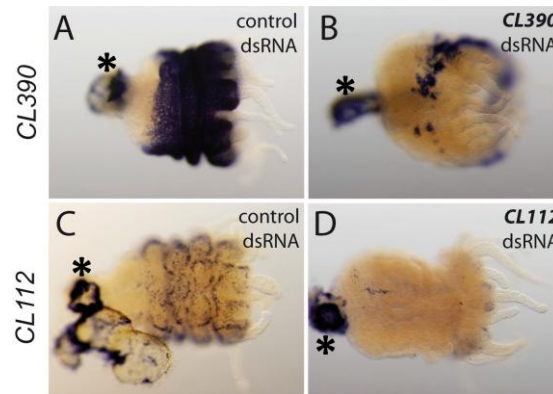


Fig. 27 RNAi by electroporation. (A) Electroporation of *GFP* dsRNA does not influence the expression of *CL390*. (B) After the electroporation with *CL390* dsRNA, expression of *CL390* is strongly down-regulated and remains only in several patches of the ectodermal cells. (C) Electroporation of *GFP* dsRNA does not influence the expression of *CL112*. (D) After the electroporation with *CL112* dsRNA, expression of *CL112* is strongly down-regulated. *, unspecific staining of the foot (probe is sticking to podocyst)

Finally, to examine the influence of *CL390*, *CL112* and *CL631* on induction of strobilation, I developed RNAi technology for *Aurelia*. As shown in Fig.27, by electroporating early strobila with dsRNA of *CL390* or *CL112*, the expression of the corresponding genes can be repressed. Electroporation of control dsRNA (*GFP* or *CL1008*) does not influence gene expression (see Fig.27A, C). To test the function of genes potentially involved in strobilation, induced polyps (incubated at +10°C for 6 days) with dsRNA of *CL1008* (ephyra-specific gene used as a control), *CL390*, *CL112* and *CL631* were electroporated. As shown in Fig.28, no difference in strobilation kinetics between animals electroporated with *CL1008*, *CL631* and *CL112* is observed. In contrast to that, animals electroporated with *CL390* dsRNA strobilate considerably slower than the control animals (*CL1008*). These results, therefore, clearly indicate that *CL390* is involved in strobilation in *Aurelia* and might represent the strobilation inducer.

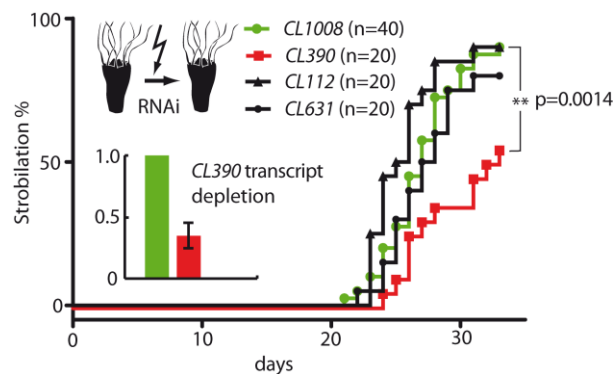


Fig. 28 Influence of *CL390*, *CL112* and *CL631* knock-downs on the temperature-induced strobilation. dsRNA of *CL1008* (ephyra-specific gene) was electroporated as control. Expression of *CL390* is down-regulated for about 60% (qRT-PCR data \pm SD in the insert). n = total number of electroporated polyps in three experiments. Strobilation curves compared by Log-rank (Mantel-Cox) test ($p=0.0014$).

2.1.7 Promoter analysis of *CL390*

As described above, retinoic acid signaling pathway plays a critical role in the induction of strobilation. *CL390* is a temperature dependent timer and might be the strobilation inducer. The results of RT-PCR (see Fig.21) show that *RxR* is up-regulated earlier than *CL390*. This led me to hypothesize that the expression of *CL390* might be regulated by the retinoic acid signaling pathway. In order to test this, the promoter of *CL390* was isolated by splinkerette

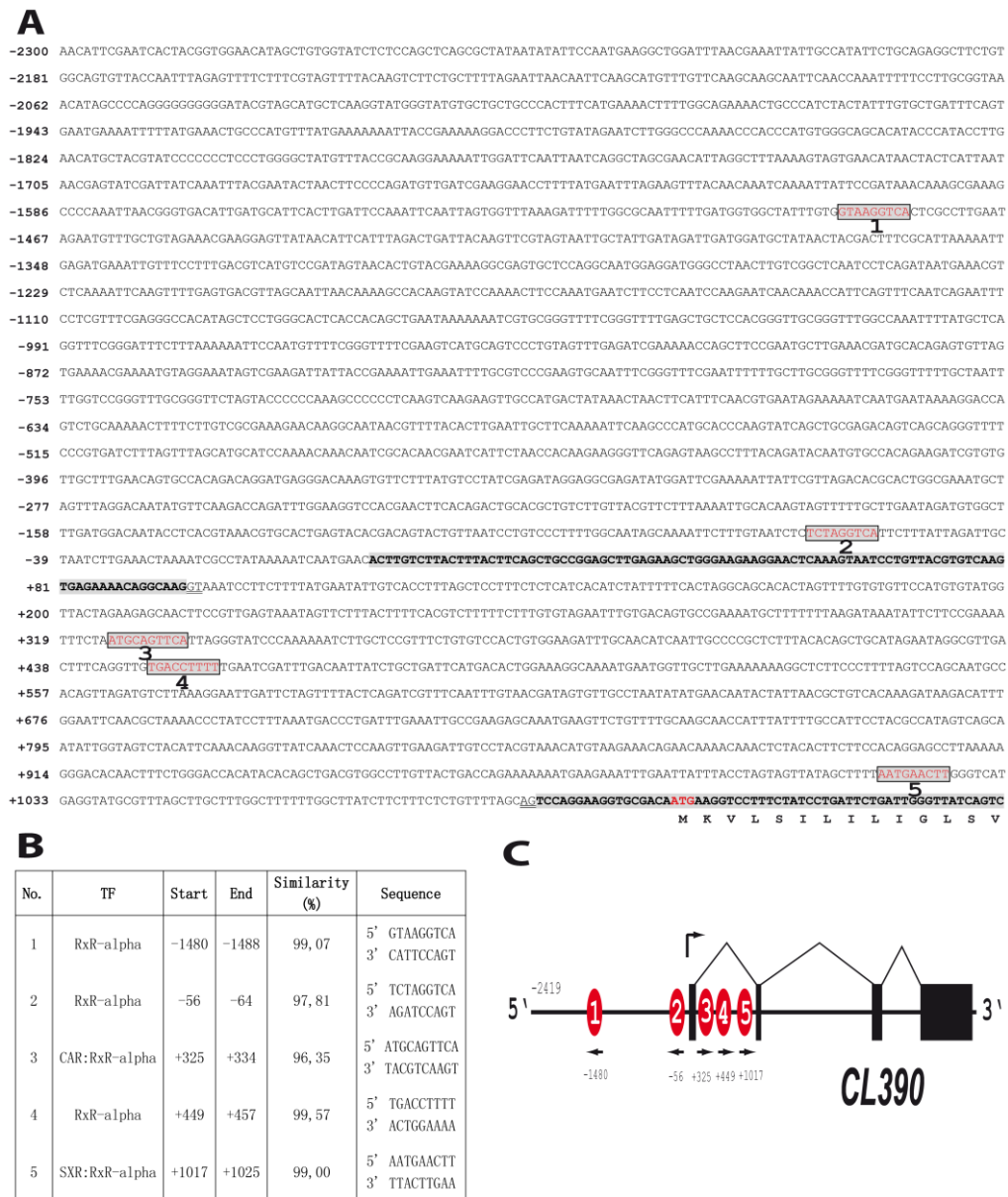


Fig. 29 Promoter and the first intron of *CL390* contain three high score binding sites for RxR receptor. (A) Sequence of 2300bp of the *CL390* 5' flanking region. RxR binding sites are boxed and numbered. Exon sequences are highlighted in gray. Splice donor and acceptor sites are underlined. Start codon (ATG) is shown in red. (B) Positions and sequences of the RxR, CAR:RxR and SXR:RxR binding sites. (C) Putative binding sites for CAR:RxR and SXR:RxR are present in the first intron of *CL390*. 1, 2, 4 - RxR binding sites; 3, 5 - CAR:RxR and SXR:RxR binding sites. CAR, constitutive androstane receptor; SXR, steroid and xenobiotic receptor.

PCR approach (see Methods 5.4). As shown in Fig.29, ConSite program (<http://www.phylofoot.org/consite>, Sandelin *et al.*, 2004) detects five putative high affinity binding sites for RxR nuclear hormone receptor in the close proximity to the CL390 coding region. Among them, two RxR sites are located in the 5' flanking region and another one is located in the first intron. Two additional putative sites for CAR:RxR-alpha and SXR:RxR-alpha heterodimers are located in the first intron of *CL390* (see Fig.29). Thereby, *CL390* might be the direct target gene of the retinoic acid signalling pathway.

2.1.8 Strobilation inducers in *Aurelia*

2.1.8.1 Recombinant CL390, CL112 and CL631 proteins

To directly test the function of CL390, CL112 and CL631 in strobilation, recombinant proteins fused to GFP were produced in *E. coli* Rosetta 2(DE3)pLysS cells (see Method 5.8) and purified by Ni-NTA chromatography. Protein yield and purify were checked by SDS-PAGE and Western blots (see Fig.30B). During expression, GFP-CL390 behaves very differently to the other proteins. The bacteria containing *pET-28a(+)-GFP-CL390* construct

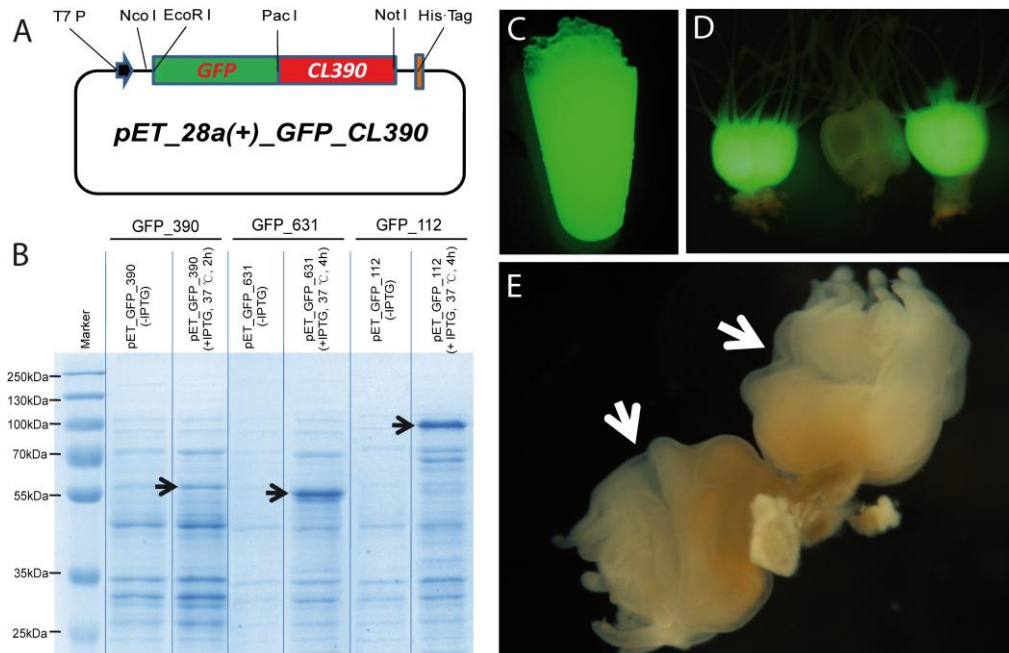


Fig. 30 Recombinant protein expression, purification and feeding. (A) Map of the *pET-28a(+)-GFP-CL390* construct used for the production of recombinant GFP-CL390 protein. (B) Expression of recombinant proteins, SDS-PAGE. (C) His-Tag purified recombinant GFP-CL390 protein in 10% gelatine matrix. (D) *Aurelia* polyps two hours after feeding them with 10% gelatine mixed with GFP-CL390 protein. Polyp in the middle was fed with 10% gelatine. (E) Polyps were fed once per day with GFP-CL390 recombinant protein in 10% gelatine. Control polyps were fed with recombinant GFP. After 72 hours constriction developed below the head of the polyps fed with GFP-CL390.

cannot reach a high optical density ($OD_{600} < 1.0$) after IPTG induction. After purification, I got relatively small amounts of GFP-CL390 recombinant protein compared to the others.

Purified recombinant proteins were desalted with Amnicon[®] Ultra Centrifugal Filters (Millipore) and mixed with gelatin (see Fig.30C). Gelatin cubes containing recombinant proteins were fed to the polyps (see Fig.30D). Alternatively, proteins were directly diluted in ASW for incubation experiments. Feeding or incubation with CL390 causes formation of segment-like constriction below the head of *Aurelia* polyps (see Fig.30E), but segmentation does not progress further. CL112 and CL631 proteins do not cause any physiological changes.

2.1.8.2 Synthetic peptides

CL390 encodes a secreted protein with an unusual C-terminal part where arginine repeats separate di- and tri-peptides with the sequences SF, LSF, WS, WL, FSY, WS, SL and FSF (see Fig.31A). It is possible that not the whole protein but its part induces strobilation. To test this the peptides representing sub-fragments of CL390 were synthesized, and used in incubation experiments (see Fig.31B). A synthetic peptide with the sequence WSRRRWL induces strobilation within 72 hours of incubation at +18⁰C (see Fig. 33). Other tested peptides (see Fig.31B) do not induce strobilation. This result indicates that CL390 might be the precursor of the strobilation inducer which becomes biologically active after being

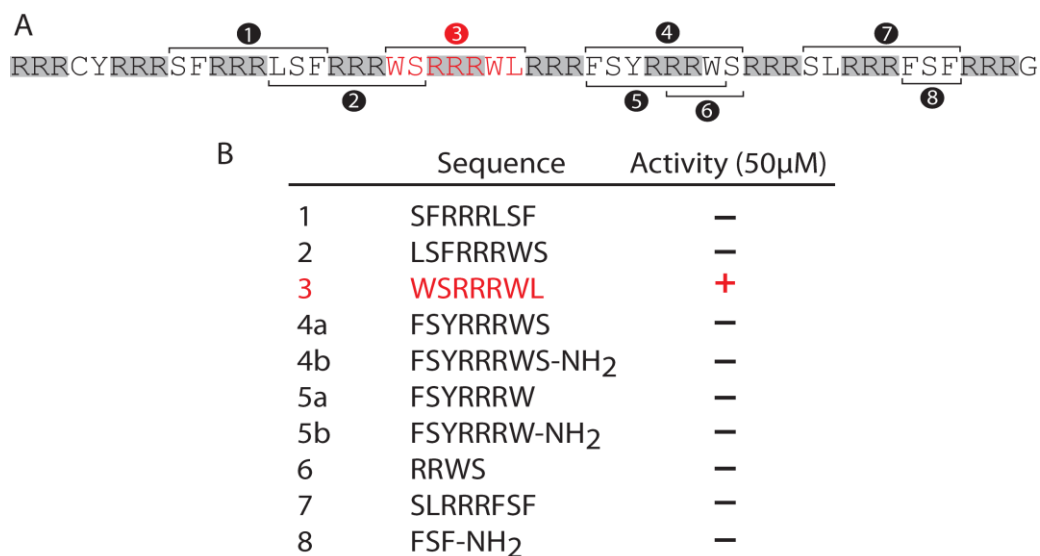


Fig. 31 Synthetic peptides. (A) C-terminal part of CL390 protein. Synthetic peptides are highlighted by brackets (1-8). Active fragment is shown in red. (B) Sequences of synthetic peptides used in incubation experiments. Peptides were diluted in DMSO and polyps were incubated in 50 μ M peptide solution.

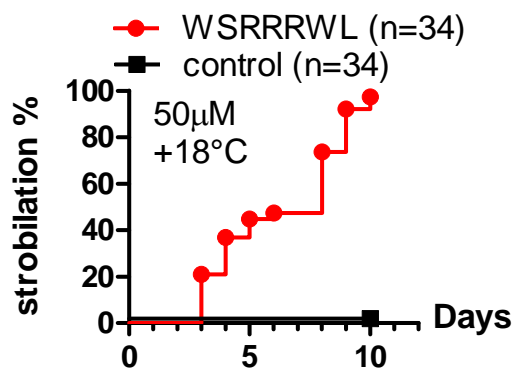
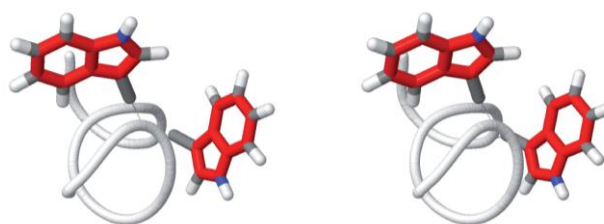


Fig. 32 Strobilation is induced by WSRRRWL peptide. control, DMSO incubation. n=total number of polyps incubated.

processed into smaller fragments. According to *in silico* structure prediction, indole rings of two tryptophans in WSRRRWL peptide are located in close proximity in mutually perpendicular planes (see Fig.34).



<http://bioserv.rpbs.univ-paris-diderot.fr/PEP-FOLD/>

Fig. 33 Structure of the RRWSRRRWL peptide was predicted using PEP-FOLD server (Maupetit *et al.*, 2009; <http://bioserv.rpbs.univ-paris-diderot.fr/PEP-FOLD/>). 3D structure was visualized using JMOL 13.0.4.

2.1.8.3 Chemical inducers

As shown in Fig.34, according to *in silico* structure prediction, C-terminal part of CL390 forms a helix where aromatic amino acids separated by three arginins are located in the close

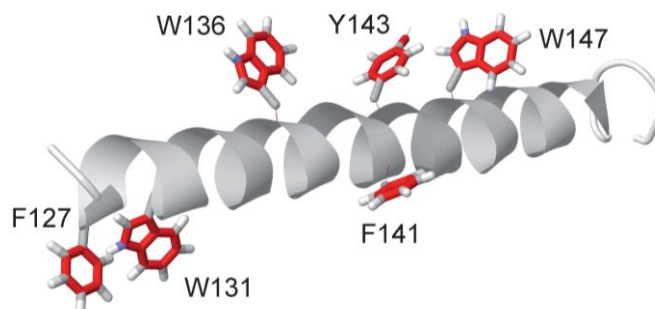


Fig. 34 Predicted structure of the C-terminal part of CL390. Aromatic rings are highlighted in red.

proximity to each other (F127 - W131 and Y143 - W147). Such a close positioning of the aromatic rings is similar to the core part of the indole derivative indomethacin (see Fig.35) which has been recently shown to induce strobilation in the Japanese strain of *Aurelia aurita* (Kuniyoshi *et al.*, 2012). Indomethacin is an anti-inflammatory drug which functions via inhibition of cyclooxygenases (COX1/2) (Weigert, *et al.*, 2008). In *Aurelia aurita* as well as in the genomes of *Nematostella*, *Hydra* and *Acropora* clear homologs of *COX-1* and *COX-2* are not present. Thus, in light of the observations described above, inductive activity of indomethacin might be explained by its structural similarity to the naturally occurring strobilation hormone of *Aurelia* encoded by *CL390*.

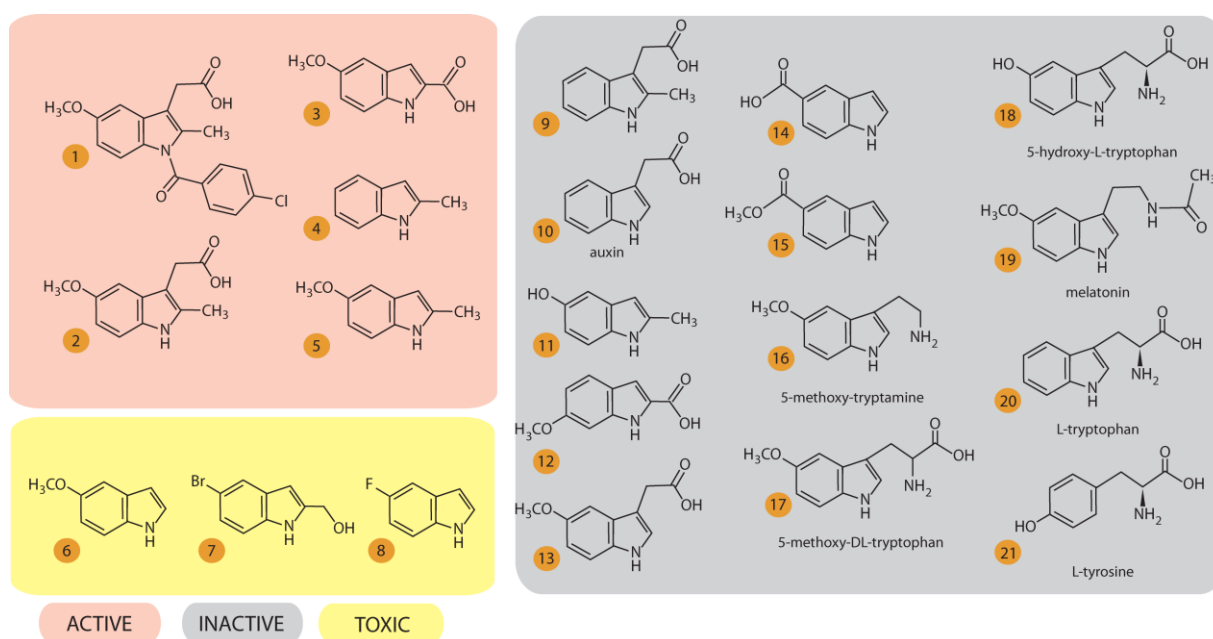


Fig. 35 Indole and tryptophan derivatives tested for their strobilation induction activity. IUPAC names and Sigma-Aldrich catalogue numbers are listed in the Table 18. Chemicals are grouped in three categories - active, toxic, inactive. Tests were performed using polyps of the Roscoff strain and 50 μ M solution of the chemicals.

In order to identify the minimal pharmacophore able to activate strobilation I further screened indole and tryptophan derivatives and identified four substances with a strong capacity to induce strobilation at 50 μ M (see Fig.35 and Table 18 for the complete list of compounds tested). As shown in Fig.36A, all the active compounds share core structure made by indole ring and methyl or carboxylic groups at the position two. Despite of the high structural similarity, compounds (1)-(5) are characterized by drastically different inductive capacities in Roscoff strain of *Aurelia* (see Fig.36B). Indomethacin induces strobilation only after 6 days of incubation; 5-methoxy-2-methylindole acetic acid (2) and 5-methoxyindole-2-carboxylic acid (3) after 4-5 days; 2-methylindole (4) after 3 days and 5-methoxy-2-methylindole (5) within

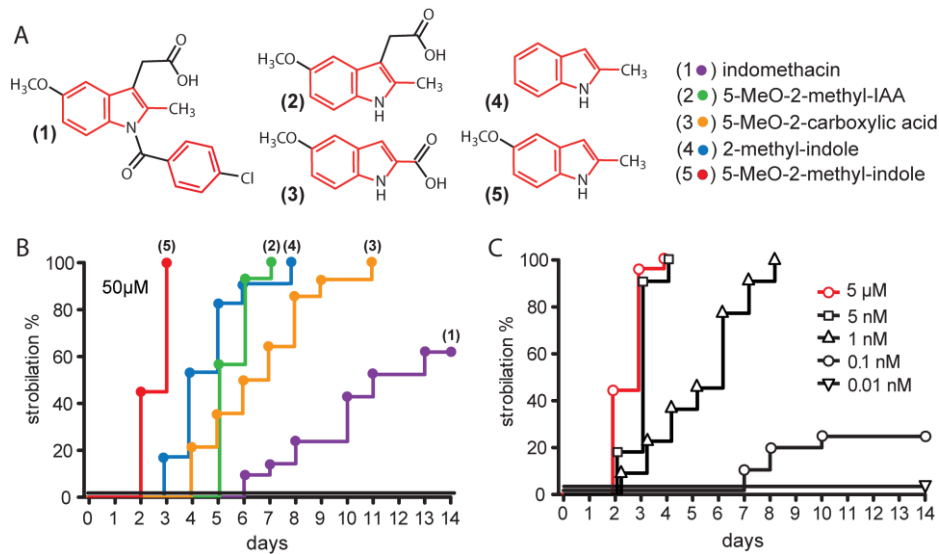


Fig. 36 Chemical induction of strobilation. (A) Chemical inducers of strobilation. Aromatic rings highlighted in red. (B) Strobilation curves in 50µM solution of indomethacin (1), 5-methoxy-2-methyl indole acetic acid (2); 5-methoxy-2-cyrbohylic acid (3); 2-methyl indole (4); 5-methoxy-2-methyl indole (5).(C) Strobilation curves at different concentrations of 5-methoxy-2-methyl indole.

48 hours. Interestingly, 5-methoxy-2-methylindole at concentration of 50µM induces strobilation with the identical kinetics as feeding with strobila rings. Inductive capacity of 5-methoxy-2-methylindole remains identical within the concentration range between 50µM and 5nM, spanning four orders of magnitude (see Fig.36C). Even at the concentration of 1nM strobilation is induced after 48 hours and 100% of the incubated polyps will start to metamorphose within 8 days. Only at a concentration of 0.1nM the inductive effect is considerably reduced and is completely absent at concentration of 0.01nM.

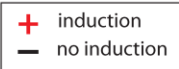
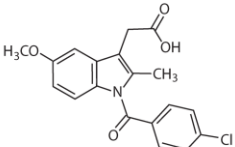
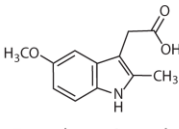
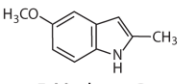
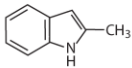
Aurelia strain				
	 indomethacin	 5-methoxy-2-methyl-3-indoleacetic acid	 5-Methoxy-2-methylindole	 2-methylindole
Roscoff	+	+	+	+
Baltic sea	-	+	+	+
White sea	-	-	+	+

Fig. 37 Aurelia strains vary in their response to chemical inducers. 5-methoxy-2-methylindole and 2-methylindole are able to induce strobilation in all three strains tested. 50µM solutions of chemicals were used.

It is interesting that *Aurelia* strains vary in their response to chemical inducers (see Fig.37). So far, three genetically different lines of *Aurelia* (Roscoff, Baltic sea and White sea strains) originating from geographically distant locations were tested (see Fig.3). Indomethacin

induces strobilation only in Roscoff strain (and Japanese animals as reported by Kuniyoshi *et al.*, 2012). 5-methoxy-2-methylindole acetic acid induces Roscoff and Baltic sea strains, but not the White sea animals. Only 5-methoxy-2-methylindole and 2-methylindole are able to induce strobilation in all three animal lines, being the universal chemical inducers. This observation strongly parallels the results of the feeding experiments (Fig.6E-H) where strobila rings of Roscoff strain fed to Roscoff polyps induce their strobilation within 48 hours, but will never induce strobilation in the Baltic sea or White sea polyps (Fig.8). Taken together, *CL390* gene appears to encode the precursor of the strobilation hormone in *Aurelia aurita* and 5-methoxy-2-methylindole may represent the minimal pharmacophore with the highest inductive capacity. My data also imply that the natural inducers vary in their structure among different *Aurelia* strains.

2.2 Strobilation inhibitors in *Aurelia*

2.2.1 Synthetic peptides

The peptide WSRRRWL has the ability to activate strobilation. Structurally, this peptide has two aromatic amino acids separated by several other residues which are located in the close proximity to each other (see Fig.33). This type of the structure might be necessary for the receptor binding. Thus, synthetic peptides with the similar structure, but with another combination of aromatic amino acids might also bind to the receptor. I noticed that CL390 protein contains several such peptides in its sequence. Such peptides might bind to the receptor but instead of activating it might function as antagonists.

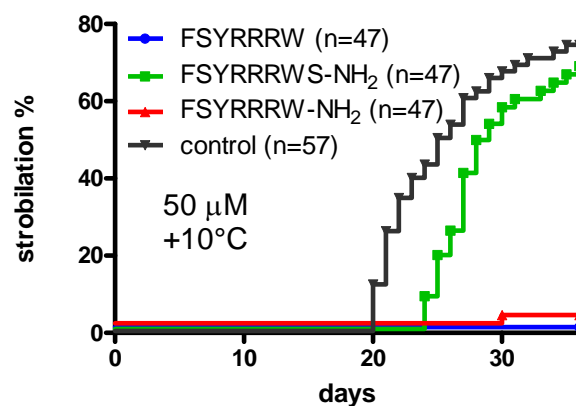


Fig. 38 Strobilation is inhibited by FSYRRRW and FSYRRRW-NH₂ peptides. No inhibition in FSYRRRWS-NH₂ peptide. control, DMSO incubation. n=total number of polyps incubated.

In order to test this idea, the influence of the synthetic peptides 1, 2, 4a, 4b, 5a, 5b and 7 (see Fig.31B) on strobilation has been examined. Polyps were kept at +10°C in the 50µM solutions of these peptides. Interestingly, polyps never strobilate in the presence of the peptides FSYRRRW and FSYRRRW-NH₂ (see Fig.38). This result indicates that CL390 might also be the precursor of the strobilation inhibitor. Most probably the structures of these two peptides are nearly the same as WSRRRWL (indole ring of tryptophan and benzene ring of tyrosine are also located in close proximity). It is also important to mention that in the solution of FSRRRWS-NH₂ peptide which has just one additional serine residue at the C-terminal, the animals can strobilate normally (see Fig.38).

2.2.2 Chemical inhibitor

The core part of the chemical strobilation inducers is an indole ring with different functional groups. Among all the chemical compounds tested (see Fig.35), only five molecules have the ability to induce strobilation (see Fig.36). The others have similar structures, but were inactive.

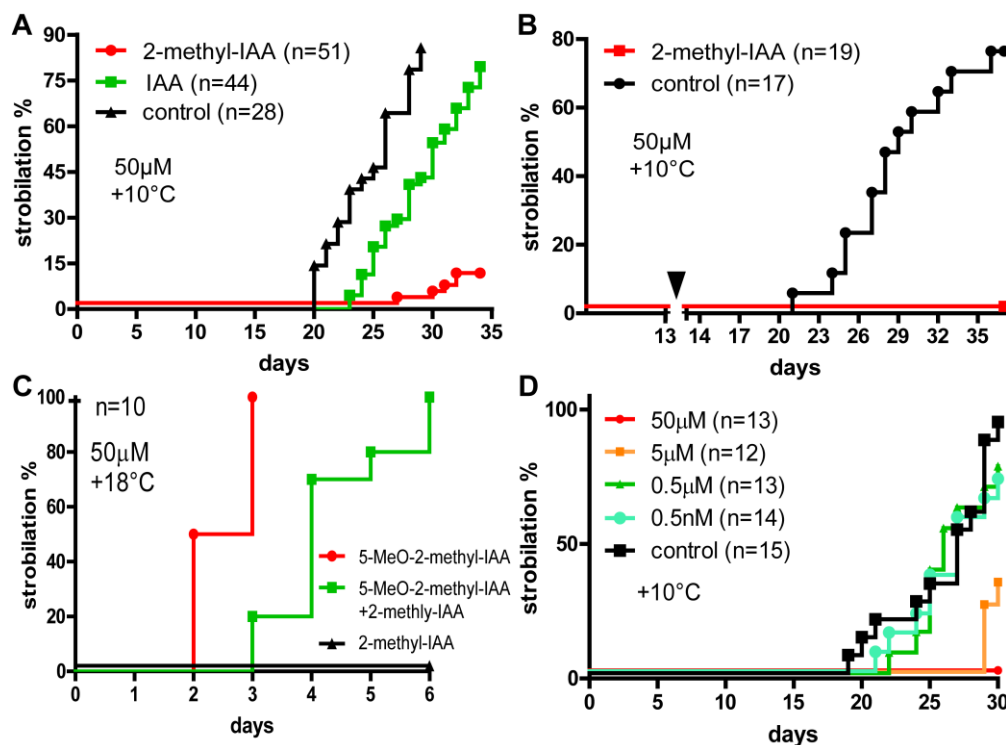


Fig. 39 Chemical inhibition of strobilation. (A) Temperature induced strobilation is inhibited in the presence of 50µM 2-methyl-3-indoleacetic acid. 50µM 3-indoleacetic acid (IAA) slows down strobilation; control, solvent (EtOH) in ASW. (B) 50µM 2-methyl-3-indoleacetic acid inhibits strobilation. Polyps were kept at +10°C for 13 days and then the chemicals has been added; control, solvent (EtOH) in ASW. (C) Co-incubation of polyps in 50µM 2-methyl-3-indoleacetic acid and 50µM 5-methoxyl-2-methyl-3-indoleacetic acid slows down strobilation. (D) Strobilation curves at different concentrations of 2-methyl-3-indoleacetic acid.

2.3 Segmentation and ephyra morphogenesis in *Aurelia aurita*

2.3.1 Segmentation process and ephyra development

Segmentation and ephyra development follow each other during strobilation. The wave-like segmentation process starts at the apical part of the polyp and progresses downwards (see Fig.5B-E). As shown in Fig.52 in Appendix, ephyra morphogenesis starts with the appearance of eight protrusions and then a rhopalium appears at the tip of each protrusion. Afterwards, the distal part of each protrusion splits into two lobes which are located at each side of a rhopalium and lappets start to extend. At this time point brown pigmentation of segments starts to appear (see Fig.5D). Finally, mature ephyrae detach from the strobila. They possess manubrium, mouth opening, gastric filaments, rhopalia, stomach and three types of canals - adradial canal, perradial canal and interradianal canal (see Fig.53 in Appendix).

It is important to know the timeline of strobilation. Only after having this knowledge it is possible to correctly interpret the results of chemical interference and RNAi experiments. To measure the kinetics of segment formation and ephyra development, one has to set a starting (“zero”) time point. So, I waited until the “zero” segment (see Fig.40A) had been completely formed and afterwards measured the time needed for the development of different structures in the following segments of the stobila (segments number 1, 2, 3 etc.).

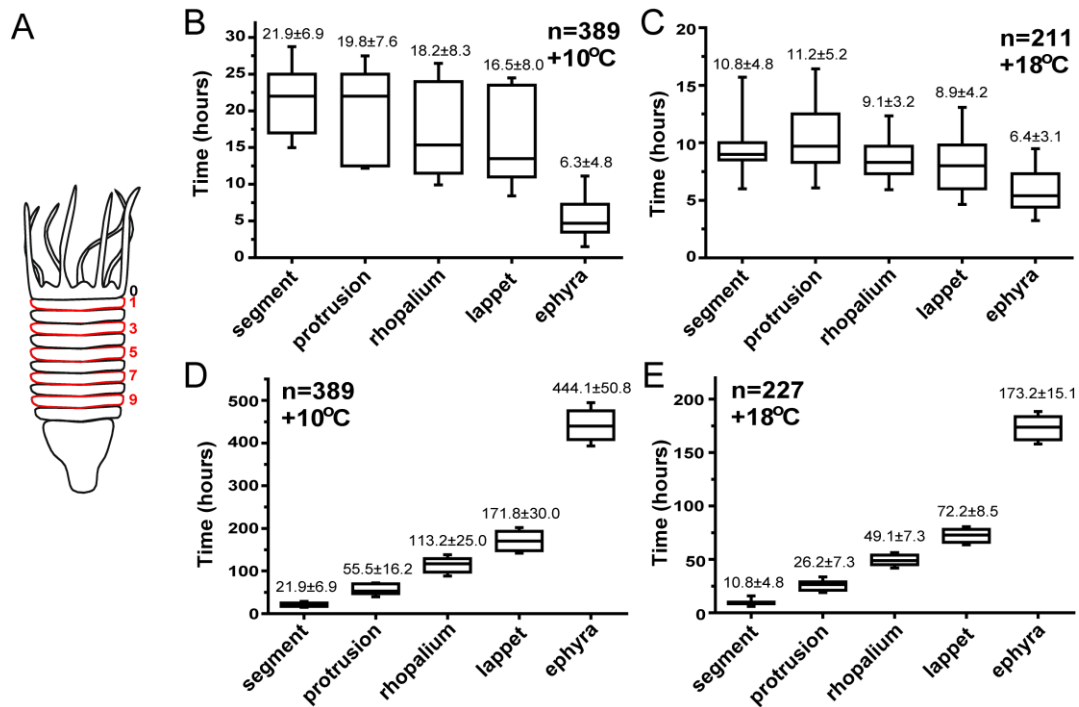


Fig. 40 Timing of segmentation and ephyra development. (A) Strobila with 10 segments. The number of segments is 1 – 10 from the anterior side to the posterior side, respectively. The head with tentacles defines as “0” segment. (B, C) Time needs for the development of a new segment, protrusions on the segment, rhopalia and lappets in two adjacent segments at +10°C (B) or +18°C (C). (D, E) Time needs for individual segments development from the moment of segment formation till ephyra detachment at +10°C (C) or +18°C (D). n: number of segments; box: 25%-75%; line: medium; error bar: mean values ±SD.

First, I measured the time difference between the development of the same structures (protrusions, rhopalia and lappets) in two adjacent segments. In total, 389 pairs of segments in 42 animals at +10°C and 211 pairs of segments in 41 animals at +18°C were observed. As shown in Fig.40B-C, at +10°C, development of a segment takes 21.9±6.9 hours. The time difference for the formation of protrusions in two adjacent segments is 19.8±7.6 hours. Rhopalia need 18.2±8.3 hours for their development and lappets need 16.5±8.0 hours. The time difference for ephyrae detachment is much shorter than for the other processes, just 6.3±4.8 hours. As shown in Fig.40C, development of a segment at +18°C takes 10.8±4.8 hours. Time differences for the emergence of protrusions, rhopalia development, lappets growth and ephyrae detachment in two adjacent segments are 11.2±5.2, 9.1±3.2, 8.9±4.2 and 6.4±3.1 hours, respectively.

Next, I followed 389 individual segments at +10°C and 227 segments at +18°C and measured the time needed for their complete development from the moment of segment formation till ephyra detachment. As shown in Fig. 40D, in average 21.9±6.9 hours are necessary to form a

segment at +10⁰C. After 55.5±16.2 hours, eight protrusions emerge. Rhopalia appear after 113.2±25.0 hours and lappets start to grow after 171.8±30.0 hours. At +10⁰C, complete development from the segment formation till ephyra detachment takes 444.1±50.8 hours. As shown in Fig.40E, the development is much quicker at +18⁰C and takes only 173.2±15.1 hours. The detachment of ephyra is the most temperature sensitive process as it is much slower at +10⁰C than at +18⁰C. In nature, young jellyfishes appear in late spring when it is already warm and easier to find enough food. So, the detachment might require a temperature sensitive enzyme which is activated by high temperature to liberate the matured ephyra from the strobila.

2.3.2 Conserved signalling pathways which influence the segmentation and ephyra development

2.3.2.1 Retinoic acid signaling pathway

Retinoic acid signaling pathway is important for various aspects of pattern formation in animals. Thus, it is a promising candidate for defining anterior-posterior polarity of segments as well as the location of lappets during strobilation of *Aurelia*. To address this question the expression patterns of *RxR*, *RDH1* and *RDH2* were examined by *in situ* hybridization.

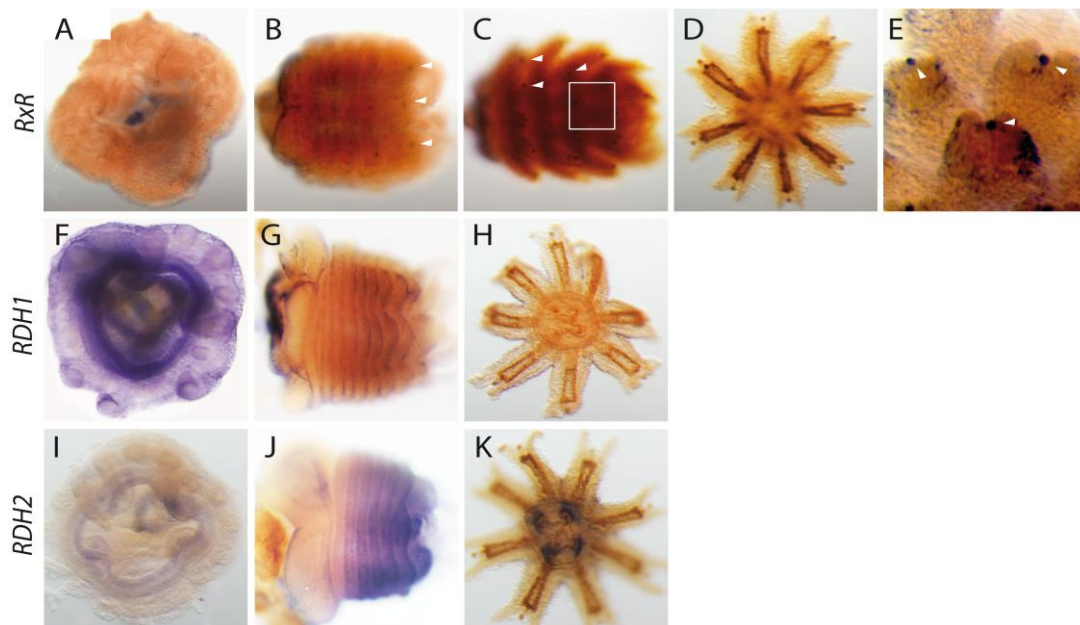


Fig. 41 Transcript localization of *RxR*, *RDH1* and *RDH2* during strobilation. (A-E) *RxR* is specifically expressed in rhopalia regions. (F-H) *RDH1* is strongly down-regulated during strobilation. (I-K) *RDH2* is exclusively expressed in the segments of strobila and in the manubrium of ephyra.

As shown in Fig.41A-E, during strobilation *RxR* is expressed only in the regions where lappet protrusions will emerge, and in the rhopalia in the ectoderm at the later stages. There is no expression in polyps and ephyra. *RDH1* which is down-regulated during strobilation, is expressed everywhere in polyps and especially strong around the mouth opening (see Fig.41F). During strobilation, *RDH1* is expressed in ectoderm at the anterior side of each segment which has protrusions. In a newly formed segment and the other parts of strobila, the expression is not retained. In ephyra (see Fig.41H), there is no expression of *RDH1*. This perfectly corresponds to RT-PCR results (see Fig.17A and Fig.21). In contrast, *RDH2* is up-regulated during strobilation (see Fig.17A and Fig.21). *RDH2* is specifically expressed in the segment rings and in the manubrium of ephyra (see Fig.41J, K). These interesting expression patterns support our assumption that retinoic acid signaling pathway is involved in the segmentation and ephyra development.

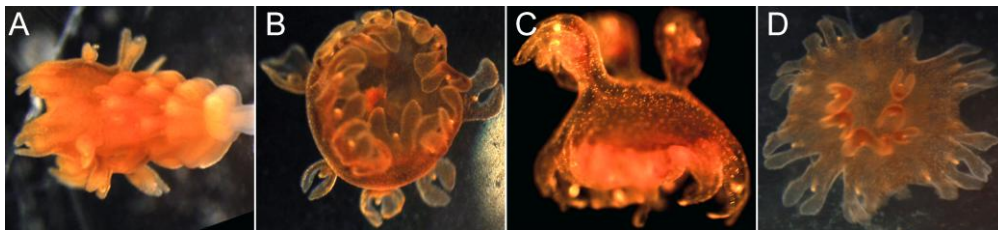


Fig. 42 Ephyrae with additional lappets caused by retinoic acid treatment. (A) Nearly mature ephyra with lappets on the umbrella; (B) Oral side view of detached ephyra with additional lappets; (C) Oral side is down of detached ephyra; (D) Umbrella side view of ephyra.

To further characterize the function of retinoic acid signaling, chemical interference experiments were done by incubating polyps in 1 μ M retinol, *9-cis* RA or *all-trans* RA solution at +10 $^{\circ}$ C. The morphology of the segments and ephyrae were recorded and compared with the controls. Animals incubated in retinol, *9-cis* RA or *all-trans* RA develop morphologically aberrant ephyrae which have additional lappets and incomplete development of endodermal structures (see Fig.42). Instead of eight lappets, these ephyrae have more than 16 lappets (see Fig.42D). In most of them, the additional lappets appear at the position between two normal lappets. They have the same structure, but are smaller than the normal ones. Some of RA incubated ephyrae have lappets on the umbrella which show the same anterior-posterior polarity but wrong position compared to the normal ones (see Fig.42C). These wrongly positioned lappets are contracting and carry rhopalia. The canal system in RA treated ephyrae is frequently deformed (or even completely absent), manubrium and mouth opening are underdeveloped or absent as well. However, regardless of such a drastic malformation, all ephyrae are alive.

2.3.2.2 *Hedgehog* signaling pathway

In the transcriptome three genes belonging to the *hedgehog* signaling pathway have been identified. Among them there are one patched receptor (*Ptc*) and two putative ligands (*SHH1* and *SHH2*). *Ptc* is drastically up-regulated during strobilation (see Fig.21). In polyp, *Ptc* is not detectable by *in situ* hybridization (see Fig.43A). In contrast, strong expression is evident in

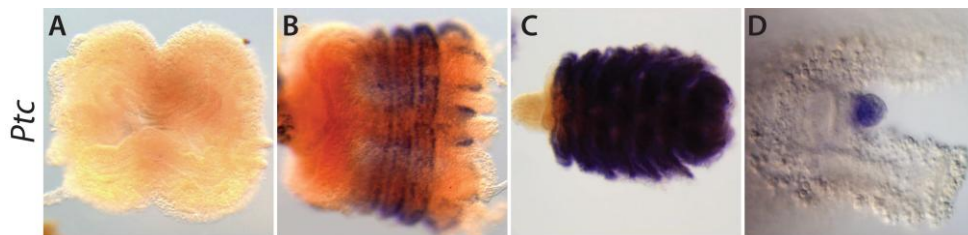


Fig. 43 Drastic up-regulation of patched (*Ptc*) during strobilation. *Ptc* is (A) not expressed in polyps, (B) only expressed in strobila segments, (C) strongly up-regulated during ephyra morphogenesis and (D) specifically expressed in ropania region of ephyra.

ectodermal epithelia cells on both edges of the strobila segments (see Fig.43B). *Ptc* is not expressed in non-segmented part of a strobila but appears at the boundary of pre-segmentation area. During ephyra morphogenesis, the signal of *Ptc* is even stronger than in strobila stage (see Fig.43C). The specific expression pattern of *Ptc* in ropania (see Fig.43D) most probably indicates the importance of *hedgehog* signaling for the development of the nervous system and sensory organs. RT-PCR (see Fig.21) shows that *SHH1* and *SHH2* are also up-regulated during strobilation, but *SHH2* seems to appeared only very late. *SHH1* is up-regulated quite early during strobilation induction and is down-regulated at the beginning of segmentation. Therefore, these two genes might play different roles during strobilation, but their functions were not analyzed further.

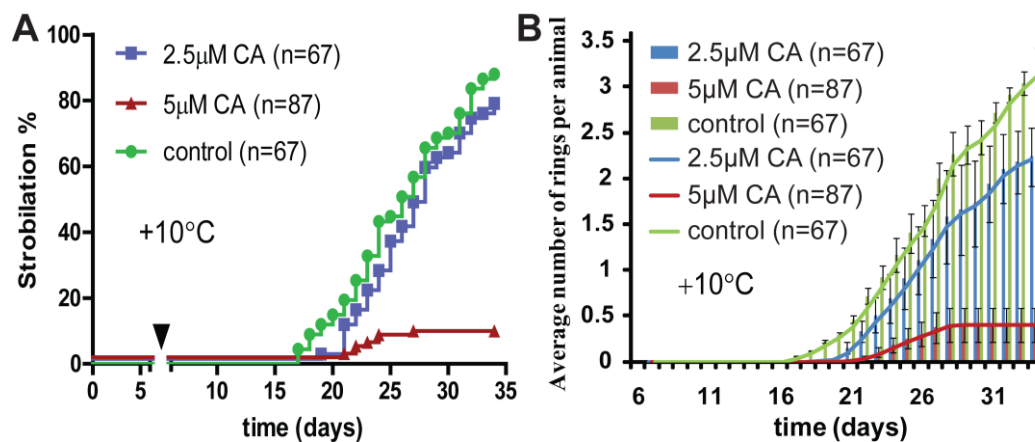


Fig. 44 Inhibition of *hedgehog* signalling pathway by cyclopamine represses strobilation. Temperature induced polyps for 6 days, and then cyclopamine was added for incubation. CA - cyclopamine; control - solvent (EtOH) in ASW. (A) strobilation curve, (B) segmentation curve.

The influence of the *hedgehog* signaling pathway on the segmentation was examined by chemical interference with cyclopamine (Chen *et al.*, 2002). Cyclopamine inhibits the *hedgehog* signaling pathway by binding to the Smoothed protein (Chen *et al.*, 2002; Glibert & Singer, 2006). In our experiments, polyps were induced at +10°C for 6 days and then incubated in 2.5µM and 5µM cyclopamine. As shown in Fig.44A, strobilation is repressed and segmentation process is negatively influenced in a concentration dependent manner (see Fig.44A). After 28 days of treatment with either ethanol or cyclopamine, 88% of the control animals strobilate, whereas only 8% of animals strobilate in 5µM cyclopamine. As shown in Fig.44B, the average number of formed segments per strobila is 3.2 in the control and 0.4 in the animals treated with 5µM cyclopamine. Interestingly, the animals incubated in 2.5µM cyclopamine can strobilate normally at the beginning, but after several days the strobilation is suddenly stopped.

2.3.2.3 *Wnt*, *BMP* and *ETS*

In the *Aurelia* transcriptomes, 8 contigs encoding *Wnt* gene were identified. Interestingly, *Wnt1* is up-regulated during strobilation. As shown in Fig.45A-E, *Wnt1* is expressed in ectoderm of polyps as a ring at the basis of every second tentacle and in a small group of endodermal cells inside of the tentacles. During strobilation *Wnt1* is asymmetrically expressed in ectoderm at the anterior side of each segment. Initially the expression domain is a ring and later the expression is retained only in the regions where protrusions will emerge and

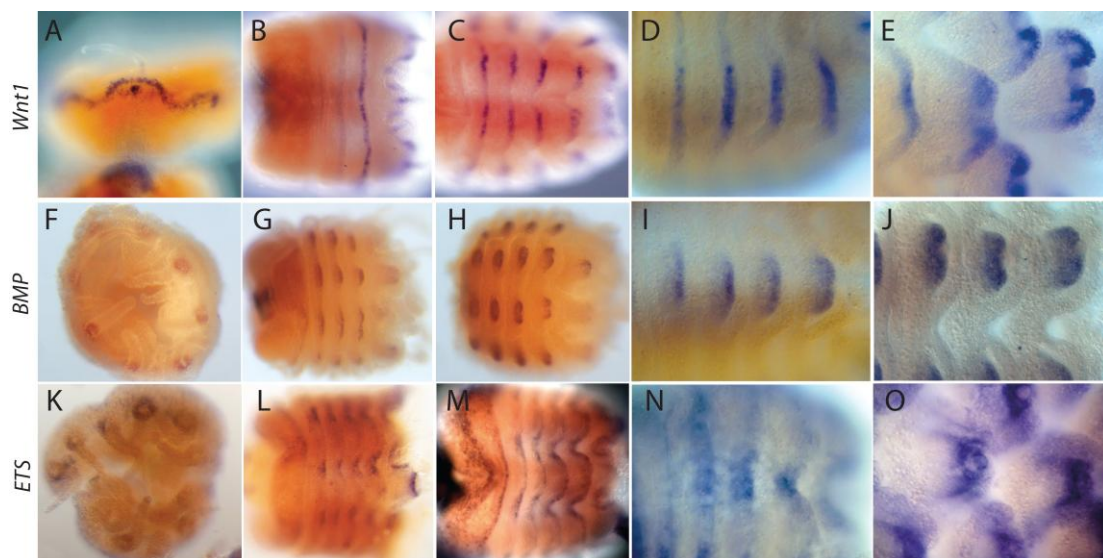


Fig. 45 Transcript localization of *Wnt1*, *BMP* and *ETS*. (A-E) *Wnt1* is specifically expressed in the ectoderm at the anterior side. (F-J) *BMP* is strongly expressed in the endoderm at the anterior end. (K-O) *ETS* is exclusively expressed in the ectoderm between lappets. *BMP*, bone morphogenetic protein; *ETS*, erythroblast transformation specific transcription factor.

disappears between them. At the later stages of ephyra morphogenesis, *Wnt1* is expressed at the tips of developing lappets in the ectoderm (see Fig.45D) and is excluded from the region where ropalia development takes place (see Fig.45E).

In a polyp which always has 16 tentacles, *BMP* is only expressed in every second one (see Fig.45F). During strobilation *BMP* expression strikingly corresponds to the expression of *Wnt1*, exhibiting the same expression pattern and dynamics, but in the endoderm (see Fig.45G-J). Initially, it is expressed as a ring at the anterior edge of each newly developed segment and later is retained only in the endodermal cells of protrusions which give rise to the tips of lappets (see Fig.45I). Similarly to *Wnt1*, expression of *BMP* is excluded from the cells which later develop into ropalia (see Fig.45J).

ETS transcription factor is expressed at the basis of tentacles in a polyp (see Fig.45K) and during strobilation expression pattern is perfectly complementary to those of *Wnt1* and *BMP* (see Fig.45L-O). *ETS* is most probably involved in the establishment of normal numbers of lappets in ephyra. Interestingly, *ETS* is expressed in the unsegmented region of strobila where the new segment will be built (see Fig.45M). Thus, it might define the pre-pattern of the segmentation.

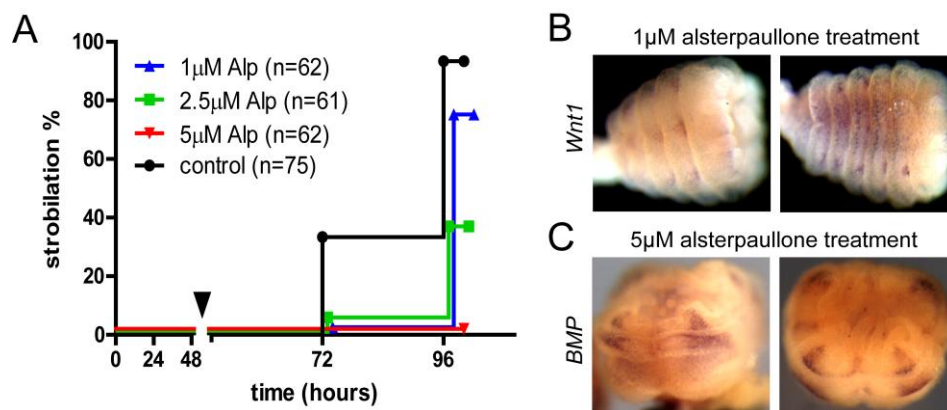


Fig. 46 Alsterpaullone treatment represses segmentation. (A) Animals were chemically induced to strobilate and after 48h, alsterpaullone was added. Alp – alsterpaullone; control - solvent (EtOH) in ASW. Transcript localization of *Wnt1* (B) and *BMP* (C) in alsterpaullone treated animals.

Similar to its role in establishing polarity in *Hydra* and *Nematostella* (Lee *et al.*, 2006; Holstein, 2008), *Wnt1* seems to be important for defining anterior-posterior polarity of segments and ephyrae in *Aurelia*. In order to test this, chemical interference experiments were performed. Very early strobilae were incubated in alsterpaullone which activates the canonical *Wnt* pathway (Guder *et al.*, 2006; Leost *et al.*, 2000). Polyps were chemically

induced to strobilate and after 48h, alsterpaullone was added to the final concentration of 1 μ M, 2.5 μ M and 5 μ M. As shown in Fig.46A, the segmentation process is repressed in a dose dependent manner by alsterpaullone. 74% of the animals have strobilated in 1 μ M alsterpaullone, whereas no animals have strobilated in 5 μ M alsterpaullone. Interestingly, alsterpaullone (1 μ M and 2.5 μ M) not only represses strobilation, but also influences the diameter of the segments which decreases from anterior to posterior (see Fig.46B). Normally all segments have the similar fixed diameter, but in alsterpaullone they are getting smaller and smaller in the anterior-posterior direction. In alsterpaullone treated animals, *Wnt1* expression region is extended (see Fig.46B) compared to the control animals (see Fig.45A-E). Instead of only appearing at the anterior end of each protrusion (see Fig.45B), *Wnt1* signal spreads to the middle of the segment and even shows a ring-shaped expression domain in the middle of the segment (see Fig.45B).

As shown in Fig.46C, we also examined the expression pattern of *BMP* in alsterpaullone treated animals. Similar to *Wnt1*, the expression region of *BMP* is extended and detects not only in the anterior side, but also in the middle or even at the posterior side of the segment. In 5 μ M alsterpaullone, the expression domain of *BMP* is reduced to just four regions (instead of eight regions in the normal animals). *BMP* transcript is distributed throughout the body from the anterior to the posterior end (see Fig.46C).

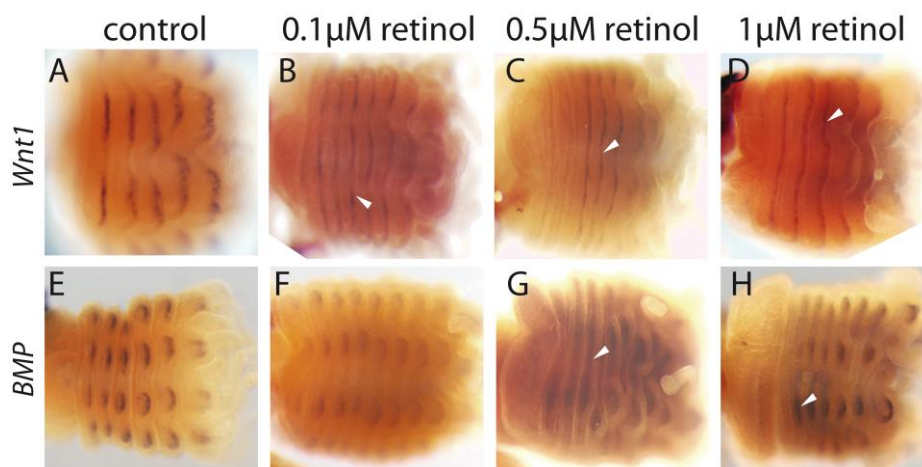


Fig. 47 Expression of *Wnt1* and *BMP* in retinol treated animals. (A) In control animals, *Wnt1* is expressed in the ectoderm at the anterior end of the segments and at the tips of protrusions. (B) 0.1 μ M retinol treated animals have extended *Wnt1* expression in the ectoderm at the tips of the protrusions. (C) *Wnt1* appears in the area between protrusions (white arrow) in the 0.5 μ M retinol treatment. (D) In 1 μ M retinol, the expression domain of *Wnt1* is corrugated at the oral side of the developing ephyra. (E) *BMP* is expressed at the tips of protrusions in the endoderm in the control group. (F) – (H) Pattern of *BMP* expression is disturbed in retinol treated animals.

To investigate the effect of retinol on the expression of *Wnt1*, whole mount *in situ* hybridization was used. As shown in Fig.47A, control animals show the normal ring-shaped expression of *Wnt1* before the formation of protrusions. When the protrusions start to appear, no *Wnt1* expression can be detected between the protrusions. However, in the animals treated with 0.1 μ M retinol the expression region of *Wnt1* is extended (see Fig.47B). In 0.5 μ M retinol solution, *Wnt1* signal is detectable even between the protrusions (Fig.47C). Interestingly, in some of the animals the expression of *Wnt1* can be detected not only at the anterior part of the segment but also at the posterior end of the segment. In 1 μ M retinol, the animals show the same expression pattern of *Wnt1* as in 0.5 μ M retinol (see Fig.47D).

Similar to *Wnt1*, *BMP* expression is also influenced by retinol. In the control, animals show endodermal, ring-shaped *BMP* expression pattern at the anterior end of each segment (see Fig.47E). There is no *BMP* expression between protrusions. In 0.1 μ M retinol, the expression of *BMP* is the same as in the control animals (see Fig.47F). However, an extended area of *BMP* expression is detected in 0.5 μ M retinol incubated animals (see Fig.47G). Moreover, *BMP* is expressed between the developing protrusions of the segments. In some animals, instead of appearing at the anterior edge of each segment only, *BMP* is expressed at posterior end as well. Animals in 1 μ M retinol show the same disturbed expression pattern of *BMP* as in 0.5 μ M retinol (see Fig.47H).

Dickkopf-like gene, which function as the *Wnt* signaling antagonist in vertebrates and cnidaria is expressed in the endodermal gland cells, in a pattern similar to that in *Hydra* (Nakamura *et al.*, 2011). *Dickkopf-like* is weakly expressed during strobilation and shows no signal in polyp and strobila. In ephyra, it is specifically expressed in the gastric filaments (see Fig.55A in Appendix).

BMP is important for anterior-posterior polarity establishment in *Hydra* and *Nematostella* (Bode *et al.*, 2008). Most probably *BMP* has the same function in segmentation and ephyra development *Aurelia*. In ephyra stage *BMP* antagonist *chordin* is up-regulated more than 10 fold (>118 12.8x; >3169 17.8x). According to *in situ* hybridization *chordin* is not expressed in the body of the polyp and strobila. In ephyra, it is strongly expressed in the ectoderm, but without any detectable gradient (see Fig.55B in Appendix).

2.3.3 Taxonomically restricted genes (*TRGs*) in segmentation

Other candidate genes that could be involved in segmentation are secreted morphogens. These secreted morphogens can create a concentration gradient by passive diffusion and define the morphogenetic field. Based on the local concentrations of these morphogens, the undifferentiated cells can determine their own location in the tissue and differentiate according to it (Glibert & Singer, 2006).

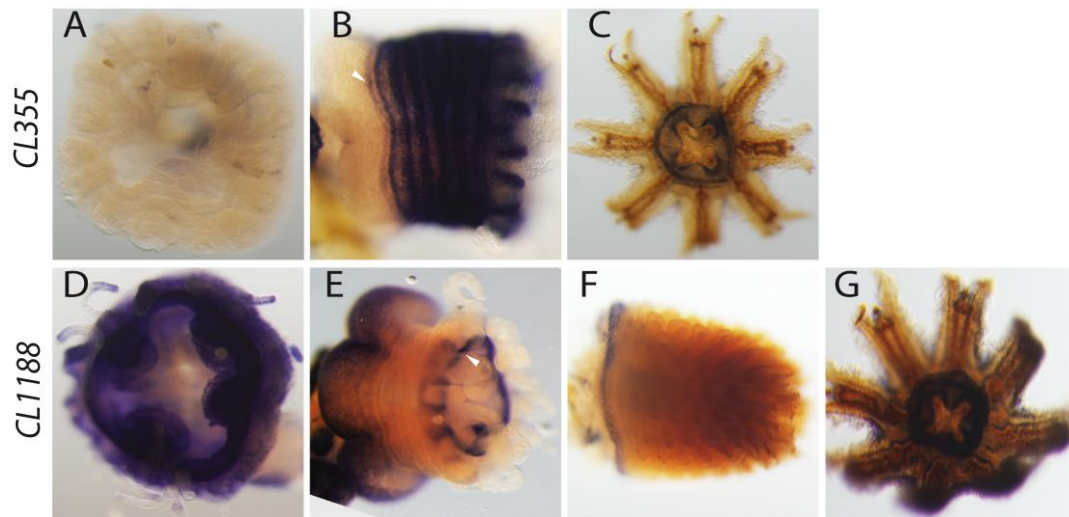


Fig. 48 Transcript localization of *CL355* and *CL1188*. (A-C) *CL355* is specifically expressed in the segments and the area which will form a new segment in strobila. (D-G) *CL1188* is strongly expressed in the polyp ectoderm, polyp part of strobila and a ring around the mouth.

Based on 454-sequencing, microarray data and *in situ* hybridization, several genes were identified which might have a potential impact on segmentation. Among them, two genes (*CL355* and *CL1188*) attracted my special attention due to their interesting expression patterns during strobilation. Both genes (*CL355* and *CL1188*) encode proteins with no similarity to other sequences in Genbank (BLASTP e-value < 1e-5). That means they are taxonomically restricted genes (*TRGs*) and may even represent *Aurelia*-specific gene. As shown in Fig.48A-C, *CL355* is not expressed in the polyp. In strobila, *CL355* is expressed in ectoderm at the posterior side of each segment. Interestingly, *CL355* is also expressed in the pre-segmentation area of the strobila (see Fig.48B). Manubrium and the ectoderm of ephyra are also *CL355* positive (see Fig.48C). *CL1188*, in contrast to *CL355*, is strongly expressed in the ectoderm of the polyp (see Fig.48D). During strobilation, expression of *CL1188* disappears in the segments. *CL1188* is expressed only in the non-segmented part of strobila and around the mouth (see Fig.48E). In ephyra, *CL1188* is detectable in the ectoderm of the manubrium (see Fig.48G).

3 Discussion

3.1 Regulation of life cycle in *Aurelia aurita*

3.1.1 Temperature induction of strobilation

Temperature shift induces metamorphosis in species- and strain-specific manner (Sugiura, 1965; Prieto *et al.*, 2010). For example, in some jellyfishes such as *Mastigias papus* and *Cassiopea andromeda* not the temperature decrease, but its increase functions as a signal for metamorphosis (Sugiura, 1965; Hofmann *et al.*, 1978). In *Aurelia aurita*, temperature shift of a defined range (ΔT) induces strobilation within a strictly defined time interval. In Roscoff strain polyps, which I use in my experiments, with $\Delta T=8^{\circ}\text{C}$ (from $+18^{\circ}\text{C}$ to $+10^{\circ}\text{C}$) first strobila will appear exactly after 18-19 days (see Fig.15). With $\Delta T=10^{\circ}\text{C}$ (from $+20^{\circ}\text{C}$ to $+10^{\circ}\text{C}$) strobilation will start after 13-14 days of incubation (see Fig.15). In a carefully maintained *Aurelia* culture where water temperature and feeding regime are stable, time between the temperature decrease and the onset of strobilation is surprisingly stable with deviations of just 24 hours for the induction periods of 13 or 19 days. Hence, as soon as polyps are transferred to $+10^{\circ}\text{C}$, a relatively precise "timer" is activated which counts the number of days spent at low temperature. As soon as strain-specific time threshold is reached, strobilation program is initiated.

What are the temperature sensors in *Aurelia*? So far, nothing is known about temperature perception in Cnidaria and I did not address this issue in this project. Most probably thermosensory receptors are constitutively expressed in all life stages and should not be up- or down-regulated during metamorphosis. Transient receptor potential cation channel subfamily A member 1 (*TRPA1*) and transient receptor potential cation channel subfamily M like (*TRPM-like*) ion channels, which are responsible for temperature perception in *C. elegans*, *Drosophila* and higher animals (Koltzenburg, 2004) are present in the genomes of *Hydra* and *Acropora* (HM147132, XM_002155179, EZ019701). In *Aurelia CL18127* and *CL9872* (partial sequences) are homologs of *TRPA1* (temperature sensing below $+15^{\circ}\text{C}$) and *TRPM-like* ion channels respectively (Sawada *et al.*, 2007). Involvement of these genes in temperature perception has not been tested, but their presence indicates that temperature sensing machinery is conserved between cnidarians and bilaterians.

3.1.2 *CL390* as a temperature dependent molecular timer

Temperature perception *per se* has a limited value for making a decision whether to strobilate or not. Necessary component is a "memory" unit which has to record the duration of the low temperature period. Water temperature is a much more stable parameter than air temperature in terrestrial habitats. It is less subjected to regular day / night fluctuations and rapid changes in case of adverse weather conditions. In marine environment drastic temperature fluctuations in supralittoral zone where *Aurelia* polyps normally live are rare. However, in order to monitor seasonal changes, polyps must be able to distinguish between short-time reversible temperature fluctuations and season-related temperature decrease in the winter period. Thus, depending on the geographical location (and correspondingly the strain of *Aurelia*) there must be minimal threshold temperature and threshold duration at this temperature which leads to irreversible activation of the strobilation cascade.

Indeed, Roscoff strain polyps maintained for 6 days at +10°C and then returned back to +18°C would not strobilate, while polyps which stayed 9 days at +10°C would undergo strobilation even after being returned back to +18°C (see Fig.22). My data indicate that *CL390* most probably plays a role of the temperature-sensitive "memory" which allows such a differential response. At low temperature the amount of *CL390* transcript steadily increases with time and at high temperature the transcript level drops. After exceeding a threshold of 15 fold up-regulation, transcription of *CL390* increases exponentially and independent of the temperature input, ultimately resulting in strobilation (see Fig.24). Such expression behavior indicates that *CL390* plays a role of a temperature dependent "timer" which measures the duration of a winter period. In this aspect induction of strobilation in *Aurelia* resembles the vernalization process in plants.

3.1.3 *CL390* as a precursor of the strobilation hormone

CL390 gene is strongly up-regulated at the cold temperature and in transplantation and feeding experiment. Moreover, GFP-*CL390* protein causes the formation of segment-like constrictions, but the segmentation does not go further (see Fig.30E). One of the possible explanations is that the protein must be processed before it is turned into the active inducer. For checking that, we synthesized peptides representing sub-fragments of *CL390* protein. Indeed, one of the peptides – WSRRRWL is active, thereby directly proves that *CL390* is the precursor of the strobilation inducer in *Aurelia*.

There is one striking analogy between metamorphosis in vertebrates and *Aurelia*. Thyroid hormone in vertebrates is a condensation product of an aromatic amino acid tyrosine and in *Aurelia* the minimal pharmacophore of the strobilation hormone is based on an indole ring structure which is nothing else, but the core element of another aromatic amino acid - tryptophan. Indole derivatives in general are widely utilized as signalling molecules in nature. These are plant hormone auxin (indole-3-acetic acid), neurotransmitter serotonin and the hormone melatonin to name just a few. The strobilation inducer of *Aurelia* adds one more example to the list of biologically active indole derivatives.

3.1.4 The molecular toolkit controlling induction of strobilation

In *Aurelia*, 9-*cis* RA is responsible for the strobilation induction via RxR and a secreted taxon-specific protein from the epithelium (CL390) functions as a precursor of the strobilation hormone (see Fig.49). Thus, in *Aurelia*, similar to that in insects and amphibians, the molecular machinery of metamorphosis consists of a conserved and a taxon-specific counterpart. This data, therefore, strongly suggest that the general principle of metamorphosis regulation is universal throughout the animal kingdom.

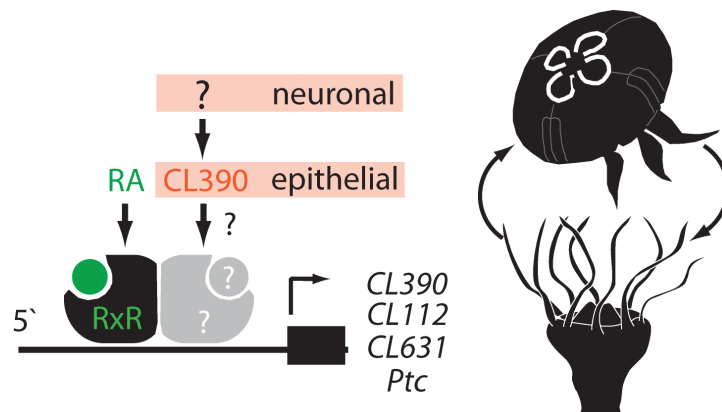


Fig. 49 Molecular machinery of metamorphosis in *Aurelia*. A previously unknown receptor is directly or indirectly activated by CL390 and forms a heterodimer with the RxR receptor which is activated by RA. The heterodimer binds to the responsive elements of target genes and activates their transcription. Among the target genes in the ectoderm include *CL390*, *CL631* and *Ptc*, and *CL112* in the endoderm.

During strobilation both *RxR* and *CL390* genes are up-regulated and seem to function cooperatively. In support of this view, 5' flanking region and the first intron of *CL390* contain five putative high score binding sites for RxR nuclear hormone receptor and its heterodimers (see Fig.29). Thus, the signals from the metamorphosis induction cascades are integrated in the structure of *CL390* promoter. *CL390*, thereby, might be the direct target gene of the

retinoic acid signaling. As shown in Fig.26, transplantation of strobila segments induces local up-regulation of *CL390* in the region adjacent to the transplant. After that, the signal spreads to the whole animal, which indicates that *CL390* could positively influence its own expression. Moreover, in the animals which were returned from +10°C to +18°C (see Fig.22 and Fig.23), the expression of *CL390* oscillates. Most probably there is a signalling loop which consists of *CL390* and the second gene which can regulate the expression of each other. We know that *RxR* is up-regulated during strobilation and its transcript will increase earlier than that of *CL390* (see Fig.21). It might be that *RxR* is a second member of the feedback loop (see Fig.49).

At the moment we do not know which nuclear hormone receptor might function together with *RxR* in *Aurelia*. I show that strobilation can be induced by the peptide derived from *CL390* protein or by several indole-based chemical compounds. It is hard to predict whether these inductors can bind directly to the corresponding nuclear hormone receptor (NHR) or additional cascade starting with G-protein coupled receptor is involved.

The major difference in the metamorphosis induction between *Aurelia* and bilaterian animals is that we have not identified any neuronally derived factor regulating strobilation. In contrast to that in the cnidarian *Hydractinia echinata*, metamorphosis of larvae into a polyp is regulated by KPPPGLW-NH₂ neuropeptide belonging to the GLW-amide family (Schmich *et al.*, 1998). Members of this neuropeptide family are present in *Hydra*, *Nematostella* and *Anthopleura* (Levieu *et al.*, 1997; Schmich *et al.*, 1998). In *Aurelia*, a gene which encodes neuropeptide belonging to GLW-amide family with the putative sequence QPPGTW-NH₂ (KC767904) have also been identified. GTW-amide positive neurons, however, are present both in polyp and ephyra stages (see Fig.56 in Appendix). Thus, metamorphosis induction in *Aurelia* might be simpler than that in Bilateria. One of the explanations might be the fact that in *Aurelia* polyps, in contrast to higher animals, centralized nervous system is not present. Taking into consideration that cells in Cnidaria are more multifunctional than in higher organisms (Hwang, *et al.*, 2007; Hemmrich *et al.*, 2012) it is feasible that in contrast to insects and vertebrates, a metamorphosis induction system of *Aurelia* consists of just one stage and the ectodermal epithelial cells of *Aurelia* combine the functions of neurosecretory and endocrine cells of the bilaterian animals.

3.2 Synthetic inhibitors of strobilation

Peptides FSYRRRW and FSYRRRW-NH₂ can inhibit strobilation and their structures are similar to indomethacin which has a close positioning of two aromatic rings (see Fig.38, 34). There is a clear difference between the functional groups associated with tyrosine (Y) and tryptophan (W) in the peptides and the functional groups of indomethacin. Two electron donor groups (chloro- and methoxy-) which might be essential for binding to the receptor are missing in the peptides. Instead, tyrosine has one electron acceptor group. As a result the peptides most probably can bind to the receptor, but do not have the ability to activate it.

Spangenberg (1967, 1971) showed that iodide can induce strobilation in the polyps which were continuously incubated in iodide-free ASW. Actually, 3- and 5- positions in the benzene ring of tyrosine can be iodinated to provide the missing electron donor groups (De Blois *et al.*, 2012). So, FSYRRRW peptide might be turned into an activator by iodination. FSYRRRWS-NH₂ peptide which cannot block strobilation, might be simply too large for the sub-pocket of the receptor, and, therefore, cannot bind to it (see Fig.38). The inhibitory function of two sub-fragments of CL390 protein indicates that *CL390* gene might encode not only the precursor of the inducer, but also the inhibitors. Thus, the fate of strobilation is controlled not only at the transcription level, but also at the protein level. There might be an enzyme which converts inhibitor into inducer.

2-methyl-3-indoleacetic acid is a chemical inhibitor of strobilation (see Fig.39). High concentration of this substance can even inhibit strobilation of the polyps which have been induced at +10⁰C for 13 days (see Fig.39B). “back to +18⁰C experiment” (see Fig.22) shows that the strobilation is irreversible after 9 days of incubation at +10⁰C, but 2-methyl-3-indoleacetic acid can still block the strobilation. 5-methoxy-2methyl-3-indoleacetic acid is a quite powerful inducer which differs to 2-methyl-3-indoleacetic acid just by the presence of an additional electron donor group - methoxy group at the position 5. Most probably both chemicals bind the same receptor. The chemical with an electron donor group functions as activator and the chemical without it as inhibitor. I think that the 2-methyl-3-indoleacetic acid or its analogs can be used to control jellyfish blooms in the future.

3.3 Segmentation and ephyra morphogenesis

3.3.1 Retinoic acid signalling pathway controls the formation of segments and ephyrae

Retinoic acid signalling pathway regulates the metamorphosis of insects and amphibians (Ollikainen *et al.*, 2006). During the embryogenesis of quail, mouse, and *Xenopus laevis* the retinoic acid signaling pathway is also involved in segmentation (somitogenesis). Quail embryos which lack retinol (Vitamin A) can only develop a half the number of somites (Maden *et al.*, 2000). In *Raldh2* knockout mice which cannot synthesize RA, the number of somites is also significantly reduced (Niederreither, 1999; Vermot *et al.*, 2005). Moreno and Kintener (2004) treated embryos of *Xenopus* with RA to enhance the activity of the retinoic acid signaling pathway which led to larger somites. Moreover, the anterior-posterior axis in the nervous system in *Danio rerio* is formed by the interaction of RA, *Wnt* and *FGF* (Glibert & Singer, 2006) and the metabolizing enzymes of the retinoic acid signaling pathway are necessary for the establishment of the morphogenetic field (Sandell *et al.* 2012). Our data indicate that retinoic acid signaling is also important in the basal Metazoa.

Both *9-cis* RA and retinol have a dramatic effect on the morphology of ephyra (see Fig.42). If they are present in high concentrations, the positional information is getting lost and as a result ephyrae get lappets at the wrong position. Extra lappets sprout in the space between the normal ones and some of them appear even on the umbrella. However, they keep the right anterior-posterior orientation. Interestingly, the same phenomenon was found in vertebrates. The famous Minnesatas' deformed frogs which were noticed in the mid-1990s get extra legs by RA induction through the manipulation of a parasite called *Riberioia ondatrae* (Szuroczi *et al.*, 2012). Both cases indicate that RA alone can induce formation of complete organs at the wrong places (frog legs or ephyra lappets). These results illustrate that the retinoic acid signaling might be upstream of several signaling pathways and can control them to build a completely new organ. In my *Aurelia* experiments, the formation of manubrium, endoderm and canal system in ephyra has been hampered. Hence, retinoic acid signaling plays a critical role in the formation of endodermal structures.

Due to its specific expression in the segments of strobila (see Fig.41J), *RDH2* has the potential to regulate the amount of retinoids in the tissue. Depending on the location of *RDH2*, a RA gradient could be established within each segment rising from the posterior end to the

anterior end. Interestingly, at +10⁰C DEAB treated animals can strobilate normally (see Fig.18E) despite of the fact that DEAB is a retinoic acid cascade inhibitor. It is known that the synthesis of RA can be completely inhibited by 10µM DEAB in a zebrafish embryo (Perz-Edwards *et al.*, 2001). In *Aurelia*, however, it is not the case. This indicates the presence of the DEAB insensitive retinoic aldehyde dehydrogenases or an independent RA synthesis pathway. *RxR* also shows a regionalized expression in every segment (see Fig.41) and thereby could also regulate the distribution of RA.

3.3.2 Inhibition of *hedgehog* signalling pathway represses segmentation

Hedgehog signaling pathway plays an important role in embryonic development (Choy & Cheng, 2012; Ingham *et al.*, 2011). *Hedgehog* genes were first discovered in *Drosophila*. They are involved in cell proliferation and cell fate decision (Nüsslein-Volhard & Wieschaus, 1980; Singh *et al.*, 2012; Oosterveen *et al.*, 2012). Three homologs of *hedgehog* were identified in vertebrates: desert hedgehog (*DHH*), indian hedgehog (*IHH*) and sonic hedgehog (*SHH*). *SHH* acts as a morphogen that regulates cellular differentiation in a concentration dependent manner (Strigini & Cohen, 1997). *SHH* is involved in several important developmental processes such as the development of central nervous system, appendages and somite polarity (Gilbert, 2010, Briscoe *et al.*, 2001).

In *Aurelia*, *SHH1* and *SHH2* are up-regulated during metamorphosis (see Fig.21), which suggests that they are directly involved in strobilation. *SHH1* and *SHH2* are expressed in different time windows. *SHH1* appears earlier, is down-regulated at the beginning of segmentation, and might be involved in strobilation induction. *SHH2* is mainly expressed during the segmentation. Most probably it is directly participating in the formation of the segments. At the same time, *Ptc* receptor is expressed only after the segmentation has started. This illustrates that *Ptc* is engaged in the segment formation and ephyra morphogenesis. It has been shown that *Ptc* functions as a negative feedback regulator of the *hedgehog* signaling pathway in the vertebrate brain (Ruiz i Altaba *et al.*, 2002). In *Aurelia*, *SHH1/2* and *Ptc* are expressed at the different time points which indicates that a similar negative feedback loop might be present.

Cyclopamine which is a well know inhibitor of *hedgehog* pathway inhibits segmentation in *Aurelia*. Hence, *hedgehog* signaling pathway is directly involved in segmentation. Interestingly, animals incubated in 2.5µM cyclopamine can normally strobilate at the

beginning, but after several days the segmentation suddenly stops. It means that an important product (or products of the *hedgehog* signaling pathway) run(s) out in the presence of the inhibitor.

3.3.3 *Wnt* signaling and segmentation

Wnt genes are involved in the formation of the posterior-anterior axis in vertebrates and invertebrates (McGinnis & Krumlauf, 1992). In *Hydra*, *Wnt* plays a key role in the head organizer (Broun *et al.*, 2005). In human, *Wnt3* is mainly involved in the formation of the body axis of the embryo (Liu *et al.*, 1999). In *Aurelia*, *Wnt1* is highly up-regulated during segmentation (see Fig.21), which indicates that *Wnt1* is directly involved in the segment formation. It has been shown (Koop *et al.*, 2010) that in vertebrates, high concentration of RA could up-regulate the expression of *Wnt3*. In *Aurelia*, the expression of *Wnt1* in RA treated animals is higher than in the control (see Fig.47) which confirms that *Wnt1* is also a target gene of the retinoic acid signaling.

By activation of *Wnt* signaling pathway using alsterpaullone treatment, the segmentation is repressed (see Fig.46A) and the expression pattern of *Wnt1* has been changed (see Fig.46B). Instead of asymmetrical expression at the anterior side of each segment, *Wnt1* appears in the middle of the segment and even spreads to the posterior end. My results indicate that the location of *Wnt1* is used to mark the segmentation area. If the expression field of *Wnt1* is too large, the animals stop to build new segments as they might consider the whole body area to be one segment. Taken together, *Wnt1* is directly involved in the segmentation of *Aurelia aurita*.

Interestingly, the size of segments in alsterpaullone treated animals is getting progressively smaller from oral side to the foot. Each alsterpaullone treated strobila looks like an inverted frustum of cones (see Fig.46B). This result suggests that the *Wnt* signaling somehow also controls the diameter of the segments.

3.3.4 *BMP* and *ETS* in segmentation and ephyra development

BMPs are well known for their roles in the formation of the dorso-ventral axis. In vertebrates, they serve as ventralization signal, and in invertebrates as a signal for the dorsal cell fate (Eivers *et al.*, 2009). In *Xenopus* *BMP-4* is involved in the formation of the intestinal tract

(Ishizuya-Oka & Hasebe, 2008). *BMP4* is a target gene of *Wnt* signaling pathway and the overexpression of *Wnt1* and *Wnt3a* induces the expression of *BMP4* in transgenic mice (Kuroda *et al.*, 2013).

BMP in *Aurelia* has an interesting endodermal expression pattern which suggests that *BMP* might be involved in the establishment of the gastro-vascular system. In this study, the expression pattern of the *BMP* was examined in normal and in alsterpaullone treated animals (see Fig.46C). When *Wnt* signaling pathway is activated by alsterpaullone, the expression area of *BMP* expands and spreads to the middle of the segments and even appears at their posterior side. This high up-regulation by alsterpaullone treatment indicates that *BMP* is also a target gene of *Wnt* signaling pathway and can be directly involved in the segmentation of *Aurelia aurita*. In 5 μ M alsterpaullone experiment, instead of eight slim lines in the tips of the protrusions (see Fig.45), the animals have four large areas of *BMP* expression which nearly cover the whole body (see Fig.46C). This phenomenon suggests that in cooperation with *Wnt1*, *BMP* is most probably involved in the establishment of normal numbers of lappets in ephyra and marks the region for segmentation.

Expression area of *BMP* is getting larger in RA treated animals (see Fig.47). In some cases, the transcript is present not only in the anterior side of the segments, but also at the posterior end. Taken together, *Wnt1* and *BMP* are critical for the positional information. Both genes seem to be regulated by RA gradient within the segments. This regulation is disturbed by the excess of RA and leads to the formation of lappets at the wrong positions.

ETS plays an important role in the embryogenesis of sea urchin, *Xenopus*, *Drosophila* and mouse (Chen *et al.*, 1988; Remy & Baltzinger, 2000; Lai & Rubin, 1992, Ristevski, *et al.* 2004). In *Aurelia*, *ETS* is strongly expressed in strobila (see Fig.45) which indicates that *ETS* also plays a role in the segmentation. Liu, *et al.* (2012) showed that *ER71*, an *ETS* transcription factor in mouse, can inhibit *Wnt* signaling. Interestingly, the expression pattern of *ETS* is perfectly complementary to *Wnt1* in *Aurelia* strobila. This indicates that similar to that in mice, *ETS* inhibits *Wnt* signaling and might regulate the establishment of normal numbers of lappets in ephyra. Interestingly, *ETS* is down-regulated in RA-induced embryonal carcinoma cells (Martin, 1992). In *Aurelia*, RA treated animals have more lappets (see Fig.42) which might be due to the inhibition of *ETS*. So, the addition of retinoids activate retinoic acid signaling pathway which further up-regulates *Wnt* and *BMP* signaling and repress the

expression of *ETS*. As a result, the position information for lappet development is disturbed and extra lappets grow.

3.3.5 Novel genes in segmentation and ephyra development

Two *TRGs* (*CL355* and *CL1188*) have been described in this work (see Fig.48). Both of them mark the segmentation area but in opposing and complementary ways. *CL355* is only expressed in segments. In contrast, *CL1188* never appears in the segmented part. *CL355* and *CL1188* are not equally distributed in those areas. *CL355* is specifically expressed in the posterior side of each segment and as a stripe in the pre-segmentation area. *CL1188* disappears from the body region as soon as the segmentation starts. Hence, *CL355* works as a marker of the posterior boundary for each segment and *CL1188* marks the unsegmented area.

3.3.6 Model for the regulation of segmentation and ephyra development

Using the stage-specific transcriptomes, RT-PCR and *in situ* hybridization I identified genes which regulate segmentation and ephyra morphogenesis. Involvement of retinoic acid, *hedgehog* and *Wnt* signaling pathways was tested by chemical interferences. Besides, two *TRGs* are good candidates for the direct regulators of segmentation due to their expression patterns. Most probably, in every segment RA is synthesized by *RDH2*, and *RxR* controls the expression pattern of downstream genes - *Wnt1*, *BMP* and *ETS*. At the same time, *Ptc* marks

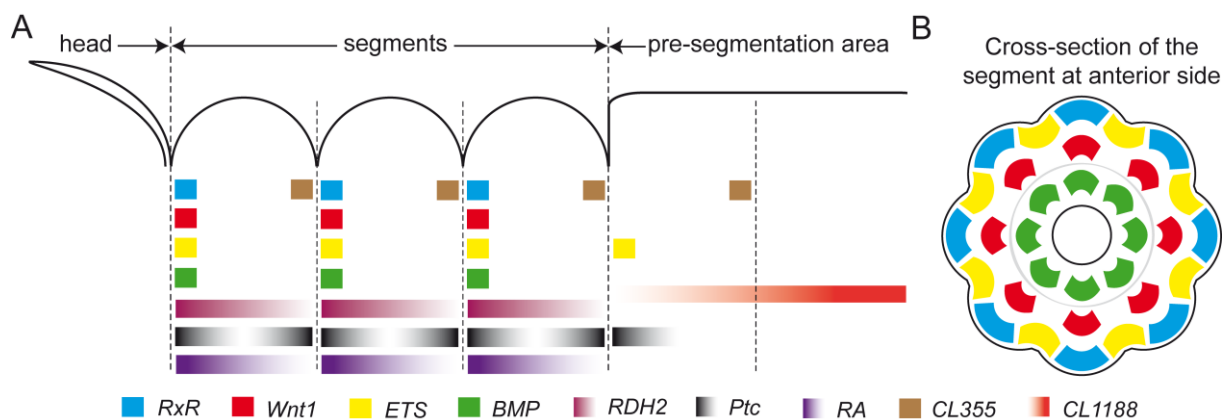


Fig. 50 Model for the establishment of anterior-posterior polarity during segmentation in *Aurelia aurita*. (A) Expression domains of genes involved in the establishments of anterior-posterior polarity. Body wall is represented as a black line and the segment boundaries are marked with dotted lines. Colored solid squares represent the expression domains of genes. *RxR* - blue, *Wnt1* - red, *ETS* - yellow, *BMP* - green, *RDH2* - fuchsia, *Ptc* - grey, *RA* - purple, *CL355* - brown and *CL1188* - pink. (B) Cross-section of the segment at the anterior side at the beginning of ephyra morphogenesis. *RxR* (blue) and *Wnt1* (red) are expressed in the ectoderm of protrusions, *ETS* (yellow) is located between protrusions. Gray line marks the border between ectoderm and endoderm. *BMP* (green) is expressed in the endoderm of each protrusion.

both sides of the segment and specifies the polarity by its expression gradient. *CL355* is used to mark the posterior side of each segment and the gradient of *CL1188* defines the non-segmented area.

A model of presumed segment polarity elements in *Aurelia aurita* is shown in Fig.50A. Firstly, the RA synthesizing enzyme *RDH2* (fuchsia) shows decreasing gradient from the anterior side to the posterior boundary in the segment. RA (purple) might show the same distribution as increasing gradient from the posterior end of the segment to the anterior side. *RxR* (blue), *Wnt1* (red) and *ETS* (yellow) are specifically expressed at the anterior side of each segment in the ectoderm and *BMP* (green) in the endoderm. Meanwhile, *CL355* (brown) appears at the posterior end. In the forming segment, *ETS* (yellow) and *CL355* (brown) mark the boundaries of the segment at the anterior and posterior sides, respectively. *Ptc* (grey) is expressed as a gradient from both boundaries of one segment to the middle and in the anterior part of the forming segment. In non-segmented part, *CL1188* (pink) is expressed as a gradient and its transcript disappears as soon as the segment is formed. When the protrusions emerge, the cross-section of the segment at the anterior side is shown in Fig.50B. *RxR* (blue) and *Wnt1* (red) are expressed in the ectodermal cells of the protrusions, while *BMP* (green) is located in the endoderm. Meanwhile, the expression of *ETS* (yellow) is complementary to *RxR* and *Wnt1* and appears between two protrusions in the ectoderm. In sum, these data indicate that retinoic acid signaling, *ETS* transcription factor, *hedgehog*, *Wnt* and *TGF β* pathways in conjunction with two novel genes, play a key role in controlling segmentation and the development of lappets in ephyra.

3.4 What is the ancestral cnidarian life cycle?

Based on the research in the basal Metazoa we know that the last common ancestor of Cnidaria and Bilateria was a genetically complex organism which shared most of the gene families with extant representatives of Deuterostomia. Was this ancestral form a planula-like organism, or polyp-like? Or did it have a life cycle with several life forms following each other? Among the major difficulties in answering these questions is the bias of cnidarian research towards model systems with abridged life cycles. All cnidarian genomes sequenced so far (*Nematostella*, *Hydra*, *Acropora digitifera* and *Acropora millepora*) come from species which lack medusoid stage (Putnam *et al.*, 2007; Chapman *et al.*, 2010; Shinzato *et al.*, 2011).

Surprisingly little is known at the molecular level about scyphozoan and cubozoan jellyfishes that represent complete life cycles with larvae, polyps and medusa. Does life cycle regulation in Scyphozoa and Cubozoa represent the ancestral molecular framework from which life cycle regulation of the bilaterian organisms has emerged?

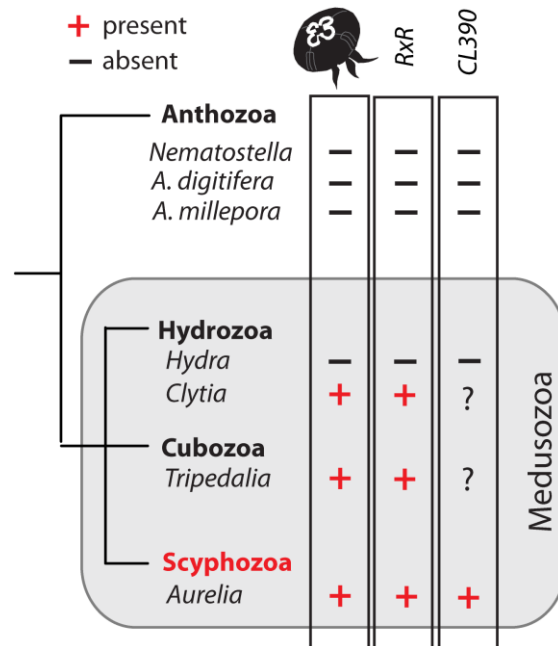


Fig. 51 Molecular machinery of the archetypical life cycle of Cnidaria. The RxR nuclear hormone receptor is present in scyphozoa (*Aurelia*), cubozoa (*Tripedalia*) and Hydrozoa (*Clytia*) which possess complete life cycle with a jellyfish stage. RxR receptor is absent in Anthozoa and *Hydra*.

One of the important differences between *Aurelia* and *Hydra*, *Nematostella* and *Acropora* is the presence of genes which are necessary for the retinoic acid signalling. The RxR receptor has an intriguing phylogenetic distribution among cnidarians. Genomes of three anthozoan species sequenced so far as well as the genome of *Hydra* contain no *bona fide* RxR receptors. None of these animals have a jellyfish stage in their life cycle. To the contrary, *Tripedalia*, *Aurelia* and *Clytia* which all have a jellyfish stage, also possess RxR receptors (see Fig.51). Is that a pure coincidence?

We know that in *Aurelia* the RxR is up-regulated during the strobilation induction and is down-regulated in ephyra stage. Incubation in RA and retinol can directly induce strobilation while RxR inhibitors repress it. In *Tripedalia*, it has been shown that RxR receptor has a strong affinity to 9-*cis* RA and binds consensus DNA sequences in the promoters of other genes (Kostrouch *et al.*, 1998). The RxR protein of *Tripedalia* is highly abundant in small

polyps and polyps undergoing metamorphosis and disappears sharply (<1 day) after the young ephyra were released (Kostrouch *et al.*, 1998). Interestingly, according to the same paper of Kostrouch and colleagues, the RxR receptor was not detected in the polyp lysate of *Aurelia*. Results in *Tripedalia*, therefore, fit well to the observations in *Aurelia* and support my hypothesis about the general importance of RxR for metamorphosis.

The phylogenetic distribution of the RxR receptor and the involvement of retinoic acid signaling in the regulation of the magnetic life cycle underscore the importance of gene loss in animal evolution (Miller *et al.*, 2005; Technau *et al.*, 2005). Taking into consideration the fact that RxR receptor homologs are necessary for life cycle regulation in Cnidaria (*Aurelia* and *Tripedalia*), insects and amphibians, it is feasible that the Urmetazoan ancestors of currently living cnidarians were animals with the complete life cycle and that the absence of the medusoid stage in Anthozoa is a secondary loss. Regarding this hypothesis it should be noticed that already in the Middle Cambrian deposits (~500 Myr) fossilized animals with jellyfish-like morphology have been reported (Cartwright *et al.*, 2007).

In sum, the molecules and pathways regulating the archetypal metagenetic life cycle of the basal Metazoa were identified. My results underscore the importance of Scyphozoa and Cubozoa for evolutionary studies and indicate that Urmetazoan ancestors might have been more complex than previously thought. Identification of the minimal pharmacophore of the strobilation inducers and an inhibitor of *Aurelia* has also a direct practical application. In the future this knowledge may lead to the development of powerful strobilation antagonists which can be used to control jellyfish blooms.

4 Material

4.1 Organisms and cell lines

***Aurelia aurita* strains :**

Baltic sea strain	Kiel bay, Germany
Roscoff strain	Pacific Ocean
White sea strain	Shupa bay, Russia

Feeding strain:

<i>Artemia salina</i>	Silver Star
-----------------------	-------------

Bacterial strains:

<i>E. coli</i> ElectroMAX™ DH5 α -E™	Invitrogen
<i>E. coli</i> Rosetta 2(DE3)pLysS	Novagen

4.2 Chemicals

Acetic acid	Roth
Acetic anhydride	Roth
Agar agar	Roth
Agarose	Roth
Ampicillin	Merck
Azur II	Merck
Boric acid	Roth
Bovine serum albumin (BSA) fraction V	Roth
Bromophenol blue	Sigma
Calcium chloride (CaCl ₂)	Roth
CHAPS	Roth
Chloroform	Roth
Dextran sulfate	Roth
Dipotassium phosphate (K ₂ HPO ₄)	Merck
dNTP mix (10mM)	Fermentas
EDTA	Roth
Ethanol	Roth
Ethidium bromide	Roth
Euparal	Roth
Ficoll	Sigma
Formamide	Roth
Gelatine	Sigma
Glucose	Roth
Glutaraldehyde	Sigma
Glycerol	Roth
Glycine	Roth
Heparin	Roth

Hoechst	Calbiochem
Hydrochloric acid (HCl)	Roth
Isopropanol	Roth
Levamisole	Roth
Magnesium chloride (MgCl ₂)	Merck
Magnesium sulfate (MgSO ₄)	Merck
Maleic acid	Roth
Methanol	Roth
Methylene blue	Merck
Monopotassium phosphate (KH ₂ PO ₄)	Merck
Mowiol 4-88	Calbiochem
TES	Sigma
NBT/BCIP	Roche
Nitrogen (N ₂)	Westfalia
Paraformaldehyde	Sigma
Peptone	Roth
Phalloidin-Tetramethylrhodamine	Sigma
Phenol	Roth
Polyvinylpyrrolidone	Sigma
Potassium chloride (KCl)	Roth
Procaine hydrochloride	Sigma
Rhodamine B Isothiocyanate-Dextran R9379	Sigma
Rotiphorese [®] Gel 40	Roth
Sea salt (Reef crystals [™])	Aquarium Systems
Sheep serum	Sigma
Sodium acetate	Roth
Sodium cacodylate	Sigma
Sodium chloride (NaCl)	Roth
Sodium citrate (Na ₃ (C ₆ H ₅ O ₇))	Roth
Sodium deoxycholate	Sigma
Sodium hydroxide (NaOH)	Roth
Sodium pyruvate	Sigma
Sudan Black B	Merck
Tetramethylethylenediamine (TEMED)	Serva
Triethanolamine	Sigma
TRIS base	Roth
TRIS-HCl	Roth
TritonX100	Merck
tRNA yeast	Sigma
Tryptic Soy Broth	Sigma
Tween-20	Roth
Urea	Roth
Urethane	Sigma
Yeast extract	Roth

4.3 Media

<i>Artemia</i> medium	30%(w/v) Reef crystals [™] in Millipore H ₂ O
Artificial Seawater	30%(w/v) Reef crystals [™] in Millipore H ₂ O
LB agar	LB medium, add 1.5%(w/v) Agar agar, autoclaved

LB medium	1%(w/v) Peptone, 0.5%(w/v) Yeast extract, 0.5%(w/v) NaCl in Millipore H ₂ O, autoclaved
LB medium with Ampicillin	LB medium, add 50µg/ml Ampicillin (sterile)
SOB medium	2%(w/v) Peptone, 0.5%(w/v) Yeast extract, 10mM NaCl, 25mM KCl in Millipore H ₂ O, autoclaved; add 10mM MgSO ₄ and 10mM MgCl ₂ (both sterile)
SOC medium	SOB medium, add 20mM glucose (sterile)

4.4 Buffer and Solutions

4.4.1 General

Ampicillin stock solution	100mg/ml in Millipore H ₂ O, sterile, store in -20 ⁰ C
10% APS	10%(w/v) in Millipore H ₂ O, fresh
10% SDS	10%(w/v) in Millipore H ₂ O
50x Denhardt's solution	1%(w/v) Polyvinylpyrrolidone, 1%(w/v) Ficoll, 1%(w/v) BSA fraction V in Millipore H ₂ O (sterile), store in -20 ⁰ C
10x DNA loading buffer	50%(v/v) glycerol, 10mM EDTA (pH 8.0), 0.1%(w/v) SDS, 0.1%(w/v) Bromophenol blue, 0.1%(w/v) Xylene cyanol in Millipore H ₂ O
EDTA solution	0.5M in Millipore H ₂ O, pH 8.0
Heparin	10mg/ml in Millipore H ₂ O, store in -20 ⁰ C
IPTG	100mM in Millipore H ₂ O, sterile, store in -20 ⁰ C
NTM buffer	100mM NaCl, 100mM Tris-HCl, 50mM MgCl ₂ in Millipore H ₂ O, pH 9.5
NTMT buffer	NTM + 0.1%(v/v) Tween-20
Paraformaldehyde/ASW	4%(w/v) in ASW, fresh
Paraformaldehyde/PBT	4%(w/v) in PBT, fresh
PBS	150mM NaCl, 80mM Na ₂ HPO ₄ , 20mM NaH ₂ PO ₄ in Millipore H ₂ O, pH 7.34
PBT	PBS + 0.1%(v/v) Tween-20
50x TAE buffer	2M Tris base, 0.05M EDTA, 5.71%(v/v) Acetic Acid in Millipore H ₂ O, pH 8.3
10x TBE buffer	1.3M Tris base, 0.45M Boric Acid, 25mM EDTA in Millipore H ₂ O, pH 8.5
Urethane relaxing solution	2%(w/v) in ASW
X-Gal	20mg/ml in Dimethylformamid, store in -20 ⁰ C

4.4.2 *In situ* hybridization

Blocking solution	20%(v/v) Sheep serum in MAB-B
Glycine solution	4mg/ml in PBT
Hybridization solution	50%(v/v) Formamide, 5x SSC, 0.1%(v/v) Tween-20, 0.1%(w/v) CHAPS, 1x Denhardt's, 100µg/ml Heparin in Millipore H ₂ O
HybMixII	50%(v/v) Formamide, 5x SSC in Millipore H ₂ O
MAB	100mM Maleic Acid, 150mM NaCl in Millipore H ₂ O, pH 7.5
MAB-B	1%(w/v) BSA fraction V in MAB
MAB-T	MAB + 0.1%(v/v) Tween-20
Triethanolamine	100mM in Millipore H ₂ O, pH 7.8

20x SSC	3M NaCl, 0.3M Sodium Citrate in Millipore H ₂ O, pH 7.0
Sheep serum	inactivation at +56 ⁰ C for 30 min, store in -20 ⁰ C
Levamisole	1M in Millipore H ₂ O, store in -20 ⁰ C

4.4.3 Protein purification

1x Ni-NTA bind buffer	300mM NaCl, 50mM Tris-HCl, 10mM Imidazole, 5%(v/v) Glycerol, 0.5%(v/v) Tween-20 in Millipore H ₂ O, pH 8.0, add Protease Inhibitor Cocktail tablet (one in 10ml) before use
1x Ni-NTA wash buffer	300mM NaCl, 50mM Tris-HCl, 20mM Imidazole, 5%(v/v) Glycerol, 0.5%(v/v) Tween-20 in Millipore H ₂ O, pH 8.0
1x Ni-NTA elute buffer	300mM NaCl, 50mM Tris-HCl, 350mM Imidazole, 5%(v/v) Glycerol, 0.5%(v/v) Tween-20 in Millipore H ₂ O, pH 8.0

4.4.4 gDNA extraction

CTAB buffer	1.4M NaCl, 0.02M EDTA, 0.1M Tris-HCl (pH 8.0), 2%(w/v) Cetyltrimethylammonium Bromide (CTAB), 0.2%(v/v) β-Mercaptoethanol in Millipore H ₂ O
TE buffer	10mM Tris-HCl, 1mM EDTA in Millipore H ₂ O, pH 8.0

4.4.5 Western blot

Separation buffer	1.5M Tris-HCl in Millipore H ₂ O, pH8.8
Stacking buffer	0.5M Tris-HCl in Millipore H ₂ O, pH6.8
5x SDS-PAGE running buffer	125mM Tris-base, 0.96M Glycine, 0.5%(w/v) SDS in Millipore H ₂ O
Coomassie brilliant blue destaining solution	50%(v/v) Methanol, 10%(v/v) Acetic acid in Millipore H ₂ O
Coomassie brilliant blue staining solution	0.05%(w/v) Coomassie brilliant blue R250 in Coomassie brilliant blue destaining solution
5x SDS-PAGE loading buffer	200mM Tris-HCl (pH 6.8), 20%(v/v) Glycerol, 10%(w/v) SDS, 0.05%(w/v) Bromphenol blue in Millipore H ₂ O; when uses it add 10%(v/v) β-Mercaptoethanol
Transfer buffer	48mM Tris-base, 39mM Glycine, 0.0375%(w/v) SDS, 20%(v/v) Methanol in Millipore H ₂ O, store in +4 ⁰ C

4.4.6 DNA sequencing

Sequencing gel for LI-COR (41 cm)	10.5g urea, 14ml Millipore H ₂ O, 3.75ml Rotiphorese [®] Gel 40, 2.5ml 10x TBE, 38μl TEMED, 175μl 10% APS
-----------------------------------	---

4.5 Kits

Amnicon [®] Ultra Centrifugal Filters	Millipore
DIG RNA Labeling Kit (SP6/T7)	Roche
DNeasy [®] Blood & Tissue Kit	Promega
First Strand cDNA Synthesis Kit	Fermentas

GoTaq [®] qPCR Master Mix	Qiagen
illustra [™] QuickPrep <i>Micro</i> mRNA Purification Kit	GE Healthcare
MEGAscript [®] RNAi Kit	Ambion
NucleoSpin [®] Extract II Kit	Macherey-Nagel
NucleoSpin [®] Plasmid QuickPure Kit	Macherey-Nagel
pGEM [®] -T Vector System	Promega
Sequencing Kit	Applied biosystems
SequiTherm EXCEL [™] II DNA Sequencing Kit	Epicentre

4.6 Enzymes

4.6.1 General

DNase I	Fermentas
<i>Go Taq</i> DNA polymerase	Promega
Platinum [®] <i>Taq</i> Polymerase	Invitrogen
Platinum [®] <i>Taq</i> Polymerase High Fidelity	Invitrogen
Proteinase K	Sigma
RNase A	Fermentas
T4 ligase	Fermentas

4.6.2 Restriction enzymes

<i>ApaI</i>	New England Biolabs
<i>BstXI</i>	New England Biolabs
<i>EcoRI</i>	New England Biolabs
<i>NcoI</i>	New England Biolabs
<i>NotI</i>	New England Biolabs
<i>NsiI</i>	New England Biolabs
<i>PacI</i>	New England Biolabs
<i>PstI</i>	New England Biolabs
<i>SpeI</i>	New England Biolabs

4.7 Antibodies

Anti-Digoxigenin-alkaline phosphatase linked Fab fragments	Roche
polyclonal rabbit anti-eGFP antibody	Roche
Anti-His-Tagged protein Mo MAb	Calbiochem
Anti-mouse affinity isolation Alk, Phos, Con Sheep	Millipore

4.8 Vectors

LigAF-1

Provided by K. Khalturin

pGEM [®] -T	Promega
pET_28a(+)	Novagen

4.9 Size standards

GeneRuler [™] DNA Ladder Mix	Fermentas
PageRuler [™] Plus Prestained Protein Ladder	Fermentas

4.10 Oligonucleotides (Primer)

Table 1: Oligonucleotides

Description	Primer ID	Sequence (5' → 3')	T _m [°C]
Standard primers			
BMP	aBMP1_F	GATGACCCACTTATAAGAGAAGTCG	61,3
	aBMP1_Rin	TGCATTCATATGTGCACCAAGAGG	61,0
	aBMP1_RinII	GTGCAATGATCCAGTCCTCCC	61,8
	aBMP1_Rout	CTGGTACTTCTTGAGAACAACATTGC	61,6
	aBMP1_F-872	TTCTATCAGCTTTAACCAGAAGTTGC	60,1
Chordin	aBMPreg_F	GATCTTTCTCGAAGACATTTTCATTGC	60,1
	aBMPreg_R	CTTTTCCAGTACAAAGCCACTCC	60,6
	aBMPreg_Rin	GGAGAATGTCTGCACAATGATCC	60,6
CL112	aCL112_F	AATTCAAACCGAGACTGGAGGAG	60,6
	aCL112_Fin	GCAACTGCTTCGTTGGATTTACC	60,6
	aCL112_R	TTCTTGTTTCAGTGTTGGTCTCC	58,9
	aCL112_Rin	GCTTTGTCCTGCATCAATCACC	60,3
CL355	aCL355_F1	GTGTCTCAGCATTACAGAAGAC	60,6
	aCL355_F2	GCAGAGCATGTTGAAGGCTTAGC	62,4
	aCL355_R1	GCTAAATTCTCATCGCTGAAGCC	60,6
CL390	aCL390_F	CGACAATGAAGGTCCTTTCTATCC	61,0
	aCL390_R	TCAGAGATCTTTGTAGGCTCAACC	61,0
	a390_FII	CTCAAAGTAATCCTGTTACGTGTC	59,3
	aCL390_RII	TCGTTTCCTAACACTGTTGTTGTGG	61,3
	aCL390_FIII	TGCTCGCAGGAGATGTTACAG	59,8
	CL390_g_Rin	GGTGACAATATTCATAAAAAGAAGG	55,9
	CL390_g_Rout1	GATGTGATGAGAGAAAGGAGC	57,9
	CL390_g_Rout2	TGCTCTTCTAGTAACCATACACA	57,1
CL631	aCL631_F	CCATATGAAAAGTTGCCTTGACGG	61,0

	aCL631_R	CTCATCGGAGATACTGATAGATAACC	61,3
CL1008	CL1008_F	GATTGCAAAATTGAACTGAAAAGGG	58,1
	CL1008_R	TCAGTATTTTGACTTCATTGAGGG	57,6
CL1188	aCL1188_F1	GAACACAGAGCGTGAAAGCAAGTG	62,7
	aCL1188_R1	CATCCTTCAACCTCTTCTCAGAGC	62,7
Dickkopf	aDKK1_F(33)	GACCTTCACGCCACCATC	58,2
	aDKK1_R(1008)	TCCATACTGAGCCTGCGG	58,2
DNMT1	DNMTb_F	GGCATGCACAGTTCATCGTGG	61,8
	DNMTc_R	CCAGTTTCTCCAAGAAGCTGTTTCG	61,0
	DNMTa_F	AAGATGCAGTGGATGAATCAGTGG	61,0
	DNMTb_R	GATGTATCTCACTAACGGAGTGG	60,6
	DNMTR3out	ATCCGGATTCGCCATTGTTTATATGC	61,6
	DNMTR3in	GGAAAACAGATGTTCCATTCAATGG	61,9
	DNMTR5in	CACAAAATCATCTGAGCCCATATCC	61,3
	DNMTR5out	CTTTATTCTTCTCAATTAGTCCATTGTCCG	61,0
EF1	aEF1_FII	AGTTCCAGGGGACAATGTTGG	59,8
	aEF1_RII	GCTTGGAACCAAATTGACGATAGC	61,0
	aEF1_F36	CCGGTATATCTGGTAATCAACTAAAAC	60,4
	aEF1_R233	CACAAGGCAATATCAATGGTGATAACC	61,6
ETS	ETS4522_F	CTATAACGAGGAATATTATTTTAATAAATTACACG	60,1
	ETS4522_R	TCGAATTTGTAAGCGTAACGTTTGC	59,7
	ETS11185_F	AACAGCGGTTGTATCGCATGG	59,8
	ETS11185_R	GTATGGGTTTGGTCCCATCC	59,8
	ETS11055_F	CGAGTATCTGACAAGCTGTGC	59,8
	ETS11055_R	TGAGCTTGTCGTAATTCATGTTCG	59,3
PTC	aPatch2_F	CTTTCAGAGAATGCTTTATTGCTTGG	60,1
	aPatch2_R	TCAAAACAAGGAATGGCACTATTCC	59,7
RDH1	Retinol_hy I_F	AGACGCTACTTATTATTGAAAGACATTAC	59,6
	Retinol_hy I_R	AAGCTACGAGTAACTGTTAATGATTTAG	59,3
RDH2	Retinol_hy II_F	TCATCTAGAGTCAGCTGCTTGC	60,3
	Retinol_hy II_R	CAGCATCTTTCGCAATGGCG	59,4
RxR	RXR26884_F	TGCATTTGCCCGAGAAAGTCC	59,8
	RXR26884_R	TGGCATTATTTCTTGATTTTCTGTCCG	58,9
	RXR26884_RII	CAATTCATAATGACAACCTCTACAGCC	60,1
	RXR26884RACE3_out	AGCACTATGGAGTCGTTGCATGC	62,4
	RXR26884RACE3_in	CTTCAAAAGATCTGTCAGGAACAATCG	61,9
	RXR6CWO_F	TGTGCCAGCACTGAAATCAATAGG	61,0
	RXR6CWO_R	CAATTCATAATGACAACCTCTACAGCC	60,1
	RxR16788_F	TTCCGACAAGACCTCTTGAACC	60,3
	RxR16788_R	CTCAATCAATTGTGGATTGCTTATCC	60,1

	RXR_F3	CTGGAATGGAGTATGCTTGCG	59,8
	RXR_F3A	TCTCTCCAGATGCAAAAGAACTTG	59,3
	RXR_R3	GGCTATATTCTACGTAAGTGTACAC	59,7
SHH1	SSH1_F	AACTTCAATTCAGTCCCATCATCATG	60,1
	SSH1_R	GTGCCGCTTTCTGATCTTCAG	59,8
	SSH1_Rin	CAGGCACCACTGTGCATCC	61,0
	SSH1_Fin	CCACGAGATTGTGTTAACAAGAAGC	61,6
	SHH1_ATG_F	AATGGGAGACGGACCCACC	61,0
	SHH1_end_R	CAAAGCTATCTTTGCGTTGCAAGCG	61,0
	SHH1_F1	CTCTGTGTAAACTGAACCAAATCG	59,3
	SHH1_F2	TACTGACACAGAGAAAGCAGGG	60,3
SHH2	SHH2_F	TATAAATGGCTCAGAACTGATTACAGC	60,4
	SHH2_Fin	GCTCATATGAGCTTCTTGCCATGG	62,7
	SHH2_Rin	AGTCAAGGCGTAGCAAGACGC	61,8
	SHH2_RinII	CTAAAATGGTTCCTTCTTCTGTAAGTGG	62,2
	SHH2_Rout	ACATACCAATGTAGTCCAGTCTGG	61,0
	SHH2_F1	TGAGCACTATTTCAAACGCAGAATG	59,7
	SHH2_R667	ATGGACGTCTTTCAAACCTTTATGCG	60,1
Splinkerette	SplTop_1	CGAATCGTAACCGTTCGTACGAGAATTCGTACGA GAATCGCTGTCCTCTCCAACGAGCCAAGG	80,5
	SplBot_EcoR I	AATTCCTTGGCTCGTTTTTTTTTGCAAAAA	59,9
	SplBot_Spe I	CTAGCCTTGGCTCGTTTTTTTTTGCAAAAA	62,7
	SplOutPri_2	GAATCGTAACCGTTCGTACGAG	60,3
	SplInnPri_2	CGTACGAGAATCGCTGTCCTC	61,8
Wnt1	Wnt1_F	AAAGTTGTCAAAGATGTACGAGAAGG	60,1
	Wnt1_F2	GCGAGAACTATGTTGTGGTAGG	60,6
	Wnt1_R	GAATTAATGTCCATATTCCTGCTCG	59,7
	Wnt1_R2	AGGGTGAGAAGTTATGATTACTTCC	59,7
	Wnt1comp_F2	AAGAGATTTGGCCTAAGCACTGC	60,6
	Wnt1R5in	CACCATATATAACGACATTTACAATTCTCG	61,3
	Wnt1R5out	TACAAGTATGCTGCAAACGACTGC	61,0
	Wnt1comp_F	GATACAAAAGAAGCAGCATTTGTATATGC	61,0
Primers for the generation of constructs and sequencing			
CL112	CL112_R_Not I	GAGTGCGGCCGCGTCTTTTTCATATGGAC	69,5
	a112_F_Pac	CATTTAATTAATGAAAAATCACAGCCAATTCAAA CC	62,6
	a112_R_Pst	CATCTGCAGCAAATTATCCACTATGTTTCTATGC	65,9
	aCL112_F(490)_800	CCAAAGACATAAAGGCAACTG	55,9
CL390	CL390_R_Not I	GAGTGCGGCCGCGTCACCTCTTCTTCTG	72,4
	aCL390_NR_Not	GAGTGCGGCCGCGTCACCCAGAATATAGG	73,6

	a390_F_Pac	CATTTAATTAATACAAAAGACGCAGAGGAGAAG	63,6
	a390_R_Pst	CATCTGCAGTCAACCTCTTCTTCTGAACG	66,7
	a390_R_Pst_2	CATCTGCAGTCCACCTCTTCTTCTGAACG	68,1
	aCL390_F(i1)_IRD700	GTAAACTAATCGAGGAGAGAG	55,9
	aCL390_R(i1)_IRD800	CTCCCATACTTGACCTGACG	59,4
	aCL390_P_R700	ACCCTGCTGACTGTCTCGCA	61,4
CL631	CL631_R_Not I	GAGTGCGGCCGCGTCTTGGCTTCTCTTGGC	75,0
	a631_F_Pac	CATTTAATTAATGAAGAAGATGAAAGTGAGAC	60,5
	a631_R_Pst	CATCTGCAGTCATTGGCTTCTCTTGGCAG	68,1
GFP	GFP_F_Nco I	CATCCATGGAATTCAGTAAAGGAGAAGAAC	64,0
	GFP_Not_R	GATGCGGCCGCTTAGGCGATCGCTTTGTATAG	72,1
	GFP_F_Eco	CATGAATTCAGTAAAGGAGAAGAACTTTTC	61,3
	GFP_R_Pac	CATTTAATTAACGCGATCGCTTTGTATAGTTC	63,1
	GFP_F(625)_800	CGAAAGATCCCAACGAAAAGA	55,9
	GFP_R(75)_700	GTGCCCATTAACATCACCATC	57,9
M13	M13F_IRD700	GTAAAACGACGGCCAGT	52,8
	M13R_IRD800	GGAAACAGCTATGACCATG	54,5
pET_28a	pET_28a_R_700	GGTTATGCTAGTTATTGCTC	53,2
SP6	SP6_IRD700	ATTTAGGTGACACTATAGAATAC	53,5
T7	T7_IRD800	TAATACGACTCACTATAGGG	53,2
Primers for qRT-PCR			
CL112	aCL112_F2	GAAGCTACCAGATCCGTTTGG	59,8
	aCL112_R2	TGCAAGCGCATCTGTTCACAG	59,8
CL390	aCL390_F2	AAGGTGCGACAATGAAGGTCC	59,8
	aCL390_R2	CTCTACAGGCTCAATGGTGTCT	59,8
CL631	aCL631_F2	GCCTTGACGGTGAAAGATGAG	59,8
	aCL631_R2	ACCTCGTCCTCATCCTTTTCG	59,8
	aCL631_F2_II	GGGAGTACGTTCTTGAGCTTG	59,8
DNMT1	aDNMT_F2	CATGCACAGTTCATCGTGGAG	59,8
	aDNMT_R2	CAATCGAACGCCACGTAATGC	59,8
EF1	aEF1_F2	AGTTCAGGGGACAATGTTGG	59,8
	aEF1_R2	TGGATTTTCGCCAGGATGGTTC	59,8
PTC	aPTC1_F2	TTGCTGAAGAAGCCAGCCAAG	59,8
	aPTC1_R2	GGGAAGTTGGCAGTGAATTCG	59,8
RDH1	aRDH1_Q_F	GCATTTGCAAGTCATCCAGACG	60,3
	aRDH1_Q_R	GCTTGCTTTCAGCCATTTTACTG	59,3
RDH2	aRDH2_Q_F	TCATCTAGAGTCAGCTGCTTGC	60,3
	aRDH2_Q_R	CCGTCTAGCTTTGTTACTGAGC	60,3
RxR	aRXR_Q_F	AGATGTACAGTGCCACGTTGG	59,8
	aRXR_Q_R	CAAGTGTTTCGAGTGCTTGCAG	59,8

Primers for dsRNA synthesis			
CL112	aCL112_T7_F	CATTAATACGACTCACTATAGGGCAACTGCTTC GTTGGATTAC	71,3
	aCL112_T7_R	TACTAATACGACTCACTATAGGGCTTGTTTCAGT GTTGGTCTCC	72,2
CL390	aCL390_T7_F	TACTAATACGACTCACTATAGGGCAATGAAGGT CCTTTCTATCC	71,3
	aCL390_T7_R	TACTAATACGACTCACTATAGGGGAGATCTTTGT AGGCTCAACC	72,2
CL631	aCL631_T7_F	CATTAATACGACTCACTATAGGGCCATATGAAA AGTTGCCTTGAC	71,3
	aCL631_T7_R	TACTAATACGACTCACTATAGGGCATCGGAGAT ACTGATAGATAC	71,3
CL1008	aCL1008_T7_F	CATTAATACGACTCACTATAGGGGATTGCAAAA TTGAACTGAAAAGGG	71,1
	aCL1008_T7_R	TACTAATACGACTCACTATAGGGTCAGTATTTTG ACTTCATTGAGGG	71,2
GFP	T7_GFP_F	TAATACGACTCACTATAGGGACAGTGGAGAGGG TGA	70,6
	T7_GFP_R	TAATACGACTCACTATAGGGAGGCAGATTGTGT GGA	69,5

4.11 Devices

4.11.1 PCR- Thermocyclers

7300 Real Time PCR-System	Applied Biosystems
Primus 25	MWG-Biotech
Primus 96 <i>advanced</i>	peqLab
Primus 96 <i>plus</i>	MWG-Biotech

4.11.2 Power supplies

E835	Consort
EPS-3500	Pharmacia Biotech
EPS-500/400	Pharmacia Biotech
PP3000	Biometra

4.11.3 Gel electrophoresis chambers

Mini Sub-Cell	Bio-Rad
---------------	---------

Novex Mini-Cell	Invitrogen
PerfectBlue™ Twin L	peqLab
Sub-Cell® GT	Bio-Rad

4.11.4 Incubators / Shakers

C/R5 (water bath)	Julabo
CB150 Binder Certomat Incubator	B.Braun
HIS25 Grant	Boekel
KS10 (Rotation-shaker)	Edmund Bühler
Magnetic Stirrer Heidolph	Eydam
Thermo-Incubator	Heraeus Instruments
Thermomixer compact	Eppendorf
ThermoStat plus	Eppendorf

4.11.5 Electroporation devices

Gene Pulser II	Bio-Rad
Pulse Controller II	Bio-Rad

4.11.6 Centrifuges

Centrifuge 5415 D	Eppendorf
Centrifuge 5417 R	Eppendorf
ELMI Centrifuge+Mixer	ELMI Ltd
Mini Spin	Eppendorf
Multifuge 3 S-R	Heraeus Instruments
Multi-Spin MSC-6000	Kisker-Biotech
Sorvall RC 5B	Du Pont Instruments
Universal Vacuum System Plus	Savant

4.11.7 Microscopy

Axiocam (digital camera)	Zeiss
Axioskop 2	Zeiss
Axiovert 100	Zeiss
CLSM TCS SP/UV	Leica
DC300F (digital camera)	Leica
DP71 (digital camera)	Olympus
KL1500 LCD	Schott
MS 5 Binocular	Leica
SZX 16 Binocular	Olympus
Wild M3C Binocular	Heerbrugg

4.11.8 UV-devices

Gel-Doc™ XR+	Bio-Rad
ImaGO Compact Imaging System	B&L-Systems
UV lamp Chroma 43	Vetter GmbH
UV-Stratalinker® 1800	Stratagene

4.11.9 Photometer

BioPhotometer	Eppendorf
Nanodrop ND1000 photometer	Eppendorf
Nanodrop ND3300 photometer	Eppendorf

4.11.10 Sequencers

4300 DNA Analyzer	LI-COR
454 GS-FLX Titanium	Roche

4.11.11 Other devices

1205 MP Weighing scale	Sartorius
AF-10 (ice machine)	Scotsman
Air pump	Wisa D.B.G.M
Elektrophoresis Power Suply Consort EL 231	peqLab
Freezer -20°C	Liebherr
Freezer -80°C	Forma Scientific
Kern 770 Weighing scale	Kern
Lyophilizer Alpha 2-4 LSC	Christ
Microwave	Moulinex
Milli-Q Academic System	Millipore
pH-Meter pH 211 Microprocessor	Hanna Instruments
Refrigerator	Liebherr
Vortex-Genie2	Scientific Industries

4.12 Expendable materials

1ml syringe	Braun
8-Lid chain, dome cap	Sarstedt
10ml pipettes	Sarstedt
12-well microtiter plates	Greiner bio-one
20ml syringe	Henke-Sass, Wolf
Cover slips	Roth
Electroporation cuvettes (1mm and 4mm)	Peqlab
Extra thick filterpaper	Invitrogen
Latex gloves	Roth
Membrane filter disc (0.025µm)	Millipore™
Microscope Slides	Walter-CMP
Microtube 1.5ml	Sarstedt
MultiPLY® - Pro cup 0.2ml	Sarstedt
MultiPLY® -µStrip Pro 8-strip	Sarstedt
MultiPLY® -µStrip 0.2ml chain	Sarstedt
Nitril gloves	Roth
Parafilm	Pechiney Plastic Packaging
Pasteur pipettes (150mm, 230mm)	Eydam
Petri dishes (35x 10mm, 60x 15mm, 92x 16mm)	Sarstedt

Pipette tips (2.5µl, 200µl, 1000µl, 5ml)	Sarstedt
Plastic dishes	Westmark
SafeSeal tube 2ml	Sarstedt
Scalpel blades	Merck
Tube (15ml, 50ml)	Sarstedt
UVette®	Eppendorf

4.13 Other materials

250ml tubes	Sorval
Beaker glasses	Schott
Easypet	Eppendorf
Erlenmeyer flasks	Schott
Glass bottles	Schott
Graduate zylinder	Schott
Micro cannulation needle	Hamilton Bonaduz AG
Pipettes	Eppendorf
Sieves	Nuova

4.14 URLs

AG Bosch internal BLAST server	http://134.245.171.51/blast/
BLAST searches	http://blast.ncbi.nlm.nih.gov/Blast.cgi
Compagen	http://compagen.zoologie.uni-kiel.de/
ConSite	http://www.phylofoot.org/consite .
NCBI	http://www.ncbi.nlm.nih.gov
MWG	http://www.eurofindna.com/de/home.html
Ribosomal Database Project	http://rdp.cme.msu.edu/
SMART	http://smart.embl-heidelberg.de/
UniProt	http://www.uniprot.org

4.15 Software

Adobe Illustrator CS3	Adobe
Axio Vision 3.1	Zeiss
BioEdit	http://www.mbio.ncsu.edu/bioedit/bioedit.html
Blast2Go	http://www.blast2go.com/b2glaunch/start-blast2go
Cell^A Imaging software	Olympus
DNAMAN 7	Lynnon
e-Seq 3.0	LI-COR
Feature Extraction Software 10.7	Agilent
GeneSpring	Agilent
HMMER	http://hmmer.janelia.org/
Illustrator CS3	Adobe

IM 50 4.0

InterProScan

MEGA 3.0

MEGA 4.0

MINIMUS/MUSCLE

Photoshop CS3

Leica

<http://www.ebi.ac.uk/Tools/InterProScan>

<http://www.megasoftware.net/index.html>

<http://www.megasoftware.net/index.html>

<http://sourceforge.net/apps/mediawiki/amos/index.php?title=AMOS>

Adobe

5 Methods

5.1 Cultivation of Organisms

5.1.1 Cultivation of *Aurelia aurita*

We have three different *Aurelia aurita* strains: Roscoff strain, Baltic sea strain and White sea strain. Most of the experiments were carried out using *Aurelia aurita* Roscoff strain which was kindly provided by PD Dr. Gerhard Jarms (University of Hamburg, Germany). In addition to Roscoff strain, polyps originating from the Baltic sea (Kiel bay, Germany) and the White sea (Shupa bay, Russia) were used. The Baltic sea strain was obtained by culturing planula larvae collected from adult jellyfishes and the polyps of the White sea strain were kindly provided by Dr. Tatiana Shaposhnikova (Saint-Petersburg State University, Russia). Genetic relations among strains are shown in Fig.4. Baltic sea polyps were cultured in artificial sea water with the salinity of 18‰.

Animals were cultured in 3 liter glass containers with aeration in artificial sea water (ASW, 30‰ Reef Crystals) at +18°C or +20°C. Polyps were fed twice per week with freshly hatched *Artemia salina* nauplii and washed after 24 hours. Strobilation in Roscoff strain was induced by incubating polyps at +10°C.

5.1.2 Cultivation of *Artemia salina*

First instar nauplius larvae of *Artemia salina* served as food for all *Aurelia aurita* strains. Eggs were incubated for 24h at +30°C in *Artemia* medium under the permanent air supply for hatching. Nauplii were collected for feeding.

5.1.3 Temperature induction of strobilation in *Aurelia aurita*

The polyps of *Aurelia aurita* Roscoff strain were induced by incubating at +10°C in refrigerator. After 2-3 weeks, the animals started strobilation. The number of individuals in the culture did not affect the induction.

5.2 Transplantation and feeding experiments

During transplantation and feeding experiments recipient polyps were kept at +18°C. All the tissue pieces were either transplanted or fed onto or into polyps which were conducted in 85mM Petri dishes filled with ASW and were statistically observed for the occurrence of strobilation for at least 96 h.

5.2.1 Preparation the tissue pieces for transplantation and feeding

From the animals of *Aurelia aurita* Roscoff strain, early strobilae with tentacles, no rhopalia and with light orange coloration were selected. Three different strobila tissues were investigated: the head, the rings and the foot. The head with tentacles was cut just above the first constriction of the strobila. The foot was separated underneath the youngest constriction. Two segment rings were transplanted or fed.

The polyp pieces were prepared by quartering the whole animal and discarding the foot and the tentacles. The whole ephyra was used for transplantation and quartered for feeding.

5.2.2 Transplantation setup

The tissue piece for transplant and its host polyp were put onto a fishing line (\varnothing 0.28mm) with sharpened ends to penetrate the polyp. The transplant was either punctured or easily put onto the line. Two pieces of the polyethylene tube (\varnothing 0.38mm) were put onto both sides of the fishing line to stabilize the setup. After 24 h, this set-up was removed and the healing rate was approximately 30-40%.

5.2.3 Feeding procedure

The tissue pieces were directly put into the gastric cavity of polyps and kept inside for several days. The setup was checked every 12 h. If the fed piece was spat out, it was re-fed.

5.3 Standard laboratory methods

5.3.1 Isolation of mRNA

mRNA was extracted using illuatra™ QuickPrep Micro mRNA Purification Kit (GE Healthcare) according to the manufacturer's protocol. Then mRNA precipitation was washed with 70% ethanol for twice. Afterwards, the dried mRNA was re-dissolved in 20µl Millipore H₂O.

5.3.2 Isolation of gDNA

gDNA was extracted using modified CTAB method according to the protocol described by Berntson *et al.*(1999). The extracted gDNA was purified using DNeasy Blood & Tissue Kit (Qiagen) according to the manufacturer's protocol.

5.3.3 Quantification of nucleic acids

The quantity and quality of isolated nuclear acids were determined at the absorbance at 260nm using the Nanodrop spectrophotometer (Thermo Scientific).

5.3.4 First strand cDNA synthesis

The synthesis of cDNA was performed using the First Strand cDNA Synthesis Kit (Fermentas) according to the manufacturer's protocol using Oligo(dT)₁₈ primer. For subsequent comparative analyses of gene expression by PCR, equal amounts of mRNA were used as templates for the reactions.

5.3.5 Double strand cDNA (dscDNA) synthesis

To synthesis dscDNA, the SuperScript™ Double-Stranded cDNA Synthesis Kit (Invitrogen) was used according to the manufacturer's protocol. dscDNA was used to amplify the 5'- and 3'- unknown regions of interested genes.

5.3.6 Splinkerette synthesis and ligation

5µl Splinkerette top primer and 5µl different bottom primers (100pmol/l) were hybridized to double strand Splinkerette adaptors (50pmol/l) by incubation the mixtures at +95°C for 2 min and then slowly cooled down to RT. Afterwards the Splinkerette adaptors were ligated to

dscDNA with blunt ends or overhangs gDNA produced by different restriction enzymes. The pipetting scheme for ligation is shown in Table 2. The ligation was performed at +37°C for 2 h and subsequently stopped by incubation at +70°C for 20 min. Ligation products were used as templates for Splinkerette PCR.

Table 2: Pipetting scheme for ligation Splinkerette adaptor

Component	Volume	Final concentration
dscDNA or digested gDNA	X μ l	1 μ g
Splinkerette adaptor (50pmol/ μ l)	2 μ l	100pmol
10x T4 Ligase buffer	4 μ l	1x
T4 Ligase (3U / μ l)	1 μ l	3U
Millipore water	33-X μ l	
Final volume	40μl	

5.3.7 Polymerase chain reaction (PCR)

5.3.7.1 Standard PCRs

Standard PCR and RT-PCR reactions and program for amplification the sequences from DNA or cDNA (RT-PCR) were shown in Table 3, Table 4 and Table 5. The PCR products were analyzed *via* agarose gel electrophoresis.

Table 3 Pipetting scheme for PCR using plasmid or DNA as template

Component	Volume	Final concentration
5x GoTaq Reaction buffer	10 μ l	1x
dNTP-Mix (10mM)	1 μ l	0,2mM
Forward-Primer (10 μ M)	2.5 μ l	0.5 μ M
Reverse-Primer (10 μ M)	2.5 μ l	0.5 μ M
Go- <i>Taq</i> DNA-Polymerase (5U/ μ l)	0,1 μ l	0,01U
DNA template	X μ l	10ng
Millipore water	33.9-X μ l	
Final volume	50μl	

Table 4 Pipetting scheme for RT-PCR

Component	Volume	Final concentration
5x GoTaq Reaction buffer	4 μ l	1x
dNTP-Mix (10mM)	0,4 μ l	0,2mM
Forward-Primer (10 μ M)	1 μ l	0.5 μ M
Reverse-Primer (10 μ M)	1 μ l	0.5 μ M
GoTaq DNA-Polymerase (5U/ μ l)	0,1 μ l	0,025U
cDNA template (1:20)	1 μ l	
Millipore water	12.5 μ l	
Final volume	20μl	

Table 5: Standard PCR program

Step	Temperature	Time
Initial denaturation	94 °C	3 min

Amplification (20 - 40 cycles):		
1. Denaturation	94 °C	30 sec
2. Annealing	T _m – 1 °C	30 sec
3. Elongation	72 °C	1 min/1 kb
Terminal Elongation	72 °C	5 min

T_m= melting temperature of the used primer-pair

Elongation time was depending on the length of the amplified PCR fragment. A synthesis rate of the *Taq* polymerase of 1,000 bp per minute was used to estimate the elongation time.

5.3.7.2 Colony Check PCR

Colony Check PCRs serve to analyze plasmids for insertion of DNA sequences, which were carried by transformed bacteria *E. coli* DH5 α . Single bacterial colonies were picked from agar plates and served as DNA template for a standard PCR reaction of a final volume of 10 μ l. For DNA sequences ligated into pGEM[®]-T vector, plasmid-specific primers pair SP6 and T7 were used. pET-28a(+)-inserted sequences were amplified by either using the T7 promoter primer T7_IRD800 and pET_28a_R_700 or GFP_F and pET_28a_R_700. Colony check PCRs were run for 35 cycles.

5.3.7.3 High Fidelity PCR

For amplification the DNA fragments for expression constructs, Platinum[®] *Taq* Polymerase High Fidelity with proof reading ability was used. Table 6 contains the pipetting scheme for the reaction. The used PCR program is shown in Table 7. The PCR products were analyzed *via* agarose gel electrophoresis.

Table 6 Pipetting scheme for High Fidelity PCR

Component	Volume	Final concentration
10x Reaction buffer	2 μ l	1x
MgSO ₄ (50mM)	0.8 μ l	2mM
dNTP-Mix (10mM)	0.4 μ l	0,2mM
Forward-Primer (10 μ M)	1 μ l	0.5 μ M
Reverse-Primer (10 μ M)	1 μ l	0.5 μ M
Platinum [®] <i>Taq</i> Polymerase High Fidelity (5U/ μ l)	0,2 μ l	0,05U
DNA template	X μ l	10-100ng
Millipore water	14.6-X μ l	
Final volume	20μl	

Table 7: High Fidelity PCR program

Step	Temperature	Time
Initial denaturation	94 °C	2 min
Amplification (40 cycles):		
1. Denaturation	94 °C	30 sec
2. Annealing	T _m – 1 °C	30 sec
3. Elongation	68 °C	1 min/1 kb

CTGTCCTCTC CAACGAGCCA AGG-3', and the lower strand was based on the overhangs produced by the restriction enzymes for gDNA, or blunt end of dscDNA. Then the Splinkerette outer primer and specific outer primer as well as Splinkerette inner primer and specific inner primer were used for the first and second PCR, respectively. It combined three different PCR techniques - the "nested", "Hot Start" and the "Touchdown" PCR. For increasing the specificity of the products, two successive amplifications were carried out ("nested" PCR). In the first PCR, the outer primers were used. The product of this PCR was diluted 1:100 in ddH₂O and then used as template for further amplification with the respective inner primers. The pipetting scheme for the reaction was the same as High Fidelity PCR but using Platinum[®] *Taq* Polymerase. The used PCR program is shown in Table 10. The PCR products were analyzed *via* agarose gel electrophoresis.

Table 10: Splinkerette PCR program

Step	Temperature	Time
Initial denaturation	94 °C	2 min
Touchdown PCR (3x 7 cycles):		
1. Denaturation	94 °C	30 sec
2. Annealing	T _m + 6 °C – 1 °C/cycle	30 sec
3. Elongation	72 °C	2:30 min
Amplification (20 cycles)		
1. Denaturation	94 °C	30 sec
2. Annealing	T _m – 1 °C	30 sec
3. Elongation	72 °C	3 min
Terminal Elongation	72 °C	5 min

5.3.8 Electrophoretic separation of DNA samples

Using horizontal gel electrophoresis, DNA samples were separated. 1-2 %(w/v) agarose gels were prepared in 1x TAE buffer depending on the sizes of the fragments. To visualize DNA bands, 5µl ethidiumbromide was added into 100ml gel-solution. After loaded on the gel, DNA fragments were separated at 60 – 120 V. The size of DNA fragments was estimated using the GeneRuler[™] DNA Ladder Mix (Fermentas) as a size marker under UV-illumination.

5.3.9 Extraction of DNA fragments from agarose gel

The desired bands were cut under UV light and transferred into 1.5ml reaction tubes. Afterwards, DNA was extracted using the NucleoSpin[®] Extract II Kit (Macherey Nagel) according to the manufacturer's protocol.

5.3.10 Restriction digestion of DNA

For cloning DNA into pET-28a(+) vector, insert DNA and vector were digested with restriction enzymes to generate “sticky end” for ligation. The typical pipetting scheme for digestion is shown in Table 11. The digestion was performed at +37°C for 4 h and subsequently stopped by incubation at +70°C for 20 min. Using agarose gel electrophoresis, the digested fragments were separated and then purified from the gel.

Table 11: Pipetting scheme for digestion of DNA

Component	Volume	Final concentration
DNA	X μ l	2 μ g
10x Reaction buffer	5 μ l	1x
Restriction enzyme 1 (10U / μ l)	1 μ l	10U
Restriction enzyme 2 (10U / μ l)	1 μ l	10U
100x BSA	0.5 μ l	1x
Millipore water	42.5-X μ l	
Final volume	50μl	

5.3.11 Ligation of DNA fragments

5.3.11.1 Ligation of PCR products into pGEM[®]-T vector

PCR products were ligated into the pGEM[®]-T vector (Promega) *via* TA cloning for subsequent sequencing and expression construct assembly. The *Taq*-Polymerase generates adenosine (A) overhangs on the PCR products. Using these “sticky ends”, the insert DNA was ligated into the pGEM[®]-T vector with thymidin (T) overhangs. Ligations were carried out overnight at +4°C as shown in Table 12 and subsequently terminated by 20 min incubation at +70°C.

Table 12: Pipetting scheme for ligation PCR products into pGEM[®]-T vector

Component	Volume	Final concentration
Insert DNA	X μ l	5 – 100ng
pGEM [®] -T vector (50ng/ μ l)	0.5 μ l	25ng
2x Ligase buffer	2.5 μ l	1x
T4 Ligase (3U / μ l)	0.5 μ l	1.5U
Millipore water	1.5-X μ l	
Final volume	5μl	

5.3.11.2 Ligation of DNA fragments into pET-28a(+) vector

For expression constructs, vector and insert DNA with “sticky ends” were first generated by restriction digestion. Then ligation was carried out overnight at +4°C using digested vector and insert DNA in a molar ratio of 3:1 to 1:3. The pipetting scheme is shown in Table 13. Finally, ligation was terminated by incubation at +70°C for 20 min.

Table 13 Pipetting scheme for ligation DNA fragments into pET-28a(+) vector

Component	Volume	Final concentration
Digested insert DNA	X μ l	~100ng
Digested pET-28a(+) vector	Y μ l	~100ng
10x Buffer	5 μ l	1x
T4 Ligase (3U/ μ l)	1 μ l	3U
Millipore water	44-X-Y μ l	
Final volume	50μl	

5.3.12 Desalting of ligation products

Ligation products were desalted before transformation using Amnicon[®] Ultra Centrifugal Filters (Millipore) according to the manufacturer's instructions.

5.3.13 Transformation of *E. coli*

10 μ l desalinated ligation product was mixed with 50 μ l of *E. coli* ElectroMAX DH5 α (invitrogen) cell suspension and electroporated using Gene Pulser II and Pulse Controller II (Bio-rad) with the following conditions: 1.8 kV, 25 μ F and 200 Ω . Immediately after electroporation, cells were transferred into 1ml of pre-warmed SOC medium and incubated at +37°C with shaking at 220 rpm for 1 hour. 100 μ l – 400 μ l bacteria solution was plated on LB-Amp⁺ agar plate and incubated overnight at +37°C. Only cells containing the plasmid providing Ampicillin resistance were able to grow.

5.3.14 Preparation of plasmids

Identified by colony check PCR, the positive bacterial clones were propagated in 5ml LB-Amp⁺ medium and performed to plasmid preparation using the NucleoSpin[®] Plasmid QuickPure Kit (Macherey Nagel) according to the manufacturer's instructions.

5.3.15 Sanger DNA sequencing

DNA sequencing was carried out using the SequiTherm EXCEL II DNA Sequencing Kit-LC (Epicentre Technologies) as shown in Table 14. This technique is based on the Sanger dideoxy-mediated chain-termination method (Sanger *et al.*, 1977). All primers used to generate sequence amplicons were labeled with fluorescent dye IRD-800 or IRD-700 at the 5' end (MWG-Biotech). Fragments in pGEM[®]-T vector were amplified using a T7, SP6 or fragment specific primers. For the inserts in pET-28a(+) vector, sequences were amplified by using a T7_IRD800, pET_28a_R_700, GFP_F(625)_800, GFP_R(75)_700 or fragment specific primers. Sequencing reaction products were separated and detected in a LI-COR

Gene ReadIR 4200 (MWG Biotech) automated sequencing machine and analyzed by the manufacturer's software.

Table 14 Pipetting scheme for Sanger sequencing

Component	Volume	Final concentration
3.5x Sequencing buffer	3.6 μ l	1x
Plasmid	X μ l	200 ng
IRD-labeled primer (2 μ M)	1 μ l	0.31 μ M
Sequi Therm EXCEL II DNA Polymerase (5 U / μ l)	0.4 μ l	2 U
Millipore water	3.5-X μ l	
Final volume	8.5μl	

A total of 2 μ l of this mixture was added to 1 μ l of nucleotide mix containing the dideoxy nucleotides ddATP, ddCTP, ddGTP or ddTTP, respectively. The samples were subjected to the PCR program shown in Table 15.

Table 15: Cycle-Seq program for Sanger sequencing

Step	Temperature	Time
Initial denaturation	95 °C	5 min
Amplification (30 cycles):		
1. Denaturation	95 °C	30 sec
2. Annealing	52 °C	30 sec
3. Elongation	70 °C	1 min

The reaction was stopped by adding 3 μ l loading buffer. Prior to loading 0.8 μ l of the samples on a 41 cm sequencing gel in the 4300 DNA Analyzer (LI-COR Biosciences), they were denaturated for 10 minutes at +95°C. The results were analyzed using the e-Seq 3.0 program.

5.4 Whole mount *in situ* hybridization

5.4.1 Preparation of the labeled RNA probes

The transcript fragments (500 bp to 1500 bp) were amplified from cDNA, ligated into pGEM[®]-T vector, propagated into *E. coli* DH5 α and subsequently sequenced to verify the sequence and orientation of the inserted fragment in the plasmid. Using vector specific primers M13_F and M13_R, the insert fragment was amplified by PCR. 0.5 μ g purified PCR product was used as a template for the DIG RNA Labeling Kit (SP6/T7) (Roche) according to the manufacturer's protocol.

5.4.2 Whole-mount *in situ* hybridization protocol for *Aurelia aurita*

The protocol was modified from the *in situ* hybridization of *Hydra* (Grens *et al.*, 1999). The protocol is in the Appendix 8.1.

5.5 Chemical interference experiments

Stock solutions of 9-*cis* retinoic acid (RA, 1mM), retinol (ROL, 1mM), UVI3003 (2mM) and 4-diethylaminobenzaldehyde (DEAB, 20mM) were prepared in ethanol and stored at -70°C. Single polyp was incubated in 1ml ASW containing 1µM final concentration of RA or ROL in 48-well plates. UVI3003 was added in a final concentration of 1µM and DEAB in a final concentration of 10µM. Control animals were incubated in 1ml ASW with 0.15 % ethanol, non-treatment groups in ASW. All the animals were incubated in the dark at +18°C or +10°C and solutions were exchanged every day.

DNA methyltransferase inhibitor 5-Aza-2'-deoxycytidine was dissolved in DMSO as 100mM stock solution and stored in 20µl aliquots at -70°C. 20-30 polyps were incubated in 4ml ASW containing 100µM 5-Aza-2'-deoxycytidine. Control animals were incubated in 0.1% DMSO/ASW. All the animals were kept at +10°C with new solutions every day.

Cyclopamine, a specific *hedgehog* signaling pathway antagonist, was prepared as 20mM stock solution in ethanol and stored at -70°C. At +10°C, 10-20 polyps were incubated in Cyclopamine/ASW solution with the final concentrations of 2.5µM or 5µM. Ethanol/ASW solution was used as control. All solutions were renewed every day.

Synthetic peptides were ordered from Eurogentec (See Fig.31). 25mM stock solutions in DMSO were prepared and stored in 2µl aliquots at -70°C. Groups of 5-7 polyps were incubated in 1ml ASW containing 50µM peptide in 48-well plates (2µl peptide per 1ml ASW) at +18°C. DMSO solution in ASW (0.2 %) was used as control. Indole derivatives were ordered from Sigma (see Fig.35 and Table 18). Stock solutions (50mM) were prepared in ethanol and were stored at +10°C. Animals were incubated in groups of 5-10 polyps in 2.5ml ASW in 12 well plates at +18°C. L-tryptophan, 5-methoxy-tryptamine, 5-methoxy-DL-tryptophan, 5-hydroxy-L-tryptophan and L-tyrosin were diluted in DMSO. Solvents (EtOH or

DMSO) in the corresponding dilution were used in controls. Solutions were exchanged every day.

For segmentation and ephyra development experiments, 20-30 polyps were incubated in 4ml ASW containing 1 μ M retinol, 9-*cis* RA or *all-trans* RA. The solutions were changed every day. The morphology of the segments and ephyrae were recorded and compared with the control animals under the binocular microscope. For *in situ* hybridization experiment, 10-20 polyps were incubated in retinol/ASW solution with the final concentrations of 0.1, 0.5 and 1 μ M at 10°C. Ethanol/ASW solution was used as control. All solutions were renewed every day. After formation of the first several segments, the animals were fixed for *in situ* hybridization.

For the segmentation experiment, alsterpaullone was prepared as 5mM stock solution in ethanol and stored at -70°C. 10-20 polyps were induced to strobilate by 50 μ M 5-methoxy-2-methylindole. 48h after induction alsterpaullone was added to the final concentrations of 1 μ M, 2.5 μ M and 5 μ M. 0.2% solvent ethanol were added as control. The animals were fixed for *in situ* hybridization after 100h. Animals were kept at 18°C.

5.6 5-Brom-deoxy-Uridin (BrdU) labeling and detection

As a thymidin analogues base, BrdU can be incorporated into the DNA instead of thymidin in the cell cycle. So BrdU labeling was used to determine the proliferation activity of cells. Animals were exposed for 24 h to 5mM BrdU solution in ASW, relaxed in 2% Urethane relaxing solution, fixed in ice-cold 4% Paraformaldehyde/ASW, sectioned and subjected to BrdU detection as described previously for *Hydra* (Holstein *et al.*, 1991).

5.7 RNA interference (RNAi)

For dsRNA synthesis, a DNA template was amplified by PCR with specific RNAi primers (see Supplementary Table 1) from a plasmid template containing the coding region of a gene of interest. The PCR product was gel purified, dsRNA was synthesized with MEGAscript RNAi Kit (Life Technologies). The integrity and efficiency of dsRNA duplex formation was

examined on a 1% agarose gel, and the concentration of dsRNA was calculated by measuring its absorbance at 260nm using a Nanodrop spectrophotometer (Thermo Scientific).

dsRNA was transfected into polyps by electroporation. Before electroporation, polyps were washed three times with chilled electroporation buffer (0.77M Mannitol: filtered ASW = 4:1), then transferred into a chilled electroporation corvette with a 4mm electrode gap. Electroporation was carried out in 250 μ l of the electroporation buffer containing 20 μ g dsRNA and 10 μ l 5% Rhodamine B isothiocyanate-Dextran. To minimize the possibility of degradation, dsRNA was added just before electroporation. The setting of the Bio-Rad Gene Pluser II were the following: 120 V, 400 μ F. The pulse lasted for 30 - 40 ms. After electroporation polyps were immediately transferred into chilled filtered ASW and were kept at +10°C. Three hours after electroporation the medium was exchanged. ASW was exchanged every day. Depletion of the target genes was monitored by in situ hybridization (see Fig.28) and by real-time PCR (see inset in Fig.29).

5.8 Recombinant proteins expression and purification

5.8.1 Constructs for recombinant proteins

For the GFP tag, a 744 bp fragment of *gfp* was amplified from LigAF vector (Wittlieb *et al.*, 2006; Khalturin *et al.*, 2007) and cloned into the pET-28a(+) expression vector using *NcoI* and *NotI* restriction sites.

Coding regions of CL390, CL112 and CL631 were cloned into pET-28a(+)-GFP expression vector behind GFP. The coding fragments were amplified from cDNA with primers containing the *PacI* and *NotI* cutting sites, digested by the corresponding enzymes and ligated into pET-28a (+) -GFP vector. Afterwards constructs were electroporated into *E. coli* ElectroMAX DH5 α component cells followed by colony check PCR and plasmid preparation. Subsequently, the correctness of the constructs was proved by sequencing.

5.8.2 Expression of recombinant proteins

Chemically competent *E. coli* Rosetta 2(DE3)pLysS cells were transformed with pET-28a(+)-GFP-CL390, pET-28a(+)-GFP-CL112 and pET-28a(+)-GFP-CL631. Single colonies were

selected from the overnight grown plates and inoculated in 5ml LB-Kan⁺-Cam⁺ medium for overnight culturing at +37°C. Diluting 1:50 with fresh LB-Kan⁺-Cam⁺ medium, the culture was incubated at +37°C until OD₆₀₀ reached 0.6. Adding IPTG to a final concentration of 0.25mM, the protein expression was induced. After 2-4 hours, the bacteria were harvested for protein purification or SDS-PAGE.

5.8.3 Purification of recombinant proteins

After freeze at -20°C for 15-20 min, the bacterial pellet was resuspended in 5ml 1x Ni-NTA bind buffer containing 30µl lysozyme (100mg/ml) and a half piece of Protease Inhibitor cocktail tablet (cOmplete, Mini, EDTA-free, Roche) and incubated on ice for 30 min. Then the solution was sonicated on ice 1x 10 sec for 10 times. Adding 50µl DNase I (Fermentas) and 50µl MgCl₂ for 1 h at RT, the solution was again sonicated on ice 1x 10 sec for 10 times. After centrifugation, the supernatant was mixed with 50% slurry of Ni-NTA His-Bind Resin and incubated at +4°C for 1 h. After washing with 5ml 1x Ni-NTA wash buffer three times, the protein was eluted four times by 1ml 1x Ni-NTA elute buffer. All samples were analyzed by SDS-PAGE.

5.9 Western blot

5.9.1 Preparation of samples

20µg of protein (based on the OD₆₀₀ of the bacterial culture medium) was taken. After centrifugation, the pellet was resuspended by adding 16µl ddH₂O and 4µl 5x SDS-PAGE loading buffer. Then the sample was boiled for 5 min and centrifuged at max speed for 5 min. Finally, 10µl sample was loaded on the SDS-Gel.

5.9.2 SDS-PAGE

The glass plates were cleaned and assembled. 15% separating-gels were made by mixing the following reagents as shown in Table 16.

Table 16 Pipetting scheme for two 15% separating-gels

Component	Volume	Final concentration
Rotiphorese® Gel 30	3.33ml	15%
Separation buffer	1.67ml	375mM
10% SDS	66.7µl	0.1%

Millipore water	1.6ml	
10% APS	66.7 μ l	0.1%
TEMED	6.7 μ l	0.1%
Final volume	6.74ml	

10% APS and TEMED were added just before pouring the gel. Isopropanol was layered on the top of the gels to prevent dehydration and allow polymerizing. After 30 min – 1 h, isopropanol was removed by washing with Millipore water and the glass plates were dried by filter paper. Then stacking-gel was overlaid on the top with inserting comb. Table 17 contains the pipetting scheme for two 4% stacking-gels.

Table 17 Pipetting scheme for two 4% stacking-gels

Component	Volume	Final concentration
Rotiphorese [®] Gel 30	0.44ml	4%
Stacking buffer	0.83ml	125mM
10% SDS	33.3 μ l	0.1%
Millipore water	2.04ml	
10% APS	33.3 μ l	0.1%
TEMED	3.3 μ l	0.1%
Final volume	3.38ml	

30 min later, the combs were removed carefully, and the glass plates were assembled into the device filled with 1x SDS-PAGE running buffer. After loading the samples, 75V was used to run the stacking-gel, and then increased the voltage to 150V to run the separating-gels until the marker reached the bottom. The size of protein bands was estimated using the PageRuler[™] Plus Prestained Protein Ladder (Fermentas).

5.9.3 Coomassie brilliant blue staining

The SDS-Gels were transferred into Coomassie brilliant blue staining solution and shaken overnight at RT. Afterwards the SDS-Gels were destained by Coomassie brilliant blue destaining solution until weakened background.

5.9.4 Transfer membranes

After SDS-PAGE, the SDS-Gels were soaked in Transfer buffer for 15 min. PVDF membranes (Roth) were activated in methanol for 1 min and then incubated in Transfer buffer for 5 min as 8x Waterman papers. The transfer sandwich was assembled as follows: 4x Waterman papers, PVDF membrane, SDS-Gel and other 4x Waterman papers at the top. Any air bubble was rolled out after each layer. The transblot was run using 2 mA/cm² for 1-1.5 h.

5.9.5 Western blot

The membranes were taken out and washed with PBT for 5 min following with incubation in 0.5% BSA/PBT for 30 min at RT. Adding Antibody I to replaced 0.5% BSA/PBT (1:3000), the membranes were incubated overnight at +4°C with rotation. Afterwards the membranes were washed 4 times with PBT for 10 min following with 0.5% BSA/PBT for 15 min. New 0.5% BSA/PBT with Antibody II (Anti-mouse AP, 1:3000 dilution) was used to incubate the membranes for 1 h at RT with rotation. To thoroughly wash away the Antibody, the membranes were washed four times with PBT for 10 min at RT. Then the membranes were incubated twice in NTMT for 5 min. Afterwards the solution was replaced by the staining solution containing 1% NBT/BCIP in NTMT. The membranes were kept in the dark until a clear staining was detectable. The reaction was stopped by washing two times with Millipore water for 10 min. Finally, the membranes were dried by filter paper.

5.10 Transcriptome sequencing and assembly

mRNA was isolated from whole animals using illustra™ QuickPrep Micro mRNA purification kit (GE Healthcare). Double-stranded cDNA libraries were constructed using SMART™ PCR cDNA Synthesis Kit (Clontech). Libraries were sequenced using FLX sequencer (Roche). Raw reads have been deposited at the Sequence Read Archive (SRA) of NCBI under the project accession number SRA012593. Final transcriptome assembly (db454_aurelia_celera_v02) is available at www.compagen.org/aurelia.

Raw reads from all sequenced libraries were assembled *de novo* into contigs using the Celera v5.04 assembly pipeline (Miller *et al.*, 2008) (unitigger = bog; utgErrorRate = 0.03) followed by a merging step using Minimus2 (minid = 94%; overlap = 40; maxtrim = 20; wiggle = 16; conserr = 0.06) from the AMOS v2.08 software package (Sommer *et al.*, 2007). The complete assembly is available for downloading and blast searches at www.compagen.org/aurelia. Sequence similarity was analyzed using Basic Local Alignment Search Tool (BLAST) (Altschul *et al.*, 1990) and peptides from contig sequences were predicted by ESTScan software (Lottaz *et al.*, 2003).

5.11 Microarray Experiments

Microarray (in 4X 44K format) based on the Roscoff strain transcriptome of *Aurelia aurita* was designed using eArray software (Agilent). It contains 33,236 probes (60-mer oligonucleotides) which represent 29,608 contigs (see Fig.9). For the contigs where 5'-3' orientation was not clear (3,581 contig) both sense and antisense oligonucleotides were placed onto array. 50 housekeeping genes were used as a control probe group. Raw microarray image files were processed by Feature Extraction 10.7 Image Analysis software (Agilent). Mean gProcessedSignal values across all the samples were normalized using *elongation factor 1 alpha (EF1a)* expression. Microarray results are available online in the Microarray Atlas section (www.compagen.org/aurelia/aur_atlas_ma.html) and in the form of the SQL database (www.compagen.org/aurelia/aur_sql.php). User manual for microarray data access and retrieval is available at www.compagen.org/aurelia/docs/aurelia_db_manual.pdf.

5.12 Phylogenetic Analysis

Concerning to the three different strains: Roscoff, Baltic sea and White sea which were kept in our laboratory and the other lineages (Schroth *et al.*, 2002), the DNA sequences of the 16S ribosomal DNA (rDNA) and ITS1 (Internal transcribed spacer 1)/5.8S rDNA were compared. Alignments were done using Clustal W method (Thompson *et al.*, 1994). Two phylogenetic trees were created by maximum likelihood statistical model with Neighbor Joining Algorithm (Saitou & Nei, 1987) for 10,000 bootstrap replicates.

Phylogenetic analysis of RxR receptors from Protostomia and Deuterostomia. DBD-LBD regions were aligned by Clustal W (Thompson *et al.*, 1994) and the neighbour-joining tree was generated using MEGA 5.1. Numbers at nodes are bootstrap support values calculated by 1,000 replicates.

5.13 Microscopic Analysis

Images were taken on Axioscope fluorescence microscope with AxioCam digital camera (Zeiss) and on SZX16 stereomicroscope with DP71 camera (Olympus).

5.14 IT Software and Hardware

We use MySQL server 5.5 Percona and MySQL Workbench 5.2 CE from Oracle Corporation for data analysis and storage, high-performance computing cluster (HPC) with Rocks distribution v5.4.3 for transcriptome assembly and local BLAST searches, Apache 2.0 web server for online services, Seqtools 8.4 (<http://www.seqtools.dk/>) and mpiBLAST-1.6.0 (<http://www.mpiblast.org/>) for sequence analysis.

6 References

- Agata K, Inoue T. (2012). Survey of the differences between regenerative and non-regenerative animals. *Dev Growth Differ.* 54(2):143-52.
- Altschul SF, Gish W, Miller W, Myers EW, *et al.* (1990). Basic local alignment search tool. *J. Mol. Biol.* 215:403-10.
- Arai MN. (1997). A functional biology of Scyphozoa. Chapman and Hall. 68-206.
- Berntson EA, France SC, Mullineaux LS. (1999). Phylogenetic relationship within the class Anthozoa (phylum Cnidaria) based on nuclear 18S rDNA sequences. *Mol Phylogenet Evol.* 13(2): 417-33.
- Berking S, Czech N, Gerharz M, Herrmann K, *et al.* (2005). A newly discovered oxidant defence system and its involvement in the development of *Aurelia aurita* (Scyphozoa, Cnidaria): reactive oxygen species and elemental iodine control medusa formation. *Int J Dev Biol.* 49(8):969-76.
- Bode H, Lengfeld T, Hobmayer B, Holstein TW. (2008). Detection of expression patterns in *Hydra* pattern formation. *Method Mol Biol.* 469:69-84.
- Böhm A. (2009). Zell- und molekularbiologische Untersuchungen an der Ohrenqualle *Aurelia aurita*. Diplomarbeit.
- Briscoe J, Chen Y, Jessell TM, Struhl G. (2001). A hedgehog-insensitive form of patched provides evidence for direct long-range morphogen activity of sonic hedgehog in the neural tube. *Mol Cell.* 7(6): 1279-91.
- Broun M, Gee L, Reinhardt B, Bode HR. (2005). Formation of the head organizer in *hydra* involves the canonical Wnt pathway. *Development.* 132(12):2907-16.
- Brown DD, Cai L. (2007). Amphibian metamorphosis. *Dev Biol.* 306(1):20-33.
- Cartwright P, Halgedahl SL, Hendricks JR, Jarrard RD, *et al.* (2007). Exceptionally preserved jellyfishes from the Middle Cambrian. *PLoS One.* 2(10):e1121.
- Chapman JA, Kirkness EF, Simakov O, Hampson SE, *et al.* (2010). The dynamic genome of *Hydra*. *Nature.* 464(7288):592-6.
- Chen JK, Taipale J, Cooper MK, Beachy PA. (2002). Inhibition of Hedgehog signaling by direct binding of cyclopamine to Smoothened. *Genes Dev.* 16(21):2743-8.
- Chen ZQ, Kan NC, Pribyl L, Lautenberger JA, *et al.* (1988). Molecular cloning of the ets proto-oncogene of the sea urchin and analysis of its developmental expression. *Dev Biol.* 125(2): 432-40.
- Choy SW, Cheng SH. (2012). Hedgehog signaling. *Vitam Horm.* 88:1-23.
- Chute JP, Muramoto GG, Whitesides J, Colvin M, *et al.* (2006). Inhibition of aldehyde dehydrogenase and retinoid signalling induces the expansion of human hematopoietic stem cells. *Proc Natl Acad Sci U S A.* 103(31): 11707-12.
- De Blois E, Sze Chan H, Breeman WA. (2012). Iodination and stability of somatostatin analogues: comparison of iodination techniques. A practical overview. *Curr Top Med Chem.* 12(23):2668-76.
- Devon RS, Porteous DJ, Brookes AJ. (1995). Splinkerettes—improved vectorettes for greater efficiency in PCR walking. *Nucleic Acids Res.* 23(9):1644-5.
- Dirksen P. (2010). Untersuchungen zur Regulation des Lebenszyklus von *Aurelia aurita*. Diplomarbeit.
- Eivers E, Demagny H, De Robertis EM. (2009). Integration of BMP and Wnt signaling via vertebrate Smad1/5/8 and *Drosophila* Mad. *Cytokine Growth Factor Rev.* 20(5-6):357-65.

- Fuchs BS. (2010). Identifikation und funktionelle Analyse von Genen, die den Lebenszyklus von *Aurelia aurita* kontrollieren. Dissertation.
- Furlow JD, Neff ES. (2006). A developmental switch induced by thyroid hormone: *Xenopus laevis* metamorphosis. *Trends Endocrinol Metab.* 17(2):40-7.
- Garm A, Oskarsson M, Nilsson DE. (2011). Box jellyfish use terrestrial visual cues for navigation. *Curr Biol.* 21(9):798-803.
- Glibert S, Singer S. (2006). *Developmental Biology*. Sinauer Associates Inc, 8th edition.
- Glibert S. (2010). *Developmental Biology*. Sinauer Associates Inc, 9th edition.
- Graspeuntner S. (2012). Regulation des Lebenszyklus von *Aurelia aurita*. Masterthesis.
- Grens A, Shimizu H, Hoffmeister SA, Bode HR, *et al.* (1999). The novel signal peptides, pedbin and Hym-346, lower positional value thereby enhancing foot formation in *hydra*. *Development.* 126(3):517-24.
- Gudernatsch, JF. (1912) Feeding experiments on tadpoles. I. The influence of specific organs given as food on growth and differentiation: a contribution to the knowledge of organs with internal section. *Arch Entwicklunsmech Org.* 35:457-83.
- Guder C, Pinho S, Nacak TG, Schmidt HA, *et al.* (2006). An ancient Wnt-Dickkopf antagonism in *Hydra*. *Development.* 133(5):901-11.
- Hemmrich G, Khalturin K, Boehm AM, Puchert M, *et al.* (2012). Molecular signatures of the three stem cell lineages in *hydra* and the emergence of stem cell function at the base of multicellularity. *Mol Biol Evol.* 29(11):3267-80.
- Hofmann, D. K. , Neumann, R. , Henne, K. (1978). Strobilation, budding and initiation of scyphistoma morphogenesis in the rhizostome *Cassiopea andromeda* (Cnidaria: Scyphozoa). *Mar. Biol.* 47(2):161-76.
- Holstein TW. (2008). Wnt signaling in cnidarians. *Methods Mol Biol.* 469:47-54.
- Holstein TW, Hobmayer E, David CN. (1991). Pattern of epithelial cell cycling in *hydra*. *Dev Biol.* 148(2):602-11.
- Houliston E, Momose T, Manuel M. (2010). *Clytia hemisphaerica*: a jellyfish cousin joins the laboratory. *Trends in genetics.* 26(4):159-67.
- Huang K, García AE. (2013). Free energy of translocating an arginine-rich cell-penetrating peptide across a lipid bilayer suggests pore formation. *BioPhys J.* 104(2):412-20.
- Hwang JS, Ohyanagi H, Hayakawa S, Osato N, *et al.* (2007). The evolutionary emergence of cell type-specific genes inferred from the gene expression analysis of *Hydra*. *Proc Natl Acad Sci U S A.* 104(37):14735-40.
- Ingham PW, Nakano Y, Seger C. (2011). Mechanisms and functions of Hedgehog signaling across the metazoa. *Nat Rev Genet.* 12(6):393-406.
- Ishizuya-Oka A, Hasebe T. (2008). Sonic hedgehog and bone morphogenetic protein-4 signaling pathway involved in epithelial cell renewal along the radial axis of the intestine. *Digestion.* 77 Suppl 1: 42-7.
- Khalturin K, Anton-Erxleben F, Milde S, Plötz C, *et al.* (2007). Transgenic stem cells in *Hydra* reveal an early evolutionary origin for key elements controlling self-renewal and differentiation. *Dev Biol.* 309(1):32-44.
- Khalturin K, Hemmrich G, Fraune S, Augustin R, *et al.* (2009). More than just orphans: are taxonomically-restricted genes important in evolution? *Trends Genet.* 25(9):404-13.
- Koltzenburg M. (2004). The role of TRP channels in sensory neurons. *Novartis Found Symp.* 260: 206-13.

- Koop D, Holland ND, Sémon M, Alvarez S, *et al.* (2010). Retinoic acid signaling targets Hox genes during the amphioxus gastrula stage: Insights into early anterior-posterior patterning of the chordate body plan. *Dev Biol.* 338(1):98-106.
- Kostrouch Z, Kostrouchova M, Love W, Jannini E, *et al.* (1998). Retinoic acid X receptor in the diploblast, *Tripedalia cystophora*. *Proc Natl Acad Sci U S A.* 95(23):13442-7.
- Kroiher M, Siefker B, Berking S. (2000). Induction of segmentation in polyps of *Aurelia aurita* (Scyphozoa, Cnidaria) into medusae and formation of mirror-image medusa anlagen. *Int J Dev Biol.* 44(5):485-90.
- Kuniyoshi H, Okumura I, Kuroda R, Tsujita N, *et al.* (2012). Indomethacin induction of metamorphosis from the asexual stage to sexual stage in the moon jellyfish, *Aurelia aurita*. *Biosci Biotechnol Biochem.* 76(7):1397-400.
- Künzel T, Heiermann R, Frank U, Müller WA, *et al.* (2010). Migration and differentiation potential of stem cells in the cnidarian *Hydractinia* analysed in GFP-transgenic animals and chimeras. *Dev Biol.* 348:120-9.
- Kuroda K, Kuang S, Taketo MM, Rudnicki MA. (2013). Canonical Wnt signaling induces BMP-4 to specify slow myofibrogenesis of fetal myoblasts. *Skelet Muscle.* 3:5.
- Lai ZC, Rubin GM. (1992). Negative control of photoreceptor development in *Drosophila* by the product of the yan gene, an ETS domain protein. *Cell.* 70(4):609-20.
- Lee PN, Pang K, Matus DQ, Martindale MQ. (2006). A WNT of things to come: evolution of Wnt signaling and polarity in cnidarians. *Semin Cell Dev Biol.* 17(2):157-67.
- Leitz T, Wagner T. (1993). The marine bacterium *Alteromonas espejiana* induces metamorphosis of the hydroid *Hydractinia echinata*. *Mar Biol.* 115(2):173-8.
- Lenk L. (2011). Regulation des Lebenszyklus der Ohrenqualle *Aurelia aurita*. Bachelorarbeit.
- Leost M, Schultz C, Link A, Wu YZ, *et al.* (2000). Paullones are potent inhibitors of glycogen synthase kinase-3 β and cyclindependent kinase 5/p25. *Eur J Biochem* 267:5983-94.
- Levieu I, Williamson M, Grimmelikhuijzen CJ. (1997). Molecular cloning of a rephormone from *Hydra magnipapillata* containing multiple copies of Hydra-LWamide (Leu-Trp-NH₂) neuropeptides: evidence for processing at Ser and Asn residues. *J Neurochem.* 68(3):1319-25.
- Lewis C, Long TAF. (2005). Courtship and reproduction in *Carybdea sivickisi* (Cnidaria: Cubozoa). *Mar Biol.* 147:477-83.
- Li Y. (2010). Investigation of the strobilation in the scyphozoan *Aurelia aurita*. Bachelor Thesis.
- Lindgens D, Holstein TW, Technau U. (2004). Hyzic, the *Hydra* homolog of the zic/odd-paired gene, is involved in the early specification of the sensory nematocytes. *Development.* 131:191-201.
- Liu F, Kang I, Park C, Chang LW, *et al.* (2012). ER71 specifies Flk-1 hemangiogenic mesoderm by inhibiting cardiac mesoderm and Wnt signalling. *Blood.* 119(14):3295-305.
- Liu P, Wakamiya M, Shea MJ, Albrecht U, *et al.* (1999). Requirement for Wnt3 in vertebrate axis formation. *Nat Genet.* 22(4):361-5.
- Lottaz C, Iseli C, Jongeneel CV, Bucher P. (2003). Modeling sequencing errors by combining Hidden Markov models. *Bioinformatics.* 19:103-12.
- Maden M, Graham A, Zile M, Gale E. (2000). Abnormalities of somite development in the absence of retinoic acid. *Int J Dev Biol.* 44(1):151-9.
- Martin ME, Yang XY, Folk WR. (1992). Expression of a 91-kilodalton PEA3-binding protein is down-regulated during differentiation of F9 embryonal carcinoma cells. *Mol Cell Biol.* 12(5):2213-21.

- Maupetit J, Derreumaux P, Tufféry P. (2009). PEP-FOLD: an online resource for de novo peptide structure prediction. *Nucleic Acids Res.* doi:10.1093/nar/gkp323.
- McBrayer Z, Ono H, Shimell M, Parvy JP, *et al.* (2007). Prothoracicotropic hormone regulates developmental timing and body size in *Drosophila*. *Dev Cell.* 13(6):857-71.
- McGinnis W, Krumlauf R. (1992). Homeobox genes and axial patterning. *Cell.* 68(2):283-302.
- Meyer E, Aglyamova GV, Wang S, Buchanan-Carter J, *et al.* (2009). Sequencing and de novo analysis of a coral larval transcriptome using 454 GSFlx. *BMC Genomics.* 10:219.
- Miller DJ, Ball EE, Technau U. (2005). Cnidarians and ancestral genetic complexity in the animal kingdom. *Trends Genet.* 21(10):536-9.
- Miller JR, Delcher AL, Koren S, Venter E, *et al.* (2008). Aggressive assembly of pyrosequencing reads with mates. *Bioinformatics.* 24:2818-24.
- Miyake H, Terazaki M, Kakinuma Y. (2002). On the polyps of the common jellyfish *Aurelia aurita* in Kagoshima Bay. *J Oceanogr.* 58:451-9.
- Möller H. (1980). Population dynamics of *Aurelia aurita* medusae in Kiel Bight, Germany (FRG). *Mar Biol.* 60(2-3):123-8.
- Moreno TA, Kintner C. (2004). Regulation of segmental patterning by retinoic acid signaling during *Xenopus* somitogenesis. *Dev Cell.* 6(2):205-18.
- Nahoum V, Perez E, Germain P, Rodriguez-Barrios F, *et al.* (2007). Modulators of the structural dynamics of the retinoid X receptor to reveal receptor function. *Proc Natl Acad Sci U S A.* 104(44):17323-8.
- Nakamura Y, Tsiairis CD, Özbek S, Holstein TW. (2011). Autoregulatory and repressive inputs localize *Hydra* Wnt3 to the head organizer. *Proc Natl Acad Sci U S A.* 108(2):9137-42.
- Niederreither K, Subbarayan V, Dollé P, Chambon P. (1999). Embryonic retinoic acid synthesis is essential for early mouse post-implantation development. *Nat Genet.* 21(4):444-8.
- Nüsslein-Volhard C, Wieschaus E. (1980). Mutations affecting segment number and polarity in *Drosophila*. *Nature.* 287(5785):795-801.
- Ollikainen N, Chandsawangbhuwana C, Baker ME. (2006). Evolution of the thyroid hormone, retinoic acid, ecdysone and liver X receptors. *Integr Comp Biol.* 46(6):815-26.
- Oosterveen T, Kurdija S, Alekseenko Z, Uhde CW, *et al.* (2012). Mechanistic differences in the transcriptional interpretation of local and long-rang Shh morphogen signaling. *Dev Cell.* 23(5):1006-9.
- Paris M, Brunet F, Markov GV, Schubert M, *et al.* (2008). The amphioxus genome enlightens the evolution of the thyroid hormone signaling pathway. *Dev Genes Evol.* 218(11-12):667-80.
- Paris M, Laudet V. (2008). The history of a developmental stage: metamorphosis in chordates. *Genesis.* 46(11):657-72.
- Perz-Edwards A, Hardison NL, Linney E. (2001). Retinoic acid mediated gene expression in transgenic reporter zebrafish. *Dev Biol.* 229(1):89-101.
- Petie R, Garm A, Nilsson DE. (2011). Visual control of steering in the box jellyfish *Tripedalia cystophora*. *J Exp Biol.* 214:2809-15.
- Petie R, Garm A, Nilsson DE. (2013). Velarium control and visual steering in box jellyfish. *J Comp Physiol A Neurothol Sens Neural Behav Physiol.* 199(4):315-24.
- Prieto L, Astorga D, Navarro G, Ruiz J. (2010). Environmental control of phase transition and polyp survival of a massive-outbreaker jellyfish. *PLoS One.* 5(11):e13793.

- Putnam NH, Srivastava M, Hellsten U, Dirks B, *et al.* (2007). Sea Anemone Genome Reveals Ancestral Eumetazoan Gene Repertoire and Genomic Organization. *Science*. 317(5834):86-94.
- Remy P, Baltzinger M. (2000). The Ets-transcription factor family in embryonic development: lessons from the amphibian and bird. *Oncogene*. 19(55):6417-31.
- Renfer E, Amon-hassenzahl A, Steinmetz PR, Technau U. (2010). A muscle-specific transgenic reporter line of the sea anemone, *Nematostella vectensis*. *Proc Natl Acad Sci U S A*. 107(1):104-8.
- Rewitz KF, Yamanaka N, Gilbert LI, O'Connor MB. (2009). The insect neuropeptide PTTH activates receptor tyrosine kinase torso to initiate metamorphosis. *Science*. 326(5958):1403-5.
- Ristevski S, O'Leary DA, Thornell AP, Owen MJ, *et al.* (2004). The ETS transcription factor GABPalph is essential for early embryogenesis. *Mol Cell Biol*. 24(13):5844-9.
- Ruiz i Altaba A, Palma V, Dahmane N. (2002). Hedgehog-Gli signalling and the growth of the brain. *Nat Rev Neurosci*. 3(1):24-33.
- Ruppert EE, Fox RS, Barnes RD. (2004). *Invertebrate Zoology*. Brooks/Cole. 7th edition.
- Saitou N, Nei M. (1987). The neighbor-joining method: a new method for reconstructing phylogenetic trees. *Mol Biol Evol*. 4(4):406-25.
- Sandelin A, Wasserman WW, Lenhard B. (2004). ConSite: web-based prediction of regulatory elements using cross-species comparison. *Nucleic Acids Res*. 32(Web Server issue): W249-52.
- Sandell LL, Lynn ML, Inman KE, McDowell W, *et al.* (2012). RDH10 oxidation of Vitamin A is a critical control step in synthesis of retinoic acid during mouse embryogenesis. *PLoS One*. 7(2):e30698.
- Sanger F, Nicklen S, Coulson AR. (1977). DNA sequencing with chain-terminating inhibitors. *Proc Natl Acad Sci U S A*. 74(12):5463-7.
- Satou Y, Satoh N. (2003). Genome wide surveys of developmentally relevant genes in *Ciona intestinalis*. *Dev Genes Evol*. 213(5-6):211-2.
- Sawada Y, Hosokawa H, Hori A, Matsumura K, *et al.* (2007). Cold sensitivity of recombinant TRPA1 channels. *Brain Res*. 1160:39-46.
- Schmich J, Trepel S, Leitz T. (1998). The role of GLWamides in metamorphosis of *Hydractinia echinata*. *Dev Genes Evol*. 208(5):267-73.
- Schroth W, Jarms G, Streit B, Schierwater B. (2002). Speciation and phylogeography in the cosmopolitan marine moon jelly, *Aurelia sp.* *BMC Evol Biol*. 2:1.
- Shinzato C, Shoguchi E, Kawashima T, Hamada M, *et al.* (2011). Using the *Acropora digitifera* genome to understand coral responses to environmental change. *Nature*. 476(7360):320-3.
- Siebert S, Anton-Erxleben F, Bosch TC. (2008). Cell type complexity in the basal metazoan *Hydra* is maintained by both stem cell based mechanisms and transdifferentiation. *Developmental biology*. 313:13-24.
- Singh BN, Doyle MJ, Weaver CV, Koyano-Nakagawa N, *et al.* (2012). Hedgehog and Wnt coordinate signaling in myogenic progenitors and regulate limb regeneration. *Dev Biol*. 371(1):23-34.
- Sommer DD, Delcher AL, Salzberg SL, Pop M. (2007). Minimus: a fast, lightweight genome assembler. *BMC Bioinformatics*. 8:64.
- Soza-Ried J, Hotz-Wagenblatt A, Glatting KH, del Val C, *et al.* (2010). The transcriptome of the colonial marine hydroid *Hydractinia echinata*. *FEBS J*. 277:197-209.
- Spangenberg DB. (1967). Iodine induction of metamorphosis in *Aurelia*. *J Exp Zool*. 165(3):441-9.

-
- Spangenberg DB. (1971). Thyroxine induced metamorphosis in *Aurelia*. *J Exp Zool.* 178(2):183-94.
- Steinmetz PR, Kraus JE, Larroux C, Hammel JU, *et al.* (2012). Independent evolution of striated muscles in cnidarians and bilaterians. *Nature.* 487(7406):231-4.
- Strigini M, Cohen SM. (1997). A Hedgehog activity gradient contributes to AP axial patterning of the *Drosophila* wing. *Development.* 124(22):4697-705.
- Sugiura Y. (1965). On the life-history of rhizostome medusae. III. On the effect of temperature on the strobilation of *Mastigias papua*. *Biol Bull.* 128:493-6.
- Szuroczi D, Vesprini ND, Jones TR, Spencer GE, *et al.* (2012). Presence of *Ribeiroia ondatrae* in the developing anuran limb disrupts retinoic acid level. *Parasitol Res.* 110(1):49-59.
- Technau U, Rudd S, Maxwell P, Gordon PM, *et al.* (2005). Maintenance of ancestral complexity and non-metazoan genes in two basal cnidarians. *Trends Genet.* 21(12):633-9.
- Technau U, Steele RE. (2011). Evolutionary crossroads in developmental biology: Cnidaria. *Development.* 138: 1447-58.
- Thompson JD, Higgins DG, Gibson TJ. (1994). CLUSTAL W: improving the sensitivity of progressive multiple sequence alignment through sequence weighting, positions-specific gap penalties and weight matrix choice. *Nucl Acids Res.* 22:4673-80.
- Vermot J, Gallego Llamas J, Fraulob V, Niederreither K, *et al.* (2005). Retinoic acid controls the bilateral symmetry of somite formation in the mouse embryo. *Science.* 308(5721):563-6.
- Weigert G, Berisha F, Resch H, Karl K, *et al.* (2008). Effect of unspecific inhibition of cyclooxygenase by indomethacin on retinal and choroidal blood flow. *Invest Ophthalmol Vis Sci.* 49(3):1065-70.
- Wittlieb J, Khalturin K, Lohmann JU, Anton-erxleben F, *et al.* (2006). Transgenic Hydra allow in vivo tracking of individual stem cells during morphogenesis. *Proc Natl Acad Sci U S A.* 103(16):6208-11.

7 Acknowledgements

The completion of this thesis would not be possible without the guidance, support and encouragement from many people. My supervisor, Prof. Thomas Bosch, you are in no doubt the first person on this list. Thank you for replying so quickly to my very first email to you. Doing my PhD abroad was something I always wanted to do. Thank you for making all this possible! In many ways, coming to your lab was a leap of faith and a crossing of boundaries. My time in Kiel has been immensely rewarding and for this I will never be able to thank you enough.

To PD Dr. Konstantin Khalturin, your influence covered all aspects of my work and life for the past few years. Thank you for your scientific advices throughout my entire time in the lab, and for guiding this project in a very productive and rewarding direction. Thank you for your efforts in enhancing my writing and presentation skills as well as your psychological encouragement during my depressed moments. Thank you for the scientific philosophy that you have planted in my minds, the anecdotes you have shared, and the delicious holiday meals.

I would like to thank the entire Bosch lab, past and current members, for sharing your scientific expertise and creating a friendly and cheerful working environment. Dr. Björn Fuchs and Philipp Dirksen, thank you for orientating me to the lab environment and teaching me experimental techniques in my initial period in the lab. Lennert Lenk, especially thank you for wonderful companions in my first year of PhD study and picking me up from the hospital. Simon Graspeuntner, thank you for good cooperation and insightful discussions. Eva-Maria Herbst, special thank you for kind helps in and out the laboratory. Dr. Anna-Marei Böhm and Yizhu Li, thanks for your work which provides a part of basis for my thesis. Dr. Friederike Anton-Erxleben, Dr. Alexander Klimovich, Dr. René Augustin, Dr. Sebastian Fraune, Dr. Sören Franzenburg, Dr. Juris Grasis and Dr. Mayuko Hamada, thank you for answering my naïve questions on protocols, data analysis and much more. Thank you for all the valuable comments on my project and thesis. Cleo Pietschke, Javier Andrés López Quintero, Santiago Insua, Katja Schröder, thank you for all the helps and continuous encouragement and moral support. Frau Christa Kuzel, Doris Willoweit-Ohl, Maria Franck, Jörg Wittlieb, Frau Antje Thomas and Daniel Freyer, thank you for all the behind-the-scene work to keep things in order for the lab. I truly appreciate your hard work.

To my wife Qian Li, thank you for forgiving me setting our dating time around my experiment schedule. Thank you for your listening and encouragement. Whenever I have been depressed or tired, you have been the most effective medicine on earth. It is also really a wonderful thing being married to a scientist more talented than I am, as I have a constant role model and resource for bouncing ideas. Without your love and support I have no idea where I would be now.

My most grateful thanks are extended to my parents Bohua Ding and Wenjie Wang. You may not understand the science that I am doing, but you have been giving your unconditional love to me and encouragement to whatever I am doing. Thank you for the tremendous sacrifice you have made for my education. Thank you for the echoic reminders over the phone of staying warm and healthy. In nowhere I can find a place better than home.

The China Scholarship Council is kindly acknowledged for financial support.

8 Appendix

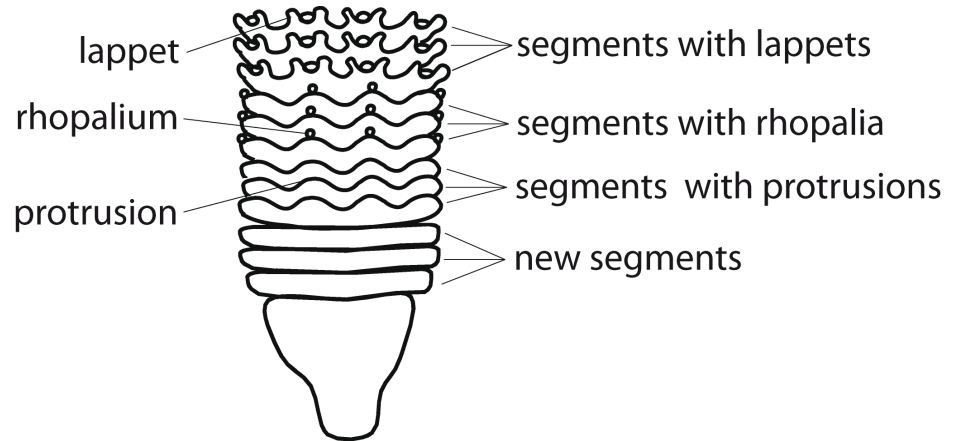


Fig. 52 Different stages of ephyra development in one strobila. In this strobila which contains 12 segments, three upper ones are well developed and contain lappets and rhopalia. Three segments below them have developed rhopalia, but still have no lappets. Six remaining segments in the basal part have no rhopalia. The most basal segments have not yet developed the protrusions.

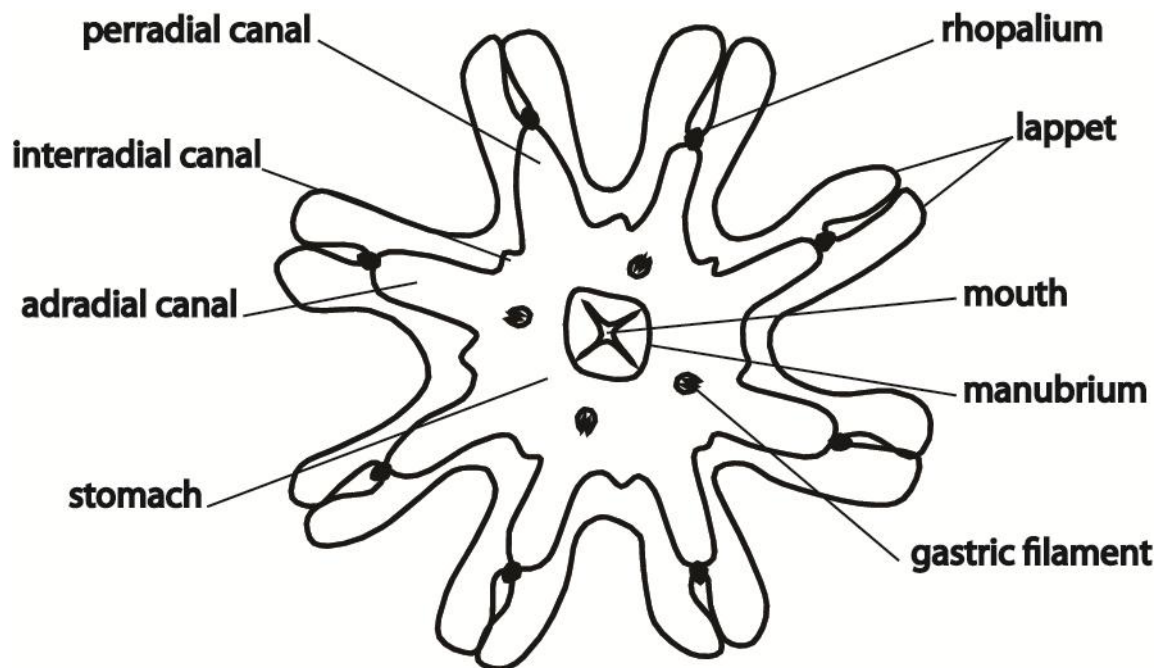
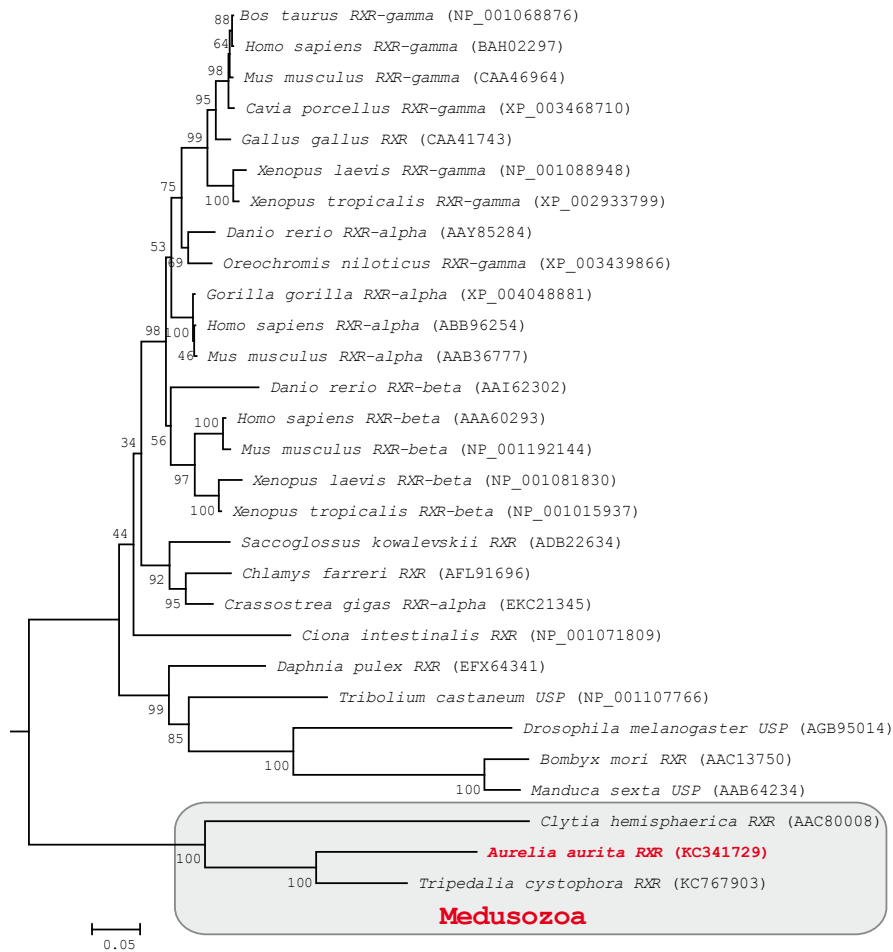


Fig. 53 Oral view of ephyra. It contains 8 lappets with rhopalia, 4 perradial canal, 4 adradial canal, 8 interradian canal, 4 gastric filament, stomach, mouth and manubrium.

A



B

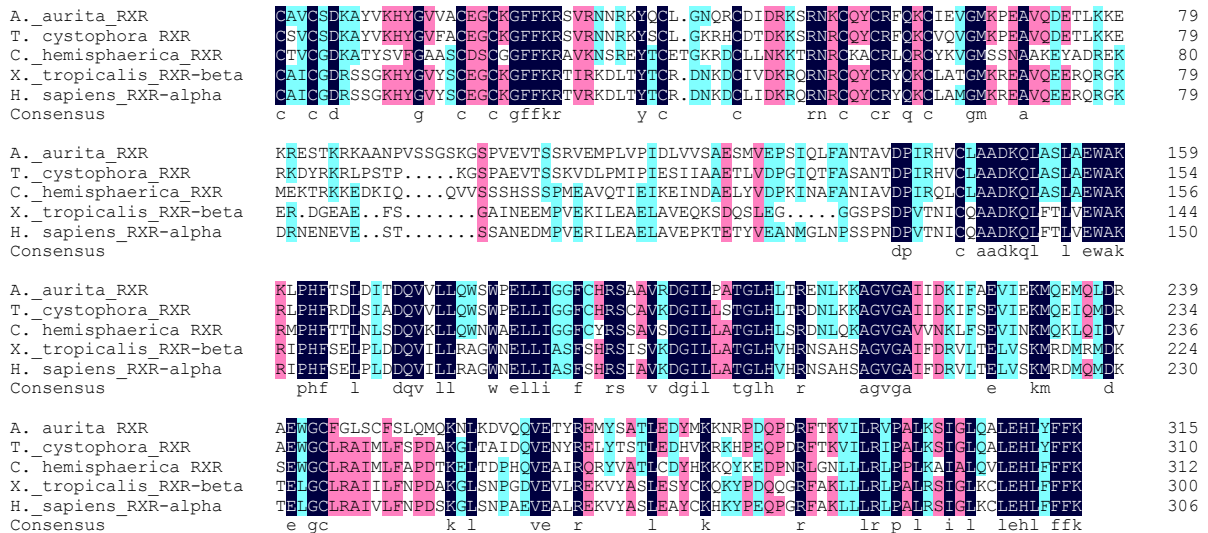


Fig. 54 (A) Phylogenetic analysis of RxR receptors from Protostomia and Deuterostomia. DBD-LBD regions were aligned by Clustal W (Thompson *et al.*, 1994) and the neighbour-joining tree was generated using MEGA 5.1. Numbers at nodes are bootstrap support values calculated by 1.000 replicates. RxR receptors from *Tripedalia*, *Aurelia* and *Clytia* group together. **(B) Alignment of DBD-LBD region of RxR receptors** from *Aurelia aurita* (KC341729), *Tripedalia cystophora* (AF091121), *Clytia hemisphaerica* (KC767903), *Xenopus tropicalis* (CR926364) and *Homo sapiens* (NP002948).

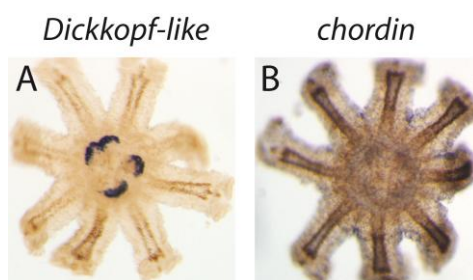


Fig. 55 (A) *Dickkopf-like* transcript is detected in the gastic filaments of ephyra. (B) *chordin* is uniformly expressed in the ectoderm of ephyra.

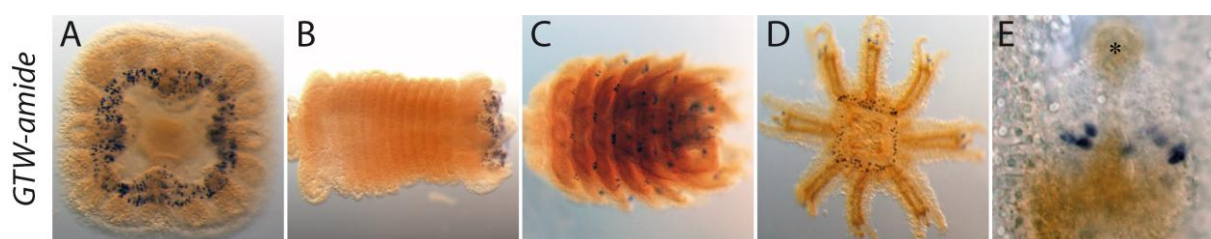


Fig. 56 Whole amount *in situ* hybridization against the precursor of neuropeptide *GTW-amide*. (A-B) The transcript of *GTW-amide* is detected in the ectodermal cells around the mouth in polyps and early strobila. (C) In late strobila, *GTW-amide* is expressed in the tips of rhopalia. (D-E) In ephyra, *GLW-amide* is expressed like a ring around the stomach and in the tips of rhopalia.

Table 18 List of the chemical compounds

No.	Chemical	Sigma SKU-Pack Size
1	Indomethacin	I7378-5G
2	5-Methoxy-2-methyl-3-indoleacetic acid	105171-1G
3	5-Methoxyindole-2-carboxylic acid	M14951-5G
4	2-Methylindole	M51407-25G
5	5-Methoxy-2-methylindole	M15451-1G
6	5-Methoxyindole	M14900-1G
7	5-Bromo-2-(hydroxymethyl)indole	736724-500MG
8	5-Fluoroindole	F9108-1G
9	2-Methyl-3-indoleacetic acid	333301-5G
10	3-indoleacetic acid	I3750-5G-A
11	5-hydroxy-2-methylindole	CDS012695-25MG
12	6-Methoxyindole-2-carboxylic acid	722014-1G
13	5-Methoxy -3-indoleacetic acid	M14935-1G
14	Indole-5-carboxylic acid	I5400-1G
15	Methyl indole-5-carboxylate	511188-1G
16	5-Methoxytryptamine	286583-100MG
17	5-Methoxy-DL-tryptophan	M4001-100MG
18	5-Hydroxy-L-tryptophan	H9772-100MG

19	Melatonin	M5250-1G
20	L-Tryptophan	T0254-1G
21	L-Tyrosine	93829-25G

Table 19 GenBank accession numbers of analyzed genes

	Gene	GenBank accession number
1	aBMP	KC357674
2	aCL112	KC341723
3	aCL390	KC341732
4	aCL631	KC341722
5	aCL1008	KC357675
6	aDNMT	KC341725
7	aEF1	KC341734
8	aETS	KC341727
9	aGTW-amide	KC767904
10	aPtc	KC341728
11	aRDH1	KC341731
12	aRDH2	KC341733
13	aRXR	KC341729
14	aWnt1	KC341730
15	BS_16S	KC767897
16	BS_ITS1	KC767902
17	R_16S	KC767898
18	R_ITS1	KC767900
19	RxR (Clytia)	KC767903
20	WS_16S	KC767899
21	WS_ITS1	KC767901

8.1 Whole-mount *in situ* hybridization protocol for *Aurelia aurita*

I. Day: Fixation of the animals:

1. Relax animals for **5-10 min** in **2% Urethane** (diluted in sea water) **on ice**
2. Fix with **fresh 4% PFA-ASW solution for 16h (overnight) at 4°C**
(Exchange **PFA with MetOH** = indefinitely long storage at -80°C is possible)

II. Day:

3. Treat with **EtOH for 10 min**
4. Rehydrate samples:
75% EtOH / 25% H₂O for 10 min, RT

50% EtOH / 50% PBT for 10 min, RT

25% EtOH / 75% PBT for 10 min, RT

Wash with PBT for 10 min, RT

5. Treat with **3% H₂O₂ for 10 min in PBT**
6. Wash with **PBT 3x for 10 min**
7. Treat with **Proteinase K in PBT for 20 min at RT** (1.25µl Proteinase K (18.5mg/ml)/25ml solution)
8. Rinse with **Glycine working solution (1x)**
9. Exchange **Glycine working solution, wash 10 min**
10. Wash with **PBT 3x 10 min**
11. Wash with **Triethanolamine 2x 10 min**
12. Exchange **Triethanolamine and add 2,5µl/ml Acetic anhydride 5 min**
13. Add **2,5µl/ml of Acetic anhydride 5 min**
14. Wash with **PBT 3x 10 min**
15. Refix with **4% Paraformaldehyde/PBT overnight at 4°C**

III.Day:

16. Wash with **PBT 3x 10 min**
17. Wash with **2x SSC 2x 10 min**
18. Heat animals in **2x SSC for 20 min at 70°C in a water bath**
19. Wash with **50% 2x SSC / 50% Hybridisation Solution (HS) for 10 min in tubes**
20. Wash with **Hybridisation Solution for 10 min**
21. Pre-hybridize for **2h in HS+40µg/ml tRNA+0.5 µg/ml dsRNA at 57°C**
22. Replace Hybridisation Solution (with tRNA & dsRNA) - 1 ml per 1.5 ml tube
23. Add **2µl of 1:50 diluted probe to 50µl of HSII (5XSSC, 50%Formamid)**
24. Denature probe 3-5 min at **70°C**
25. Add probe to the tube with animals (final probe dilution 1:25000)
Hybridise for **at least 24 hours at 57°C** with moderate agitation

Pre-incubate anti-DIG antibody (before DAY IV!):

Select fixed animals of different life stages

Wash with **PBT 3x 10 min**

Wash with MAB-T **3x 10 min**

Smash animals completely in 1ml of MAB-B, store at -20°C if necessary

Add **6 µl Anti-DIG AP antibody** (enough for 12 probes = 12 ml of Blocking Solution)

Incubate **for 12h (overnight) at 4°C with moderate agitation**

Centrifuge **at 14000g, 10min**

Use supernatant (pre-incubated antibody solution) for the probe detection on DAY IV.

IV. Day:

27. Wash away the probe with pre-warmed solutions at hybridisation temperature (**57°C**).

a) **100% HS for 10 min (without tRNA & dsRNA)**

b) **75% HS / 25% 2x SSC 10 min**

c) **50% HS / 50% 2x SSC 10 min**

d) **25% HS / 75% 2x SSC 10 min**

28. Incubate in **2x SSC + 0,1% CHAPS for 2x 30 min (at hybridisation temperature)**

29. Wash with **MAB-T 2x 10 min (at RT)**

30. Wash with **MAB-B for 1h (at RT)**

31. Incubate in **Blocking solution (80% MAB-B / 20% sheep serum) for 2h at 4°C**

32. Incubate with antibody (**final dilution 1:2000**) in **Blocking Solution**, overnight at **4°C** with moderate agitation

V. Day:

33. Wash with **MAB-T 9x 20 min**

34. Wash with **NTMT 1x 5 min**

35. Wash with **NTMT/Levamisole (1mM) 1x 5 min**

36. Discard the solution and add **NBT/BCIP in NTMT (1:50)**, incubate in the dark at **RT**

37. Check the staining every **5 min**

38. Wash animals with **Millipore-water 3x 1 min to stop colour reaction**

39. Incubate in **70% EtOH**, storage up to 2 weeks possible

VI. Day: Preparation of slides

- 40.** Incubate animals in **100% EtOH**
- 41.** Incubate in **MetOH for 30''** (**MetOH destains colour substrate!**)
- 42.** Incubate in **1-Butanol for 1-3 min**
- 43.** Incubate in **Xylol for 1-3 min**
- 44.** Embed in **Eukitt** or **Euparal**

The attached DVD contains the following data:

1. Sequences of analyzed genes
2. Constructs of recombinant proteins
3. Probes for *in situ* hybridization

9 Erklärung

Hiermit erkläre ich, dass ich die vorliegende Dissertation nach den Regeln guter wissenschaftlicher Praxis eigenständig verfasst und keine anderen als die angegebenen Hilfsmittel und Quellen benutzt habe. Dabei habe ich keine Hilfe, außer der wissenschaftlichen Beratung durch meinen Doktorvater Prof. Dr. Dr. h.c. Thomas C. G. Bosch in Anspruch genommen. Des Weiteren erkläre ich, dass ich noch keinen Promotionsversuch unternommen habe. Teile dieser Arbeit wurden bereits zur Publikation eingereicht.

Kiel, den 21. Mai 2013

Wei Wang